

1991

The Effects of Carboxyl-group Specific Modification and Triiodo-L-thyronine on Cardiac Sodium Channels

Samuel C. Dudley
masetto606@gmail.com

Follow this and additional works at: <http://scholarscompass.vcu.edu/etd>

 Part of the [Physiology Commons](#)

© The Author


Downloaded from

<http://scholarscompass.vcu.edu/etd/4527>

This Dissertation is brought to you for free and open access by the Graduate School at VCU Scholars Compass. It has been accepted for inclusion in Theses and Dissertations by an authorized administrator of VCU Scholars Compass. For more information, please contact libcompass@vcu.edu.

*School of Basic Health Sciences
Medical College of Virginia
Virginia Commonwealth University*


This is to certify that the thesis prepared by **Samuel C. Dudley, Jr.** entitled, **The Effects of Carboxyl-Group Specific Modification and Triiodo-L-Thyronine on Cardiac Sodium Channels**, has been approved by his committee as satisfactory completion of the thesis requirement for the degree of Doctor of Philosophy.


Clive M. Baumgarten, Ph.D.; Thesis Advisor



Linda S. Costanzo, Ph.D.; Committee Member


Richard M. Costanzo, Ph.D.; Committee Member


R. Michael Culpepper, M.D.; Committee Member


Hermes A. Kontos, M.D., Ph.D.; Committee Member


Roland N. Pittman, Ph.D.; Committee Member


S. Gaylen Bradley, Ph.D.; Dean, School of Basic Health Sciences

10 May 1991
Date

**The Effects of Carboxyl-Group Specific Modification
and
Triiodo-L-Thyronine on Cardiac Sodium Channels**

*A thesis submitted in partial fulfillment of the requirements for the degree of
Doctor of Philosophy at the Medical College of Virginia, Virginia Commonwealth University*

By

Samuel Calvert Dudley, Jr., M.D.

Bachelor of Arts with Highest Distinction, University of Virginia, 1985
Doctor of Medicine, Medical College of Virginia, 1989

Advisor: Clive Marc Baumgarten, Ph.D.

Associate Professor
Department of Physiology

Medical College of Virginia
Virginia Commonwealth University
Richmond, Virginia
May, 1991

ACKNOWLEDGEMENTS

My enduring gratitude goes to David Cafiso, who showed me the wonder of questioning, and to Clive Baumgarten, who instructed me in the ways of science. Whatever my achievements, they blossom from the seed of my grandparents, Andrew and Marian Cummins, who enabled my dreams. These aspirations and thirsts are lovingly attended by my partner, Victoria. I pray that I may have more fortune in the sea of unknown than Tantalus had in his pool.

I would also like to recognize the friendship of Tim Bentley, Henry Clemo, David Setchel, and Scott Duncan. They made the bafflements sufferable.

Table of Contents

	Page
List of Tables	v
List of Figures	vi
ABSTRACT	ix
CHAPTER 1. Introduction	1
<i>Sodium Channels</i>	2
<i>Single Channel Recording</i>	4
<i>Theoretical Considerations</i>	6
<i>Patch Clamp Configurations</i>	12
CHAPTER 2. Carboxyl-Group Specific Modification of Cardiac Sodium	
Channels	16
ABSTRACT	17
INTRODUCTION	19
METHODS	22
<i>Cell Isolation Procedure</i>	22
<i>Modification of Carboxyl Groups</i>	22
<i>Single Channel Recordings</i>	26
RESULTS	27
<i>Carboxyl Reagents Fail to Prevent Ca²⁺ Block of the Cardiac Na⁺ Channel</i>	28

<i>The Effect of Carboxyl Modification on Single Channel Properties in Low Ca²⁺</i>	34
<i>Effects of Carboxyl Modification on Mean Open Time</i>	39
DISCUSSION	47
<i>Why are carboxyl reagents ineffective in preventing Ca²⁺ block of cardiac Na⁺ channels?</i>	47
<i>Low Amplitude Openings</i>	52
<i>Are multiple unitary current levels substates or unique populations of modified channels?</i>	54
<i>Carboxyl Reagents' Mechanism of Action</i>	54
CHAPTER 3. Acute Exposure to 3,5,3'-Triiodo-L-thyronine Increases Bursting of Cardiac Sodium Channels	57
ABSTRACT	58
INTRODUCTION	60
METHODS	62
<i>Cell Isolation Procedure</i>	62
<i>Addition of T₃ and TAA</i>	62
<i>Single Channel Recordings</i>	63
RESULTS	66
<i>The Effect of T₃ on Na⁺ Channel Gating in Cell-Attached Patches</i>	67
<i>The Role of Second Messengers in the Effect of T₃</i>	78
<i>Patch Excision in the Presence of Pipette T₃ Increases Bursting</i>	80
DISCUSSION	84
<i>The Origin of Bursts</i>	85
<i>Kinetic Schemes</i>	87
<i>T₃'s Mechanism of Action</i>	88
Bibliography	92
Vita	108

List of Tables

	Page
Table I. Selected non-conservative substitutions related to carboxyl-reagents and group IIb metal sensitivity.	50
Table II. T ₃ requires access to the Na ⁺ channel's extracellular face to induce long events.	79

List of Figures

	Page
Figure 1. A model of the tertiary structure of the Na ⁺ channel α -subunit.	5
Figure 2. Analysis of single channel current records for unitary current amplitude and kinetics of the open state.	10
Figure 3. The four possible configurations for single channel recording.	13
Figure 4. Modification of a carboxyl group by trimethyloxonium tetrafluoroborate (TMO).	24
Figure 5. The conversion by water soluble carbodiimide (WSC) of a protein (P) carboxyl group into an uncharged amide.	25
Figure 6. Effect of Ca ²⁺ and trimethyloxonium (TMO) on unitary Na ⁺ currents in ventricular myocytes (pipette solution, 280 mM Na ⁺).	29
Figure 7. Open channel amplitude histograms at -60 mV and least squares fits to single Gaussian functions.	30
Figure 8. The effect of Ca ²⁺ and trimethyloxonium (TMO) on the current-voltage relationship.	32
Figure 9. Pretreatment of cells with 50 mM carbodiimide and 50 mM glycine methyl ester (WSC) failed to prevent block by 10 mM Ca ²⁺	33
Figure 10. Selected sweeps from TMO-treated cells exposed to 2 mM Ca ²⁺	35
Figure 11. Open channel amplitude histograms and Gaussian fits at -60 mV in one control and three TMO-treated patches (pipette solution, 280 mM Na ⁺ and 2 mM Ca ²⁺ in all panels).	36

Figure 12. Current-voltage relationships for each of the three current levels produced by TMO pretreatment.	38
Figure 13. Mean open time (MOT)-current level relationships in single patches after TMO pretreatment (pipette solution, 280 mM Na ⁺ and 2 mM Ca ²⁺).	40
Figure 14. The effect of Ca ²⁺ and carboxyl reagents on the mean open time-voltage relationship.	41
Figure 15. Transition rate constant (K) for leaving the open state - voltage relationships in 2 mM Ca ²⁺ (panel A), 10 mM Ca ²⁺ (panel B), and 10 mM Ca ²⁺ after TMO-treatment (panel C).	43
Figure 16. Ensemble averages at -30 mV in 2 mM Ca ²⁺ from control (panels A and C, 150 sweeps) and TMO-treated (panels B and D, 168 sweeps) patches.	46
Figure 17. The chemical structures of triiodo-L-thyronine (T ₃) and triiodothyroacetic acid (TAA).	64
Figure 18. Consecutive current traces at -50 mV from cell-attached patches with and without 5 nM T ₃ in the pipette solution.	68
Figure 19. Current traces and open probability diary showing runs of bursts in the presence of 5 nM T ₃	70
Figure 20. The effect of T ₃ in the patch pipette on unitary current and mean open time (MOT) in cell-attached patches.	72
Figure 21. Effect of T ₃ in the pipette on percent long events (%LE) as a function of voltage in cell-attached patches.	74
Figure 22. Effect of triiodothyroacetic acid (TAA) in the pipette on the %LE as a function of voltage in cell-attached patches.	76
Figure 23. Ensemble average of single channel currents from a cell-attached patch with 5 nM T ₃ in the pipette.	77

Figure 24. The effect of patch excision with 5 nM T_3 in the pipette.	81
Figure 25. The effect of patch excision in the presence of 5 nM T_3 on the unitary current, MOT, and %LE.	83

The Effects of Carboxyl-Group Specific Modification and Triiodo-L-Thyronine on Cardiac Sodium Channels

ABSTRACT

A thesis submitted in partial fulfillment of the requirements for the degree of Doctor of Philosophy at the Medical College of Virginia, Virginia Commonwealth University

Samuel Calvert Dudley, Jr., M.D.

Advisor: Clive Marc Baumgarten, Ph.D.

The patch clamp method was used to evaluate the effects of 3,5,3'-triiodo-L-thyronine (T_3) and carboxyl modification on adult rabbit ventricular Na^+ channels. In contrast to TTX-sensitive Na^+ channels, Ca^{2+} block of cardiac Na^+ channels was not prevented by selective carboxyl modification by trimethylxonium (TMO) or water soluble carbodiimide (WSC). In 2 mM Ca^{2+} , TMO-treated patches exhibited 3 discrete conductance (γ_{Na}) levels. An abbreviation of mean open time (MOT) accompanied each decrease in γ_{Na} . The effects on channel gating of elevating external Ca^{2+} differed from those of TMO pre-treatment. Ensemble averages after TMO showed a shortening of the time to peak current and an acceleration of the rate of current decay. WSC caused a decrease in γ_{Na} and an abbreviation of MOT at all potentials tested. We conclude that alteration of the surface potential by a single carboxyl modification is inadequate to explain the effects of TMO and WSC. Physiological concentrations of T_3 increased bursting as measured by the ratio of long events (LE) to the total number of events. In the cell-attached patch configuration, addition of 5 nM T_3 to the pipette increased the %LE at all potentials examined. The increase had a biphasic voltage-dependence and peaked at -50 mV. A similar increase in the %LE occurred with 50 nM T_3 suggesting saturation at ≤ 5 nM. LEs sometimes were grouped into runs, but the more usual pattern suggested that modal shifts occurred in ~ 1 s. Addition of T_3 to the bath but not the pipette in cell-attached patches failed to alter the MOT, unitary current, or %LE.

Na⁺ channel gating also was unaffected by patch excision or by addition of T₃ to the cytoplasmic face of inside-out patches. Nevertheless, with T₃ in the pipette, patch excision to the inside-out configuration caused a dramatic increase in the %LE, especially near the threshold potential, and an increase in the MOT. These results suggested that T₃ was not membrane permeable during the time scale of the experiments and that T₃'s action required close proximity to the extracellular face of the Na⁺ channel.

CHAPTER 1

INTRODUCTION

This section contains a brief discussion of a current model of the tertiary structure of voltage-gated Na^+ channels. Also, an overview of some of the theory and practice associated with recording currents from single ion channels is provided. For a more comprehensive discussion of the techniques and utility of single channel recording, the reader is referred to several recent reviews (Sakmann and Neher, 1983; Hille, 1984; Sakmann and Neher, 1984). These concepts form the bases for the analysis presented in Chapters 2 and 3.

Sodium Channels

By examining the presence of voltage-gated channels in different organisms, Hille (1984) speculated that these channels arose with the transition from prokaryotic to eukaryotic organisms. In eukaryotic organisms, the cell membrane is free from the maintenance of the proton-motive force, and gradients of other alkali and alkali earth metals can be exploited for information transfer. Hille reasoned that since the voltage-gated Ca^{2+} channel has a pivotal role in translating information carried by the cell membrane into cellular actions and is found in every excitable cell, this channel must have developed first. Under the pressure to communicate information rapidly over large distances in multicellular organisms, the Na^+ channel developed from the Ca^{2+} channel. The evolution of a Na^+ channel allows for a separation of the transduction and translation of information.

Along the same lines of reasoning, the development of diverse types of Ca^{2+} and K^+ channels (Tsien et al., 1987; Yellen, 1987) may have resulted from the needs of different tissues to modulate their cell membrane information content. However, since the information transmitted by an action potential in nerve and skeletal muscle was encoded as a function of time only, early investigators (e.g., Bishop, 1965) suggested that there should be only one type of Na^+ channel. The first evidence that there may be Na^+ channel subtypes came from pharmacological studies with the guanidinium neurotoxins, saxitoxin (STX) and tetrodotoxin (TTX). STX and TTX have a much lower affinity for cardiac and denervated

skeletal muscle Na⁺ channels than for nerve or innervated skeletal muscle Na⁺ channels (see Barchi, 1988; Trimmer and Agnew, 1989; Fozzard and Hanck, 1991). Na⁺ channels from brain and skeletal muscle, which are both sensitive to guanidinium toxins, differ in their binding affinities to μ -conotoxin, a polypeptide toxin isolated from sea snails (Moczydlowski et al., 1986a). Mammalian cardiac channels are more sensitive than nerve Na⁺ channels to sea anemone toxins (Renaud et al., 1986) and lidocaine (Krafte et al., 1990). Other evidence supporting subtypes of the Na⁺ channel comes from biophysical measurements. When compared under identical conditions, the cardiac and nerve Na⁺ channels have different conductances and gating properties (Baumgarten et al., 1991).

The development of molecular biological techniques confirmed the existence of a Na⁺ channel multigene family with at least three isoforms in brain (Noda et al., 1986; Auld et al., 1988; Kayano et al., 1988), one in skeletal muscle (Trimmer et al., 1989), and one in neonatal cardiac muscle (Rogart et al., 1989). The primary subunits of the Na⁺ channels have a high degree of homology with the sequences of Ca²⁺ channels (Tanabe et al., 1987; Mikami et al., 1989). Both channel types consist of ~2000 amino acid residues and have four homologous repeating domains. The K⁺ channel appears to consist of a tetramer in which each of the protein subunits is homologous with one of the four repeats in the Na⁺ or Ca²⁺ channels.

Based on the primary sequence of the Na⁺ channel and the recent biophysical data, Guy and Conti (1990) have refined a model of the Na⁺ channel's tertiary structure first proposed by Noda et al. (1986). Guy and Conti advance a model that has six membrane spanning α -helices in each repeat. Two of the helices are without charged amino acids (S5 and S6), and four are amphipathic having some charged residues (S1-S4). The S4 segment has a positively charged residue in every third position of the helix. These charges are thought to constitute the voltage sensor. There are several lines of evidence to suggest that the segments between S5 and S6, known as SS1 and SS2, fold into the center of the protein and form the selectivity filter (see Stevens, 1991). As shown in Figure 1, the current Na⁺ channel

model consists of three concentric transmembrane cylinders. The external cylinder is comprised of S1, S2, S3, and S5 α -helices from the four repeats. The middle cylinder contains the SS1 and S6 helices. In the closed state, the central cylinder is tightly packed with an S4 segment α -helix. In the open state the ion permeation pathway is formed by the SS2 and S4 segments arranged as an antiparallel β -barrel. Opening of the channel involves a complicated movement and rearrangement of the S4 segment. Finally, inactivation seems to involve amino acids in a cytoplasmic domain between repeats III and IV (Stühmer et al., 1989). This region has a net positive charge and may move in behind the ion permeation pathway to block conduction.

In 1949, Hodgkin and Katz and Hodgkin et al. proposed that an increase in sodium conductance was responsible for the upstroke of the action potential in squid giant axon. Similar results were subsequently obtained in frog sartorius muscle (Nastuk and Hodgkin, 1950), frog sciatic nerve (Huxley and Stämpfli, 1951), and dog and kid Purkinje fibers (Draper and Weidmann, 1951). The identity of the current responsible for the upstroke of the action potential was confirmed by Hodgkin and Huxley (1952a and b) using the voltage-clamp method. In this dissertation, single channel recording techniques are used to investigate the effects of chemical modification of carboxyl groups and of triiodo-L-thyronine (T_3) on cardiac Na^+ channels from acutely isolated rabbit ventricular cells. The results of these experiments suggest that both the conductance and gating of the channel are sensitive to extracellular manipulations. A susceptibility to such changes may allow for regulation of the channel function *in vivo*.

Single Channel Recording

In the investigation of channel behavior, single channel recordings have a number of advantages over analyzing macroscopic currents. The macroscopic current (I) recorded from

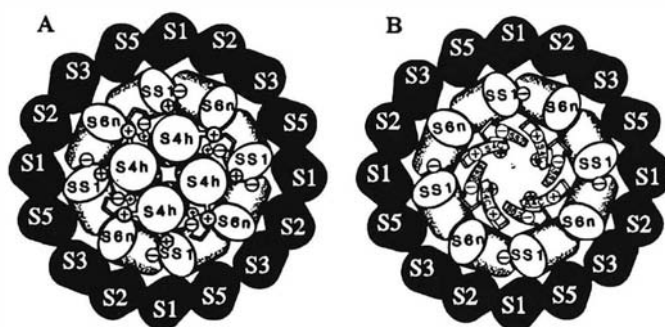


Figure 1. A model of the tertiary structure of the Na⁺ channel α -subunit. The Na⁺ channel α -subunit consists of four homologous repeats, each containing six putative transmembrane α -helices (S1-S6) and two short segments (SS1 and SS2). The α -helices are arranged in three concentric layers. In the closed configuration (panel A), the S4 helix, which contains positively charged amino acids at every third residue, occludes the central ion permeation pathway. In panel B, the S4 segment rearranges to form an eight member antiparallel β -barrel that allows for conduction. From Guy and Conti, 1990.

a cell is an average of the behavior of multiple channels

$$I = N \cdot i \cdot P_{\text{open}}(t)$$

where N is the number of channels under study, i is the unitary current, and $P_{\text{open}}(t)$ is the open probability of a single channel at time t . Fluctuation analysis techniques have been developed to estimate single channel parameters from macroscopic currents. These techniques assume that small variations in the current are the result of channels opening and closing at random. Although the variance of the macroscopic current can be related to the properties of individual channels, single channel recording can determine these parameters directly. Some of the advantages of single channel over macroscopic recordings are listed below (Aldrich and Yellen, 1983):

1. Ionic and experimental conditions can be manipulated to record from a single type of channel (e.g., Na^+ , Ca^{2+} , and K^+ channels). Records can provide evidence of the existence of separate populations or substates of channels when isolation of a single type of channel is impossible.
2. Any changes in the leak current with voltage steps can be corrected for directly without assuming the leak is a linear function of voltage. This allows for more accurate estimates of the current amplitude.
3. When recording macroscopic currents, the current is a time dependent function of all possible transitions between channel states. In single channel recording, kinetic parameters for a subset of these transitions can be estimated directly (*vide infra*) allowing for more detailed models of channel behavior.
4. In single channel recordings, open channel conductance properties can be observed directly. This information can be used to estimate the potential energy profile for ions in the permeation pathway. In turn, the energy profile can suggest structural features of the channel. In macroscopic measurements, assessment of open channel properties may be inextricable from the voltage dependence of channel opening.

5. In single channel recording, small currents reduce the artifacts caused by ion accumulation. Larger electrode apertures allow for a decreased access resistance in series with the channels.

In general, single channel recordings give a more detailed assessment of a subset of the data contained in macroscopic current measurements. Macroscopic currents can be approximated by averaging a number of single channel records to give an ensemble.

Theoretical Considerations

Single channel recording became possible with the development of field effect transistors (FETs). FETs are biased by an electric field and subsequently have high input resistances. The low power, open circuit input and low noise characteristics make FETs ideal components of operational amplifiers used in current-voltage (I-V) converters. A typical Na⁺ channel is open for 1 ms and conducts 1 pA, so only ~6000 ions move across the membrane. Consequently, amplifiers requiring little input current are critical to resolving single channel events without perturbing the system.

Even with low noise amplifiers, single channel event detection is an interplay of retaining the maximum kinetic resolution while minimizing errors related to random noise. The lower limit of the noise variance is

$$\sigma^2 = \frac{4kTB}{R}$$

where B is the bandwidth of the recordings, k is the Boltzmann constant, and R is the combined resistance of the membrane and the feedback amplifier (Nyquist, 1928). A common way to improve the signal-to-noise ratio is to reduce the recording bandwidth by low pass filtration. Filters are described by a cut-off frequency, f_c , at which the attenuation of the signal is -3 dB (i.e., $V_{out}/V_{in} = 0.71$). As shown in the equation above, filtering will decrease the baseline noise but will limit the kinetic resolution of the recordings. In the experiments

described below, the bandwidth was 2 kHz and the amplifier resistance was 50 G Ω , so the theoretical minimum standard deviation, σ , was 0.03 pA. In practice, noise from the electrode, electrode holder, membrane seal with the electrode, and I-V converter made this limit much higher.

Analog single channel currents must be converted to a digital form to allow for computer analysis. To provide for a subsequent reconstruction of the original signal and to avoid aliasing, the current data must be sampled at a minimum rate of $\geq 2\times$ the highest frequency in the record (i.e., the Nyquist sampling criterion). Because of practical considerations including the method used for interpolation of the discrete data, the sampling rate is usually $5 \times f_c$. Filtered digital current records are suitable for analysis. For automated event detection, a threshold current level (ϕ) is set. The beginning and end of an event are determined by when the current crosses ϕ . The threshold must be high enough to avoid mistaking noise for transitions while being low enough to detect as many true openings as possible. The threshold level is usually set at $\phi = 0.5i$. This ϕ level is called the half-amplitude threshold, and the time between threshold crossings provides an unbiased estimate of the channel open time. To maximize detection, the f_c of the filter must be adjusted in concert with ϕ . Colquhoun and Sigworth (1983) have shown that the rate of false events detected is proportional to ϕ/f_c and that a ratio of ~ 5 is appropriate for single channel recording. Figure 2A shows representative interpolations from digitized single channel current records at -50 mV. Panel B illustrates idealized records of openings and closings based on a half-amplitude threshold criterion.

The data available from single channel records can be divided into current amplitude and kinetic information. Filtering alters the amplitude data by time averaging the current input, and when estimating the unitary current, data affected by filtering must be omitted. Bessel-type active filters are used because they produce an output with a constant time delay that minimizes waveform distortion. The output of a multipole Bessel filter at time t depends

on the impulse response function which is proportional to $f_c \exp(-kf_c t)$ where k is a constant reflecting the characteristics of the filter. The time required for the filter output to reach the full amplitude of an applied step function is called the rise time (T_r) and is inversely related to f_c . Since channel openings are rectangular waves, the practical effect of filtering is to round the amplitude of these current pulses in the time domain which produces a roughly Gaussian rising and falling phase. Therefore, data points within one T_r of the current step will not reflect the true unitary current amplitude. Further, the measured current amplitude of channels with an open duration less than $0.538 T_r$ will never reach the half-amplitude threshold. In order to accurately estimate the unitary current with a sample rate of $5 \times f_c$, the first and last data points above threshold, which are affected by filtering, must be omitted.

The second class of available information is kinetic data. Transition rates between channel states are generally constant and independent of the previous history of the channel (i.e., stochastic). Such time homogeneous kinetics are referred to as Markovian, and imply that the channel state lifetime distribution will be exponential. For example, the relative frequency of an open channel lifetime is given by the probability density function (pdf; Colquhoun and Hawkes, 1983)

$$f(t) = \alpha \exp(-\alpha t)$$

where α is equal to the sum of the transition rates away from the open state. The mean of $f(t)$ is $1/\alpha$, known as the mean open time (MOT), and is equivalent to the time constant of the exponential decay. Therefore, the MOT contains kinetic information about the rate constants for the transitions away from the open state.

The MOT can be determined in several ways. One of the most frequently employed methods is to construct an open time histogram from the half-amplitude threshold duration information (Figure 2C). By making the bins small, the histogram will approximate the pdf for the open channel lifetime. The points in this histogram can be fitted to an exponential function, and the decay constant for the exponential will equal the MOT. Because of filtering

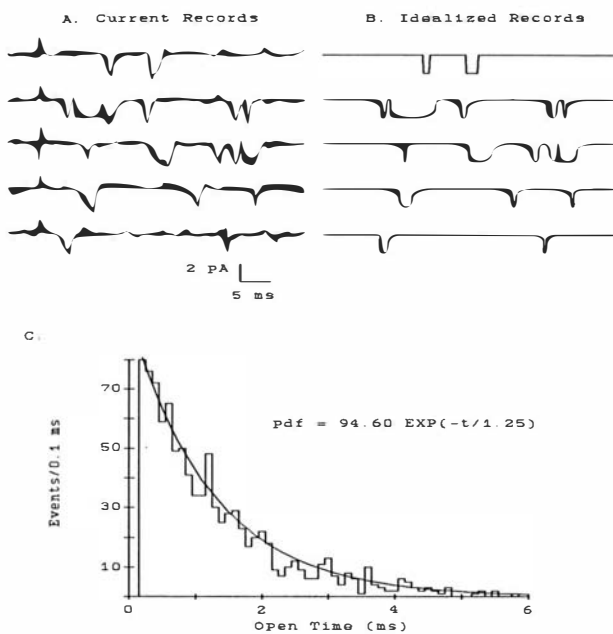


Figure 2. Analysis of single channel current records for unitary current amplitude and kinetics of the open state. Panel A shows typical current records at -50 mV interpolated from digitized data. Panel B illustrates computer assigned channel openings and closings based on a half-amplitude threshold criterion. An open time histogram can be constructed from the idealized records (panel C). The solid line represents a least squares monoexponential fit to the histogram, and the equation for this line is shown. In this example, the mean open time (τ) is 1.25 ms.

and a half-amplitude threshold for event detection, short events will be missed. Using a half-amplitude threshold, the estimated open duration will be correct for openings with an original width $> T_p$, so fitting the histogram after this time automatically compensates for missed events. An open time histogram described by the sum of exponentials implies multiple open states.

The MOT can also be obtained by averaging the open time durations. Because of missed openings, the average calculated from detectable openings (θ) will be longer than the true MOT (τ) and must be corrected. In general, the mean of this pdf is

$$\theta = \int_{t'}^{\infty} \frac{1}{\tau} t \exp(-t/\tau) dt / \int_{t'}^{\infty} \frac{1}{\tau} \exp(-t/\tau) dt$$

where $\tau = 1/\alpha$ and t' is the smallest detectable duration. Letting $x = t/\tau$ and $dx = dt/\tau$, the equation simplifies to

$$\theta = \tau \int_{x'}^{\infty} x \exp(-x) dx / \int_{x'}^{\infty} \exp(-x) dx$$

Integrating this equation with respect to x gives

$$\theta = \frac{\tau \exp(-x)[x+1] \Big|_{x'}}{\exp(-x) \Big|_{x'}}$$

and evaluating this at $x' = t'/\tau$ and ∞ reveals a surprisingly simple answer.

$$\begin{aligned} \theta &= t' + \tau \\ \tau &= \theta - t' \end{aligned}$$

I independently derived this relationship and later learned that it had been previously reported (Neher and Steinbach, 1978).

At least two graphical representations can be based on this analysis. The most obvious is the linear relationship between θ and t' . A plot of θ on the ordinate and t' on the abscissa will give a line with a slope of 1 and a y-intercept of τ . Also, it was found that the pdf multiplied by t' and plotted as a function of t' has a maximum which is equal to τ .

$$dy/dt = \frac{t'}{\tau} \exp(-t'/\tau)$$

$$dy/dt = 0 = \exp(-t'/\tau) \left[-\frac{t'}{\tau} + 1 \right]_{\max}$$

$$t' = \tau \quad \text{at the maximum}$$

The τ estimated from this relationship was less reliable than the other methods because the derivative dy/dt is very sensitive to small changes in the number of events in the adjoining time bins.

Patch Clamp Configurations

In order to record current from single channels, Hamill et al. (1981) pulled a microelectrode with a large aperture ($\sim 1-2 \mu\text{m}$). After smoothing the aperture with heat, they pressed the patch pipette against a cell. Application of suction to the pipette interior converted a low resistance seal into a gigaohm seal (see Figure 3, cell-attached configuration). In a high resistance seal, the distance between the glass and the membrane is on the order of several angstroms (Corey and Stevens, 1983). The ability to form a seal depends upon divalent cation bridging between the charges on the glass and the membrane. Other binding forces include hydrogen bonding, coulombic interactions, and Van der Waals' forces. As will be discussed later, reducing the negative membrane surface potential by chemical modification decreases the likelihood of obtaining a gigaohm seal.

The gigaohm seal acts as a diffusion barrier and is mechanically stable. These properties permit four recording configurations illustrated in Figure 3 (for review see Sakmann and Neher, 1984). All of the configurations originate from the cell-attached position. In this position, single channel currents may be recorded with minimal alteration of the membrane or the cytoplasmic milieu. Since the seal effectively separates the pipette solution from the bath solution, this configuration can be used to establish that a channel is regulated by an extracellular transmitter via a soluble cytoplasmic second messenger. If

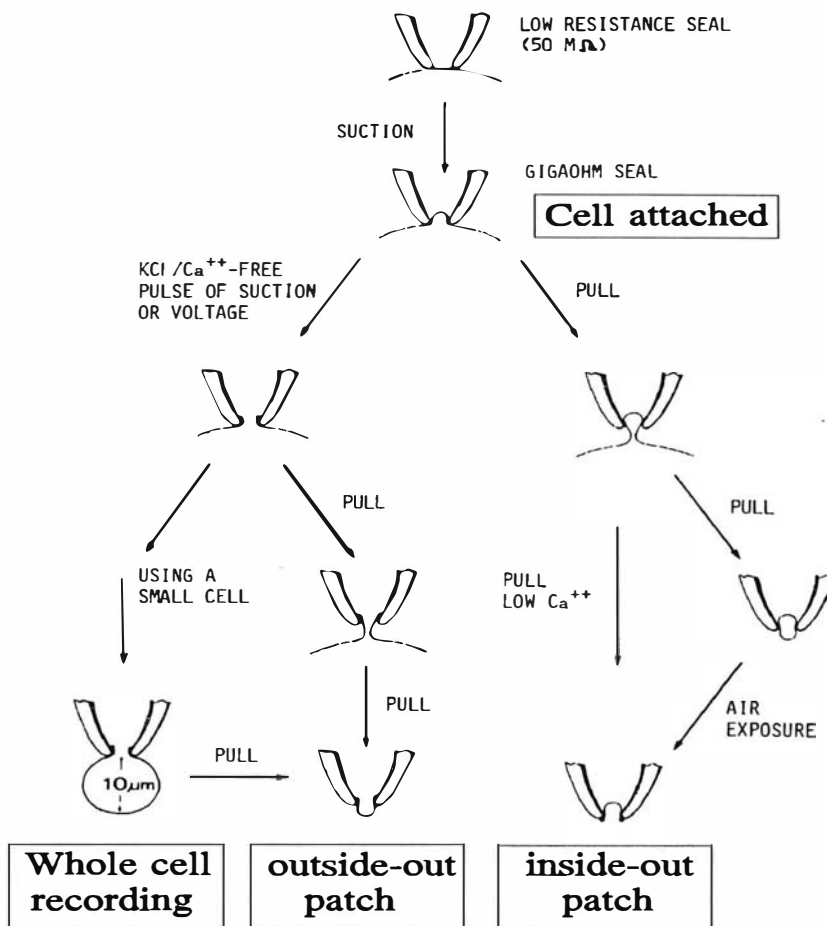


Figure 3. The four possible configurations for single channel recording. After placing a heat polished pipette on the surface of a cell, suction is applied to seal the pipette to the membrane (cell-attached). Withdrawing the pipette from this configuration in a low Ca^{2+} medium results in a membrane patch with the former cytoplasmic side facing the bath (inside-out). In the cell-attached configuration, a pulse of suction or an oscillating voltage will rupture the patch. Then, the electrode is continuous with the cytoplasm (whole cell). By withdrawing the pipette from the whole cell position, a membrane patch reseals over the pipette orifice. The former extracellular face of this patch faces the bath (outside-out). From Hamill et al., 1981.

modulation of the channel occurs with addition of a transmitter to the bath, a soluble second messenger must have diffused in the cytoplasm from the site of production to the channels isolated in the patch. This configuration also can be used to test channel properties under extreme ionic conditions. The pipette isolates solutions that would ordinarily damage the cell if the entire membrane were exposed. The limitation of the cell-attached configuration is the inability to change either the pipette or cytoplasmic solutions easily.

Upon forming a seal in the cell-attached configuration, withdrawing the pipette into a low Ca^{2+} -containing medium causes an excision of the patch from its native membrane. Because the former cytoplasmic side of the patch is left facing the bathing solution, this configuration is known as inside-out, and is well suited for studying the effects of cytoplasmic constituents on channel behavior. While it is technically difficult to change pipette solutions, bathing solutions are altered readily. This configuration can be used to screen for possible second messengers and is complimentary to the cell-attached mode for investigation of processes involving cytoplasmic components. Unfortunately, physical alteration of the membrane with excision and the loss of intracellular constituents may change the natural behavior of the channel.

If excessive suction or an oscillating voltage is applied to a cell-attached patch, the patch membrane will break, and the electrode will be in direct contact with the cytoplasm. This configuration is known as whole cell and is analogous to whole cell recording using conventional electrodes. When the patch is broken, the cytoplasm will be exchanged for the pipette filling solution. This makes the whole cell configuration similar to the inside-out configuration but with the limitation of only one cytoplasmic solution change. The bath solution may be readily exchanged, however. This configuration should be used when it is necessary to study the average properties of many channels (e.g., dose-response curves for a toxin).

The whole cell configuration is appropriate for small cells only. In the cell-attached mode conditions are ideal for voltage clamping. The electrode tip resistance is usually between 2–10 M Ω and constitutes the major access resistance in series with the channels. For a 10 pA current, the access resistance causes only a 0.1 mV deviation from the expected holding potential. The capacitance of an average patch is ~0.1 pF giving a time constant of ~1 μ s for the response of the system. In the whole cell configuration, the capacitance, access resistance, and current are increased. The cytoplasm contributes to the series resistance, and the capacitance is dominated by the cell membrane. Consequently, the time constants of the voltage clamp can be > 100 μ s. With whole cell currents typically on the order nanoamperes, the voltage drop across the series resistance can cause significant errors in the membrane holding potential. By taking the scaled output of the I-V converter and feeding it back on the command voltage, the apparent access resistance can be decreased by an order of magnitude to improve the time constant.

If the electrode is withdrawn slowly from the whole cell configuration into a bathing solution containing a moderate amount of Ca²⁺, a patch of membrane will reseal over the mouth of the pipette. This membrane will have its former extracellular surface facing the bathing solution and, therefore, is called the outside-out configuration. This configuration has similar advantages to the whole cell configuration, although the access resistance, the membrane capacitance, and the current are reduced for a better voltage clamp. This mode also allows for better dialysis of the cytoplasmic side by the pipette solution. The limitation of this configuration is the major rearrangement of the membrane required and the loss of cytoplasmic constituents which may regulate the channel.

CHAPTER 2

CARBOXYL-GROUP SPECIFIC MODIFICATION OF CARDIAC SODIUM CHANNELS

ABSTRACT

In TTX-sensitive nerve and skeletal muscle Na^+ channels, selective modification of the external carboxyl groups with trimethyloxonium (TMO) or water soluble carbodiimide (WSC) prevents voltage-dependent Ca^{2+} block, reduces single channel conductance, and decreases guanidinium toxin affinity. In the case of TMO, it has been suggested that these findings result from the modification of a single carboxyl group which causes a positive shift in the channel's surface potential. Using the cell-attached patch clamp method, I studied the effect of carboxyl modification on Ca^{2+} block of adult rabbit ventricular Na^+ channels. In unmodified channels, unitary conductance (γ_{Na}) was 18.6 ± 0.9 pS with 280 mM Na^+ and 2 mM Ca^{2+} in the pipette and was reduced to 5.2 ± 0.8 pS by 10 mM Ca^{2+} . In contrast to TTX-sensitive Na^+ channels, Ca^{2+} block of cardiac Na^+ channels was not prevented by selective carboxyl modification by TMO; after TMO pretreatment, γ_{Na} was 6.1 ± 1.0 pS in 10 mM Ca^{2+} . Nevertheless, TMO altered cardiac Na^+ channel properties. In 2 mM Ca^{2+} , TMO-treated patches exhibited 3 discrete γ_{Na} levels: 15.3 ± 1.7 , 11.3 ± 1.5 , and 9.8 ± 1.8 pS. An abbreviation of mean open time (MOT) accompanied each decrease in γ_{Na} . The effects on channel gating of elevating external Ca^{2+} differed from those of TMO pretreatment. Increasing pipette Ca^{2+} from 2 to 10 mM prolonged the MOT at potentials positive to ~ -35 mV by decreasing the open to inactivated (O \rightarrow I) transition rate constant. On the other hand even in 10 mM Ca^{2+} , TMO accelerated the O \rightarrow I transition rate constant without a change in its voltage dependence. Ensemble averages after TMO showed a shortening of the time to peak current and an acceleration of the rate of current decay. Channel modification with WSC resulted in analogous effects to those of TMO in failing to show relief from block by 10 mM Ca^{2+} . Rather, WSC caused a decrease in γ_{Na} and an abbreviation of MOT at all potentials tested. I conclude that alteration of the surface potential by a single carboxyl modification is inadequate to explain

the effects of TMO and WSC. Failure of carboxyl modification to prevent Ca^{2+} block of the cardiac Na^+ channel is a new distinction among isoforms in the Na^+ channel multigene family.

INTRODUCTION

Besides its well-known effect on surface potential (McLaughlin, 1989), Ca^{2+} blocks open Na^+ channels in a voltage-dependent manner by occluding the ion permeation pathway in nerve (Woodhull, 1973; Yamamoto et al., 1985), skeletal muscle (Weiss and Horn, 1986a and b) and cardiac muscle (Sheets et al., 1987; Nilius, 1988a). This block is too rapid to resolve but is manifest as an outward rectification at negative potentials in both the macroscopic instantaneous current-voltage relationship and the unitary current-voltage relationship. Experiments with group-specific reagents suggest that a carboxyl group is involved with Ca^{2+} block. Exposure to the carboxyl-specific, *O*-methylation reagent trimethyloxonium (TMO) prevents voltage-dependent Ca^{2+} block of reconstituted nerve Na^+ channels (Worley et al., 1986). TMO and other carboxyl-specific reagents also decrease the affinity of nerve and skeletal muscle Na^+ channels for guanidinium toxins, tetrodotoxin (TTX) and saxitoxin (STX) (Shrager and Profera, 1973; Baker and Rubinson, 1975 and 1977; D'Arrigo, 1975; Reed and Raftery, 1976; Spalding, 1980; Glden and Vogel, 1985; Krueger et al., 1986; Worley et al., 1986), and in the absence of Ca^{2+} block, decrease the nerve Na^+ channel unitary conductance, γ_{Na} (Sigworth and Spalding, 1980; Krueger et al., 1986; Worley et al., 1986; Chabala et al., 1986; Cherbavaz, 1990).

Worley et al. (1986) observed that TMO always altered Ca^{2+} block, guanidinium toxin affinity, and γ_{Na} concurrently and concluded that all three actions resulted from the modification of a single carboxyl group. Methylation by TMO of a carboxyl residue accessible from the extracellular solution decreases the negative surface potential of the channel, and Worley et al. (1986) argued that such an alteration in surface potential could explain the diverse effects of TMO on Na^+ channel properties. Other evidence also suggests that divalent cation block, guanidinium toxin affinity, and γ_{Na} may be linked. Cultured rat myoblast Na^+ channels are TTX-resistant (i.e., micromolar affinity), only poorly blocked by external Ca^{2+} ,

and possess a lower γ_{Na} than cultured rat myotube Na^+ channels, which are TTX-sensitive (i.e., nanomolar affinity) and significantly blocked by Ca^{2+} (Weiss and Horn, 1986a and b). That is to say, this naturally occurring TTX-resistant channel behaves like a TTX-sensitive Na^+ channel after modification by TMO. Furthermore, removing the negative charge from one carboxyl group by mutation of a single glutamate to a neutral glutamine in the rat brain II Na^+ channel results in a lower γ_{Na} and guanidinium toxin affinity (Noda et al., 1989).

The cardiac Na^+ channel deviates from this pattern, however. Despite the much lower affinity for guanidinium toxins (Moczydlowski et al., 1986b) and a lower γ_{Na} (Baumgarten et al., 1991) of mammalian cardiac than nerve Na^+ channels, the cardiac channel retains a relatively high affinity site for Ca^{2+} block (Sheets et al., 1987; Nilius, 1988a). Furthermore, the divalent cation blocking site in heart has a different sequence of potency and a notably higher affinity for group IIb metals than the nerve Na^+ channels (DiFrancesco et al., 1985; Frelin et al., 1986; Sheets et al., 1988; Tanguy and Yeh, 1988; Baumgarten and Fozzard, 1989; Visentin et al., 1990). These data suggest that the divalent cation blocking site may be different in heart and nerve.

In view of these differences in channel properties, I tested whether treatment with carboxyl group reagents would deter block of adult rabbit ventricular Na^+ channels by Ca^{2+} . TMO and water soluble carbodiimide (WSC), two reagents that specifically modify carboxyl groups, failed to prevent block of cardiac Na^+ channel by 10 mM Ca^{2+} . However, the reagents significantly affected several other channel properties. In 2 mM Ca^{2+} , the abatement of divalent cation block revealed that TMO pretreatment resulted in Na^+ channel openings to three distinct unitary current levels. Rather than behaving as substates, each open level appeared to reflect a population of channels with a distinct modification. Consequently, it is necessary to postulate multiple sites for the action of TMO on the cardiac Na^+ channel. Furthermore, the effect of TMO on mean open time was qualitatively different from that of elevating extracellular Ca^{2+} . Although TMO must modify surface potential, these data

indicate that a change in surface potential alone is insufficient to explain all the actions of TMO. Differences in the response of cardiac and nerve Na⁺ channels to carboxyl modifying reagents may have important implications for models of the Na⁺ channel.

Preliminary results of these studies have been reported elsewhere in abstract (Dudley and Baumgarten, 1990a and b).

METHODS

Cell Isolation Procedure

Ventricular myocytes were isolated from New Zealand white rabbits (1.5–2.5 kg) by a collagenase–protease digestion procedure modified from Poole et al. (1989). A cannula was placed in the aorta and hearts were perfused retrogradely for 4 min with a warm (37°C) Ca^{2+} -containing modified Tyrode's solution consisting of (in mM): 130 NaCl, 20 taurine, 10 creatine, 5.4 KCl, 0.75 CaCl_2 , 0.4 NaH_2PO_4 , 3.5 MgCl_2 , 5 N-2-hydroxyethylpiperazine- N' -2-ethanesulfonic acid (HEPES), 10 glucose (titrated to pH 7.25 with NaOH and bubbled with 100% O_2). After rinsing with a nominally Ca^{2+} -free Tyrode's solution to which 100 μM ethyleneglycol-bis-(β aminoethylether) N,N,N',N'-tetraacetic acid (EGTA) was added, low Ca^{2+} Tyrode's solution containing 1 mg/ml collagenase (type II; Worthington Biomedical, Freehold, NJ), 0.1 mg/ml protease (pronase E, type XIV; Sigma, St. Louis, MO), and 80 μM added Ca^{2+} (total Ca^{2+} ~200 μM) was recirculated for 15 min. Then, the ventricles were isolated, cut into small pieces (~5 × 5 mm), and divided among three flasks containing 3 ml of the enzyme solution with the addition of 10% bovine serum albumin. The flasks were gently shaken for up to 15 min in a Dubnoff metabolic shaking incubator maintained at 37°C. Single myocytes were separated from the undigested material by filtration through nylon gauze (250 μm pore size). Isolated cells were washed twice and stored at room temperature in a Kraft-Bruhe solution containing (in mM): 88 KOH, 80 glutamic acid, 11 glucose, 10 taurine, 10 KH_2PO_4 , 10 HEPES, 0.5 EGTA, 2.5 KCl, 1.8 MgSO_4 (titrated to pH 7.2 with 1 N KOH). This procedure consistently yielded >70% Ca^{2+} -tolerant, rod-shaped cells.

Modification of Carboxyl Groups

Channels were modified by two carboxyl-specific reagents (Brodwick and Eaton, 1982): trimethyloxonium tetrafluoroborate (TMO) and 1-cyclohexyl-3-(2-morpholinoethyl)-

carbodiimide metho-*p*-toluenesulfonate in the presence of glycine methyl ester (WSC). TMO modifies carboxylic acid residues by creation of a methyl ester derivative, while carbodiimide activates the carboxyl for nucleophilic substitution. Glycine methyl ester was added as the nucleophile and, in the presence of carbodiimide, should result in the formation of an uncharged amide derivative of the original carboxylic acid. However, any nucleophile present can react with a carboxyl group activated by carbodiimide, and protein crosslinking may occur.

TMO protocol. Isolated cardiac myocytes were placed in a solution containing (in mM): 90 KCl, 100 HEPES (pH 8.0). To prevent hydrolytic breakdown, TMO was weighed immediately prior to use and was added to the solution as a solid to yield a final concentration of 50 mM. The cells were stirred periodically and incubated for 10 min at ~0°C. The final pH of the reaction solution was 7.36 ± 0.04 ($n = 10$). This acidification in the presence of 100 mM HEPES buffer indicated that the TMO was active; a proton is released during the reaction of TMO with a nucleophile. To remove TMO's reaction byproducts, dimethylether and methanol, the cells were washed twice by centrifugation in 10× the volume of the cell pellet of the K-aspartate extracellular solution used during patch clamp or the Kraft-Bruhe solution (*vide infra*). The reaction of TMO with a protein carboxyl group is depicted in Figure 4.

WSC protocol. Modification of myocytes with 50 mM carbodiimide and 50 mM of a nucleophile, glycine methyl ester, was carried out in solutions containing (in mM): 50 KCl, 50 2-(*N*-morpholino) ethanesulfonic acid (MES). The pH of the reaction medium was adjusted to pH 5.5 with 1 N KOH to maximize the carboxyl selectivity of WSC (Baker and Rubinson, 1975). Both reagents were added as solids to the reaction solution which was gently agitated to insure dissolution and mixing with the cells. Cells were incubated for 15 min at 25°C and then washed by the same procedure used for TMO-treated cells. The two step conversion by WSC of a protein carboxyl group to an amide is depicted in Figure 5.

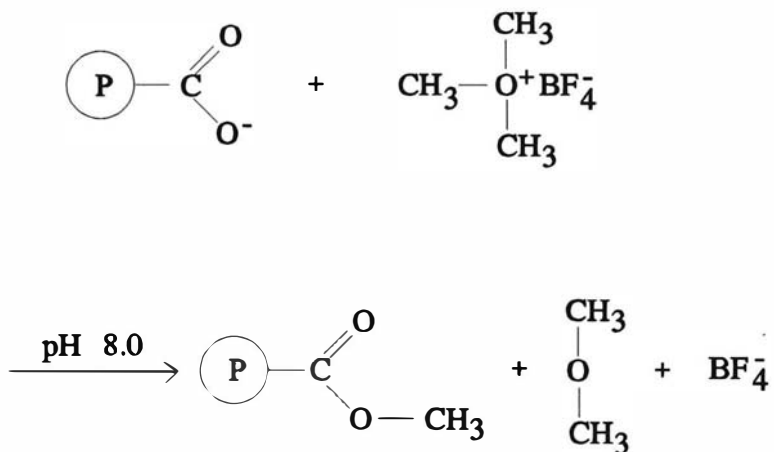


Figure 4. Modification of a carboxyl group by trimethyloxonium tetrafluoroborate (TMO). The carboxyl group is depicted as part of a protein, P. The reaction generates an uncharged methyl ester derivative and dimethylether.

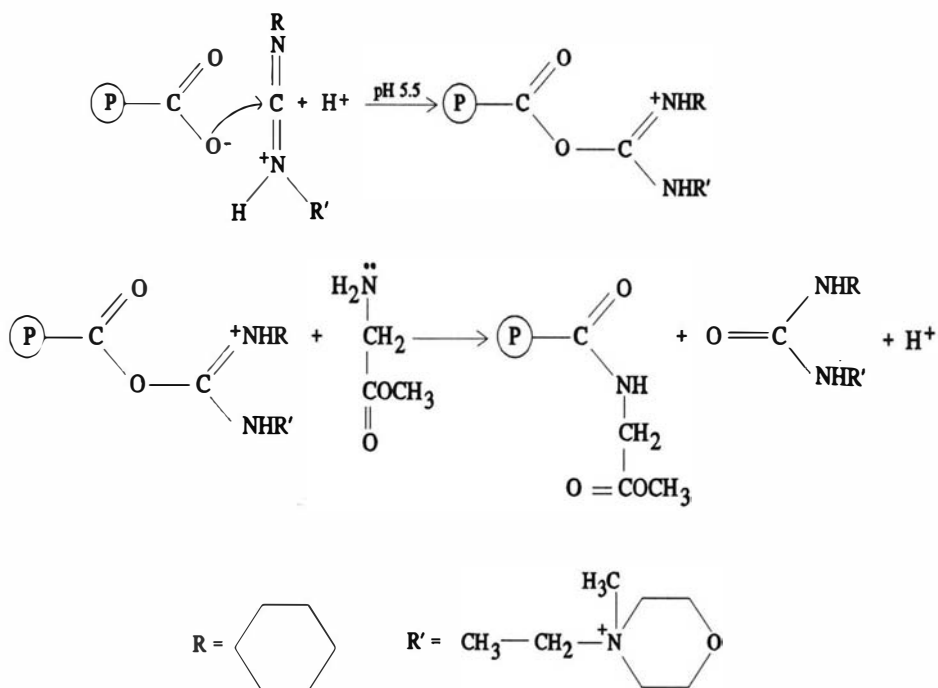


Figure 5. The conversion by water soluble carbodiimide (WSC) of a protein (P) carboxyl group into an uncharged amide. WSC promotes nucleophilic substitution at the carbonyl carbon group by forming an *O*-acylisourea intermediate. This intermediate undergoes nucleophilic substitution by the amino group of glycine methyl ester.

Initial attempts to modify Na⁺ channels utilized 100 mM WSC and pretreatment for 30 min. These conditions resulted in difficulty in forming gigaohm seals, and extremely few channels were functional upon seal formation. Even with a 50% reduction in both the concentration of WSC and the treatment time, high resistance seals were difficult to obtain, and patches exhibited a paucity of functional channels. The propensity for WSC to render tissues inexcitable also was noted by Shrager and Profera (1973).

Single Channel Recordings

Unitary Na⁺ channel currents were measured with a List EPC-7 patch clamp amplifier in the cell-attached mode (Hamill et al., 1981). Cells were affixed to the floor of a chamber with poly-L-lysine (MW > 300,000; Sigma). The membrane potential in series with the patch potential was depolarized to near 0 mV by an extracellular solution containing (in mM): 140 K-aspartate, 1 or 10 EGTA, and 5 HEPES (pH = 7.4) at 10°C. The low temperature was employed to better resolve channel openings and kinetics. To increase the signal-to-noise ratio, the pipette solution contained (in mM): 280 NaCl, 10 HEPES (pH = 7.4), and either 2 or 10 mM CaCl₂. The patch electrodes (2-5 MΩ) were pulled from 7740 glass, coated with Sylgard 184 (Dow Corning, Midland, MI) to improve their capacitive properties, and heat polished.

Pulse protocols, data acquisition, and analysis were directed by custom programs written in ASYST (Keithley, Rochester, NY) and run on an Intel 80386-based computer. Holding potential typically was -130 mV, and step depolarizations 45 ms in duration were applied at 1 Hz. Current records were digitized at 10 kHz (12 bits) after filtering at 2 kHz (-3 dB, 8-pole Bessel). Capacity transients were partially compensated for by analog circuitry, and the average current in sweeps without openings was subtracted from the original records to eliminate the residual capacity transient. In addition, the leak current was subtracted sweep-by-sweep so that the averaged current baseline was 0 pA.

The half-amplitude threshold criterion was applied in assigning openings, and open channel amplitude histograms were calculated after excluding the first and last points above threshold which were affected by filtering ($t_{50-90} \approx 0.08$ ms). Two methods for calculating MOT were employed in all cases. After excluding the first bin to allow for missed openings, a single exponential was fitted to the open time histogram using a least squares criterion. The exponential time constant was reported as the mean open time. The MOT also was calculated by the formula (Neher and Steinbach, 1978):

$$\text{MOT} = \theta - t$$

where θ is the arithmetic mean of the open duration of all openings with a duration greater than t , and t is the minimum open duration accepted for analysis, usually $250 \mu\text{s}$. This method also assumes an exponential distribution of open times. The results of the two methods rarely diverged, and in those instances, the MOT based on the arithmetic mean usually was accepted.

Statistical analyses of multiple, unpaired observations were carried out using a two-way analysis of variance. Measured values are reported as means \pm SE. Nonlinear curves were fitted by the Marquardt method with PROC NLIN (SAS Institute, Cary, NC) or with ASYST. Other statistical methods are presented with the results.

RESULTS

Carboxyl Reagents Fail to Prevent Ca²⁺ Block of the Cardiac Na⁺ Channel

Block of open cardiac Na⁺ channels by Ca²⁺ is illustrated in Figure 6. Typical consecutive sweeps showing openings on depolarizing from -130 to -50 mV are shown. Panel A is from a patch with 280 mM Na⁺ and 2 mM Ca²⁺ in the pipette solution, and panel B is from another patch exposed to 280 mM Na⁺ and 10 mM Ca²⁺. Increasing the pipette Ca²⁺ from 2 to 10 mM decreased the amplitude of the unitary current. This Ca²⁺-induced reduction of unitary Na⁺ currents has been reported previously in squid giant axon (Yamamoto et al., 1985), cultured rat skeletal muscle (Weiss and Horn, 1986a and b), rat brain (Worley et al., 1986), canine Purkinje fibers (Sheets et al., 1987), and guinea pig ventricle (Nilius, 1988a). The reduced current has generally been attributed to a decrease in the time-averaged current caused by unresolved blocking and unblocking of the open channel.

If methylation of carboxyl groups prevented Ca²⁺ block as it does for reconstituted nerve Na⁺ channels (Worley et al., 1986), the unitary currents of cardiac Na⁺ channels pretreated with TMO should be greater in amplitude than those recorded from untreated cells. Figure 6C shows consecutive sweeps obtained from a cell that was pretreated with 50 mM TMO. The pipette and bath solutions were identical to those used to record the sweeps in panel B. Contrary to the results obtained by Worley et al. (1986) in nerve, the amplitude of the openings in 10 mM Ca²⁺ appeared to be quite similar in TMO-treated and untreated cells. Since each panel represents a separate patch, inferences about the probability of channel opening cannot be drawn from these data.

Open channel amplitude histograms were used to quantitatively analyze the unitary Na⁺ currents recorded between -70 and 0 mV. Figure 7 illustrates histograms constructed from currents recorded at -60 mV. This voltage was chosen for illustration because the sensitivity for detection of the relief of block should be high at more hyperpolarized

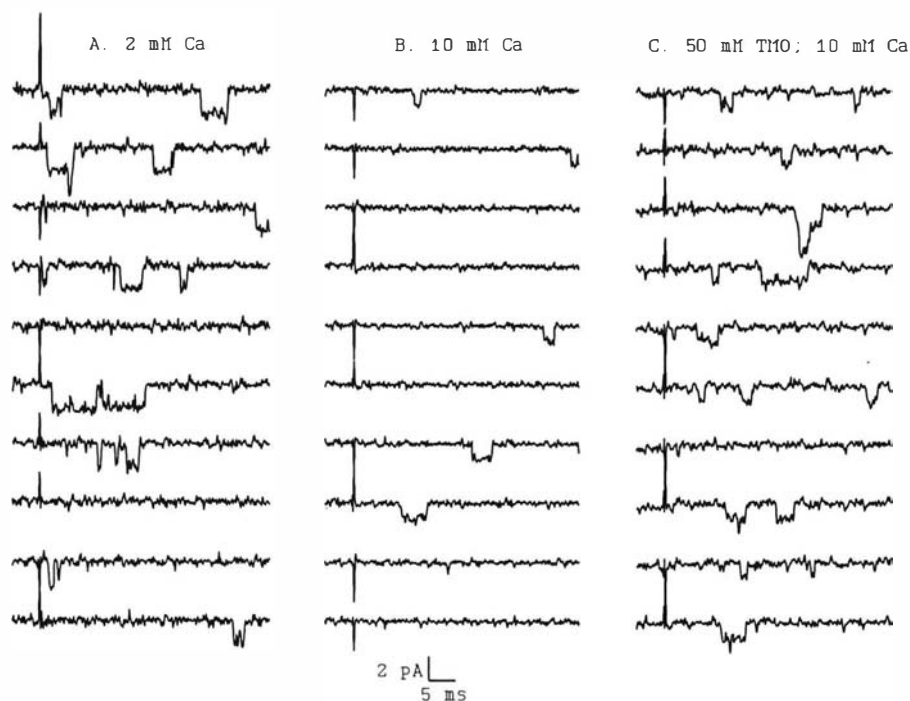


Figure 6. Effect of Ca^{2+} and trimethyloxonium (TMO) on unitary Na^+ currents in ventricular myocytes (pipette solution, 280 mM Na^+). Consecutive traces pulsing to -50 mV are shown. Increasing pipette Ca^{2+} from 2 mM (panel A) to 10 mM (panel B) decreased the unitary Na^+ current amplitude. In contrast to results in TTX-sensitive nerve Na^+ channels (Worley et al., 1986), pretreating ventricular myocytes with 50 mM TMO for 10 min failed to prevent open channel block by 10 mM Ca^{2+} . Rather than increasing unitary current, comparison of sweeps in panels B and C suggests that the unitary current amplitude of cardiac Na^+ channels is unaffected by TMO.

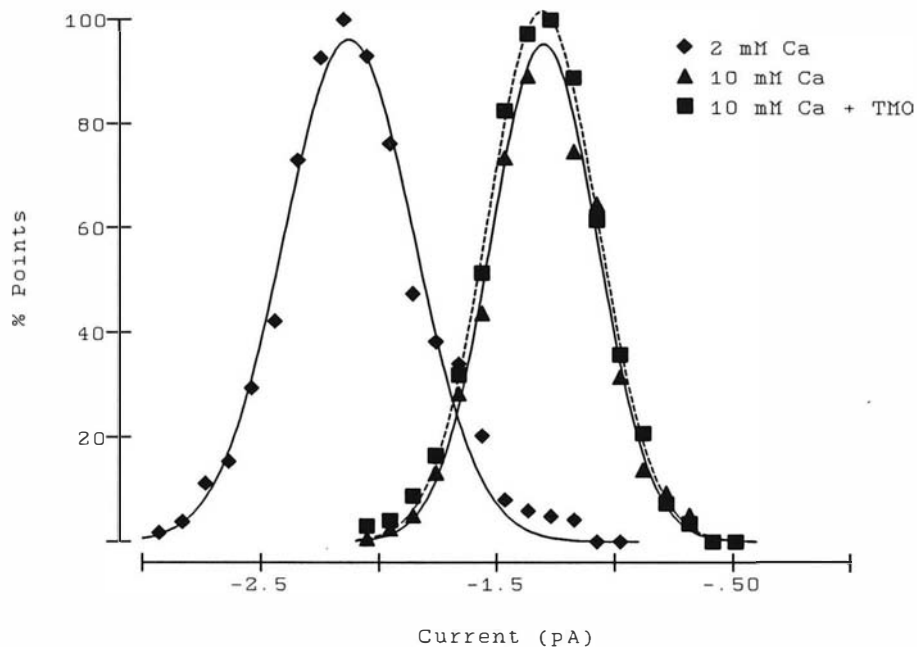


Figure 7. Open channel amplitude histograms at -60 mV and least squares fits to single Gaussian functions. Amplitude histograms were constructed after excluding the points affected by filtering, the first and last points of each opening above the 50% threshold. In 2 mM Ca^{2+} , unitary current amplitude was -2.13 pA (\diamond ; $\sigma = 0.28$ pA) and was reduced to -1.30 pA (\blacktriangle ; $\sigma = 0.23$ pA) by increasing pipette Ca^{2+} to 10 mM. The unitary current amplitude in 10 mM Ca^{2+} was unaffected by pretreatment with 50 mM TMO, -1.30 pA (\blacksquare ; $\sigma = 0.23$ pA). The ordinate of the amplitude histogram is normalized by the maximum number of open channel data points.

potentials where Ca^{2+} block is maximized. In the examples shown, increasing Ca^{2+} from 2 (\blacklozenge) to 10 mM (\blacktriangle) decreased the unitary Na^+ current from -2.13 to -1.30 pA, and an identical unitary current, -1.30 pA, was recorded in 10 mM Ca^{2+} from a cell which had been exposed to TMO (\blacksquare). On average, the unitary Na^+ current at -60 mV was -2.17 ± 0.03 pA in 2 mM Ca^{2+} ($n=9$), -1.30 ± 0.02 pA in 10 mM Ca^{2+} ($n=6$), and -1.32 ± 0.02 pA in 10 mM Ca^{2+} after exposure to TMO ($n=5$). Although increasing Ca^{2+} from 2 to 10 mM resulted in a significant reduction in unitary Na^+ current in 10 mM Ca^{2+} , currents recorded from TMO-treated cells were indistinguishable from those of control cells. This indicates that TMO failed to prevent Ca^{2+} block of open cardiac Na^+ channels.

Current-voltage curves depicted in Figure 8 show the effect of Ca^{2+} and TMO over the entire voltage range tested. Increasing pipette Ca^{2+} from 2 mM (\blacklozenge) to 10 mM (\blacktriangle) reduced γ_{Na} . The γ_{Na} after TMO pretreatment (\blacksquare) resembled that of the unmodified channel (\blacktriangle). The outward rectification of the current-voltage curve in 10 mM Ca^{2+} reflects the voltage-dependent Ca^{2+} block which is increased at more negative potentials. Based on a least squares linear regression over the entire voltage range, γ_{Na} was 18.6 ± 0.9 pS in 2 mM Ca^{2+} (\blacklozenge), 5.2 ± 0.8 pS in 10 mM Ca^{2+} (\blacktriangle), and 6.1 ± 1.0 pS in 10 mM Ca^{2+} after exposure to TMO (\blacksquare). Because of rectification, these values overestimate γ_{Na} in 10 mM Ca^{2+} at negative potentials. Nevertheless, the data points appear to overlap in 10 mM Ca^{2+} with and without TMO pretreatment. Comparison of γ_{Na} 's recorded under identical conditions with and without TMO exposure demonstrated that TMO pretreatment was ineffective over the entire voltage range ($p = 0.47$). This eliminates the possibility that an effect of TMO on Ca^{2+} block was obscured at certain voltages.

To confirm the inability of carboxyl modifying reagents to relieve Ca^{2+} block of cardiac Na^+ channels, I performed experiments with WSC, another carboxyl-specific reagent. As shown in Figure 9, pretreatment of cells with 50 mM WSC also failed to prevent the block of the unitary Na^+ current by 10 mM Ca^{2+} . The panel A shows consecutive records at

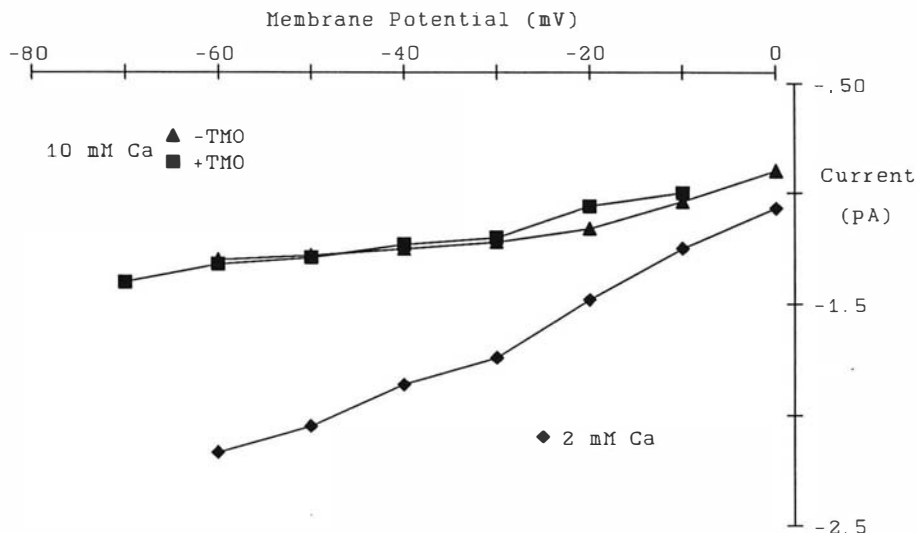


Figure 8. The effect of Ca^{2+} and trimethyloxonium (TMO) on the current-voltage relationship. Block of Na^+ channels by 10 mM Ca^{2+} was not prevented by pretreatment with 50 mM TMO. Unitary conductance (γ_{Na}) was 18.6 ± 0.9 pS in 2 mM Ca^{2+} (\blacklozenge), 5.2 ± 0.8 pS in 10 mM Ca^{2+} (\blacktriangle), and 6.1 ± 1.0 pS in 10 mM Ca^{2+} after exposure to TMO (\blacksquare). Symbols represent the mean value at each voltage, and the error bars (± 1 SE) are smaller than the symbol size. The γ_{Na} 's reported are based on a linear regression weighted for the number of observations at each potential. Tests for the homogeneity of the γ_{Na} 's based on a Student's *t* distribution suggest that raising Ca^{2+} had a significant effect ($p < 0.01$), but TMO pretreatment did not effect γ_{Na} in 10 mM Ca^{2+} ($p = 0.47$).

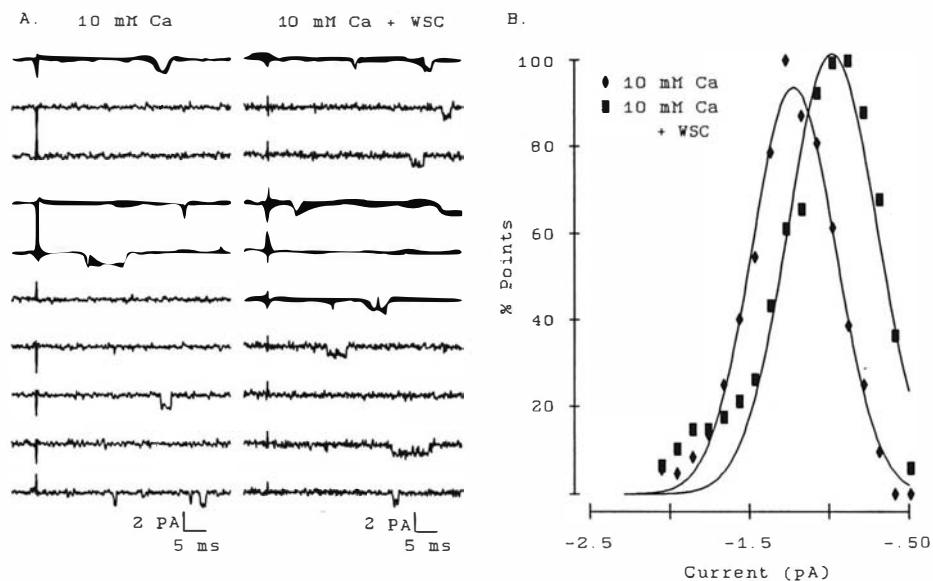


Figure 9. Pretreatment of cells with 50 mM carbodiimide and 50 mM glycine methyl ester (WSC) failed to prevent block by 10 mM Ca^{2+} . Consecutive sweeps at -50 mV from control and WSC-treated patches in 10 mM Ca^{2+} are shown (panel A). Open channel amplitude histograms and least squares fits to single Gaussian functions (panel B) show that pretreatment with WSC decreases the unitary current amplitude. Unitary current at -50 mV in 10 mM Ca^{2+} for the control patch is -1.22 pA (♦; $\sigma = 0.26$ pA), and the unitary current decreases to -0.98 pA (■; $\sigma = 0.28$ pA) after pretreatment with WSC. A decrease in the unitary current is opposite to the effect expected if WSC prevents divalent block of Na^+ channels. The ordinate of the amplitude histogram is normalized by the maximum number of open channel data points.

-50 mV from control and WSC pretreated channels exposed to the same pipette and bath solutions. Open channel amplitude histograms (panel B) indicate that the unitary Na^+ current was ~20% less in WSC pretreated channels (■) as compared with unmodified channels (◆). Unitary Na^+ currents in channels exposed to 10 mM Ca^{2+} after pretreatment with WSC were -1.05 ± 0.08 (n = 3), -0.98 ± 0.04 (n = 3), and -1.00 pA (n = 1) at -50, -40, and -30 mV respectively. Under identical conditions, unitary currents from control channels were -1.28 ± 0.04 (n = 9), -1.25 ± 0.03 pA (n = 6), and -1.22 ± 0.01 pA (n = 4). These significant decreases in unitary Na^+ current are antithetical to that expected with a relief of Ca^{2+} block. WSC differed from TMO in that a reduction in unitary current was not noted with TMO pretreatment.

The Effect of Carboxyl Modification on Single Channel Properties in Low Ca^{2+}

Although TMO did not alter γ_{Na} when the external surface of the channel was exposed to 10 mM Ca^{2+} , more complex behavior was observed with 280 mM Na^+ and 2 mM Ca^{2+} in the pipette. Figure 10 demonstrates the results of TMO pretreatment on unitary Na^+ currents in low external Ca^{2+} . Traces from patches pretreated with TMO and depolarized to -60 mV are shown, and the dotted line is the average unitary Na^+ current in unmodified channels exposed to the same pipette and bath solutions (see Figure 6). With a reduction in Ca^{2+} block, TMO-treated patches displayed openings to several current levels. Some openings appeared normal while the amplitude of others were either slightly less than normal or about half that of controls. Transitions between any of the three open current levels were not observed.

Open channel amplitude histograms were constructed at test potentials from -70 to -20 mV to quantify the multiple open current levels induced by TMO. Amplitude histograms from openings at -60 mV in one control and three TMO-treated patches are shown in Figure 11. Panel A is a typical open channel amplitude histogram from an unmodified, control channel. Control histograms showed only one peak in the vast majority of cases.

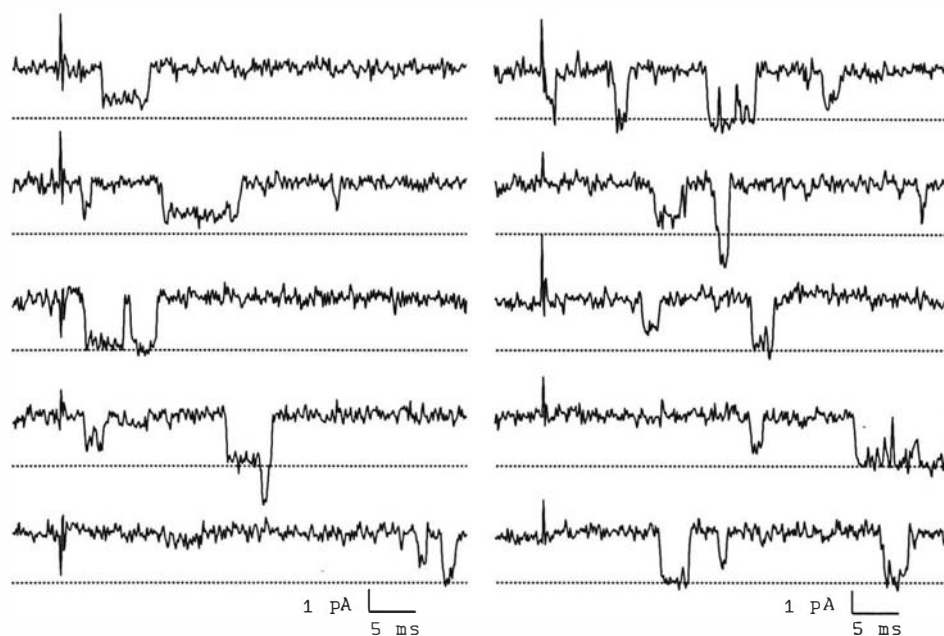


Figure 10. Selected sweeps from TMO-treated cells exposed to 2 mM Ca^{2+} . Contrary to the single γ_{Na} observed after TMO pretreatment in 10 mM Ca^{2+} , TMO-treated patches showed three current levels in 2 mM Ca^{2+} . The dotted line at -2.17 pA represents the average unitary current observed in control patches with 2 mM Ca^{2+} . Some openings appeared normal while the amplitude of others were either slightly less than normal or about half that of controls. Transitions between any of the three current levels were not observed.

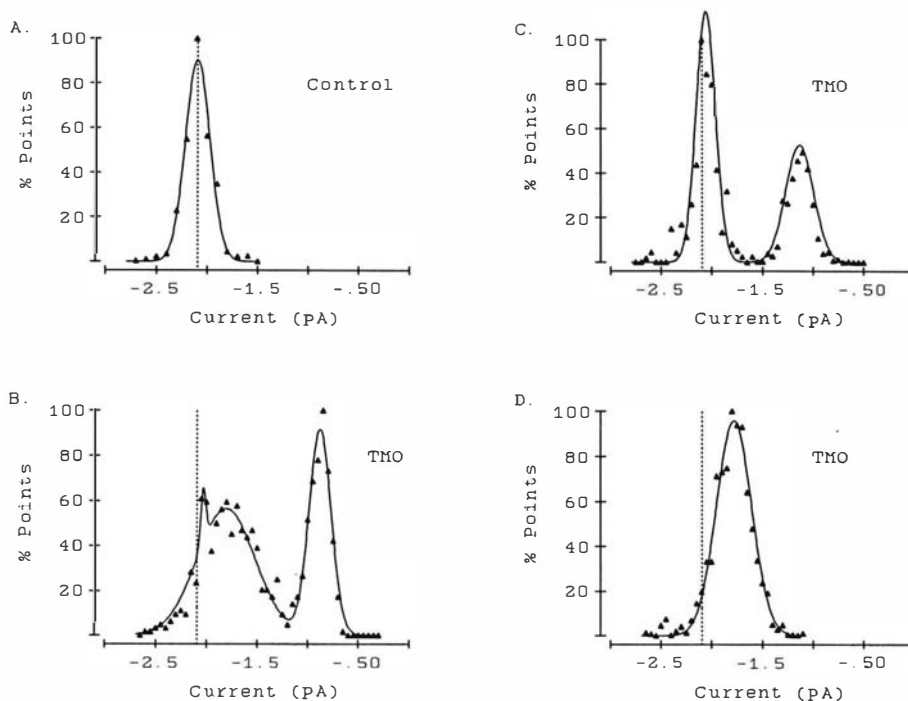


Figure 11. Open channel amplitude histograms and Gaussian fits at -60 mV in one control and three TMO-treated patches (pipette solution, 280 mM Na^+ and 2 mM Ca^{2+} in all panels). The dotted lines represent the unitary current of -2.08 pA ($\sigma = 0.12$ pA) for the control patch (panel A). With TMO pretreatment, three levels of unitary current were observed. All three levels (-2.03 pA, $\sigma = 0.03$ pA; -1.81 pA, $\sigma = 0.29$ pA; -0.88 pA, $\sigma = 0.11$ pA) are present simultaneously in the patch analyzed in panel B. In panel C, only the largest and the smallest current levels (-2.06 pA, $\sigma = 0.10$ pA; -1.13 pA, $\sigma = 0.14$ pA) are present. Panel D contains only the middle current level (-1.78 pA, $\sigma = 0.17$ pA). All combinations of the three levels were seen except that the smallest current level was never seen in isolation. To better resolve multiple current levels, the average unitary current of an opening was weighted for open time before constructing the histograms. In all histograms, the ordinate is normalized by the maximum number of open channel data points. Least squares fits to one or the sum of two Gaussian functions are shown in panels A, C, and D. In panel B, the least squares fit to the sum of three Gaussian functions gave a weight for the highest current level with a large asymptotic standard error. Therefore, the weight of this peak was adjusted by eye, and all other parameters correspond to the least squares criteria.

Rarely, a second amplitude opening was noted in unmodified patches as previously reported in cardiac channels by others (Cachelin et al., 1983; Kunze et al., 1985; Scanley and Fozzard, 1987; Patlak, 1988). The amplitude was ~40% of the more common amplitude, and in one patch with sufficient low amplitude events to permit reliable analysis, the MOT of the high and low amplitude events were similar. Because of the rarity of the lower amplitude event in control patches, further analysis was not undertaken.

In 2 mM Ca^{2+} , three levels of unitary current were observed after TMO pretreatment. All three levels were simultaneously present in the patch analyzed in the Figure 11, panel B. In panel C, only the largest and the smallest current levels are present. Panel D contains only the middle current level. All combinations of the three levels were seen except that the smallest current level was never seen in isolation.

Current-voltage curves with 2 mM Ca^{2+} and 280 mM Na^+ in the patch pipette for each of the three conductance states found in TMO-treated and the single conductance state in control patches are shown in Figure 12. In order to construct these curves, open channel amplitudes in a given patch were assigned to one of the three levels. The largest current level was easily distinguishable from the smallest level, especially if both levels existed in a patch. Otherwise, current amplitude values were assigned to the level with a mean value closest to that amplitude. Because the differences between unitary current levels were large compared to the variance of the measurements, the assignments were usually unambiguous. As estimated by a weighted least squares linear regression of the mean unitary currents, the γ_{Na^+} 's for the three current levels in TMO-treated patches were 10.7 ± 1.7 pS (■), 11.2 ± 2.2 pS (▲), and 14.8 ± 2.4 pS (◆) in 280 mM Na^+ and 2 mM Ca^{2+} . Statistically indistinguishable estimates of γ_{Na^+} , 9.8 ± 1.8 pS (n=5), 11.3 ± 1.5 pS (n=6), and 15.3 ± 1.7 pS (n=4), were obtained by averaging γ_{Na^+} 's calculated patch-by-patch. Although the largest conductance level in TMO-treated patches was ~20% smaller than that in control, 18.6 ± 0.9 pS, the difference was not statistically significant ($p = 0.17$). In contrast to the similarity of γ_{Na^+} for levels 2 and 3, the

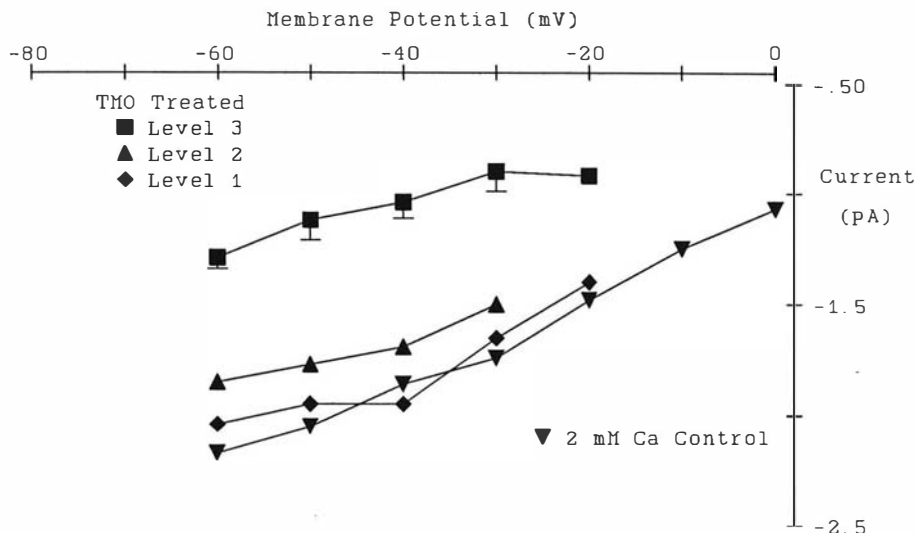


Figure 12. Current-voltage relationships for each of the three current levels produced by TMO pretreatment. Within each patch, unitary currents were assigned to one of the three levels as described in the text. The symbols represent the mean current at a given test potential, and error bars (± 1 SE) are shown when they exceed the symbol size. The γ_{Na} for each of the three levels was estimated by a weighted least squares linear regression of the mean unitary current at each voltage. The γ_{Na} 's for the three current levels in TMO-treated patches were 10.7 ± 1.7 pS (\blacksquare), 11.2 ± 2.2 pS (\blacktriangle), and 14.8 ± 2.4 pS (\blacklozenge) in 280 mM Na^+ and 2 mM Ca^{2+} . For comparison, the current-voltage curve from Figure 8 for unmodified Na^+ channels under identical conditions is superimposed (\blacktriangledown , 18.6 ± 0.9 pS). Based on a Student's t test for homogeneity of two slopes, the γ_{Na} 's for the control Na^+ channel and the largest current level in TMO-treated patches were statistically indistinguishable ($p = 0.17$).

unitary currents were clearly distinct. For example at -50 mV, the unitary currents were 55, 86, and 95% of the control unitary current. This apparent disparity arises because the extrapolated reversal potential for level 2, 107 ± 26 mV, is significantly more positive than that for level 3, 47 ± 14 mV. With the limited voltage range of the data, one cannot distinguish between differences in rectification and in the reversal potential, however.

Effects of Carboxyl Modification on Mean Open Time

When at least two different unitary current levels were observed in the same patch, analysis of the MOTs showed that a reduction in γ_{Na} was always associated with a reduction in the MOT. This relationship is illustrated in Figure 13. At each test potential, openings to different levels in the same patch are connected by a solid line. In 14 of 14 pairs, MOT was shorter for openings to a lower current level ($p < 0.01$). Thus within the same patch, there was a clear linkage between the amplitude of the unitary current and the dwell time in the open state. Analysis of the relationship between γ_{Na} and MOT for channels within the same patch excludes any confounding effects of cell-to-cell variations in Na^+ channel regulation and of E_m in series with the patch.

Na^+ channel MOT also was effected by elevating Ca^{2+} from 2 to 10 mM and by carboxyl modification in 10 mM Ca^{2+} . Figure 14 shows the relationship of MOT to voltage under several conditions. At depolarized potentials, pretreatment with TMO affected the MOT-voltage relationship in an opposite manner from elevations in Ca^{2+} alone. However, neither changes in Ca^{2+} nor TMO-treatment altered MOT at more negative potentials. By itself, increasing Ca^{2+} from 2 mM (\blacktriangle) to 10 mM (\blacklozenge) resulted in a prolongation of the MOT at potentials positive to -30 mV. In high Ca^{2+} , pretreatment with TMO (\blacksquare) resulted in a decreased MOT at potentials positive to ~ -35 mV. The decrease in MOT in 10 mM Ca^{2+} at positive potentials after TMO-treatment bore some similarity to the previously described link between TMO modification and a decrease in MOT in low Ca^{2+} . In 2 mM Ca^{2+} , however,

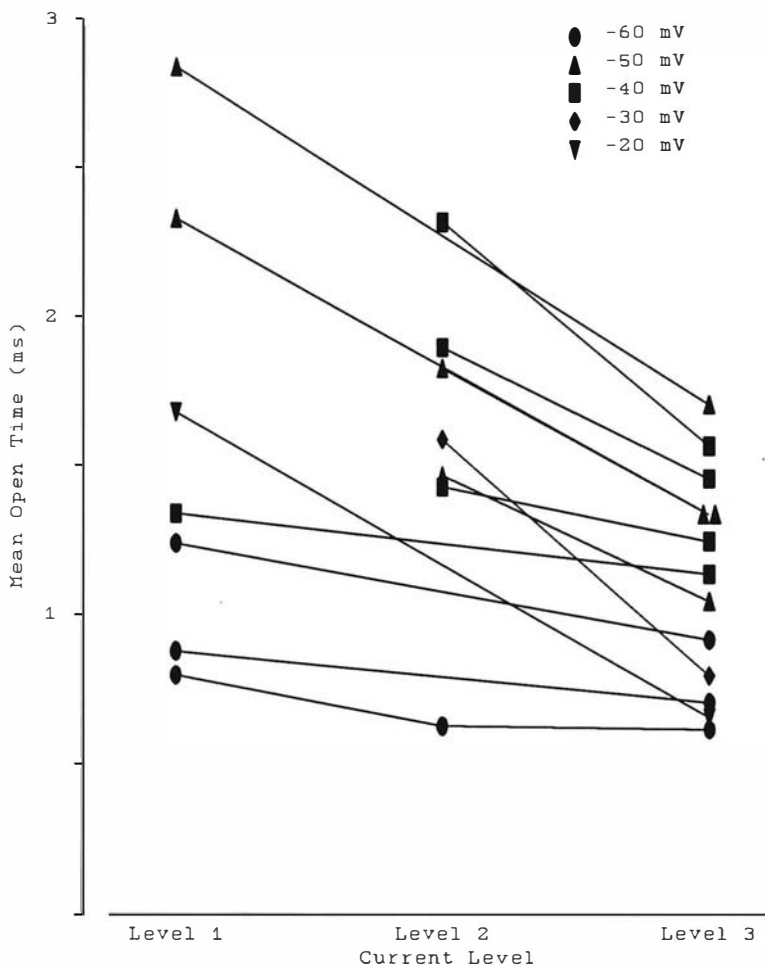


Figure 13. Mean open time (MOT)-current level relationships in single patches after TMO pretreatment (pipette solution, 280 mM Na⁺ and 2 mM Ca²⁺). Current levels present in a single patch at a given voltage are connected by a solid line. At each voltage tested (●, -60 mV; ▲, -50 mV; ■, -40 mV; ◆, -30 mV; ▼, -20 mV), a reduction in unitary current is associated with a decrease in the MOT. The linkage between a reduced unitary current and a shorter dwell time in the open state is present in all 14 pairs and is highly significant ($p < 0.01$) by a Wilcoxon signed rank sum test.

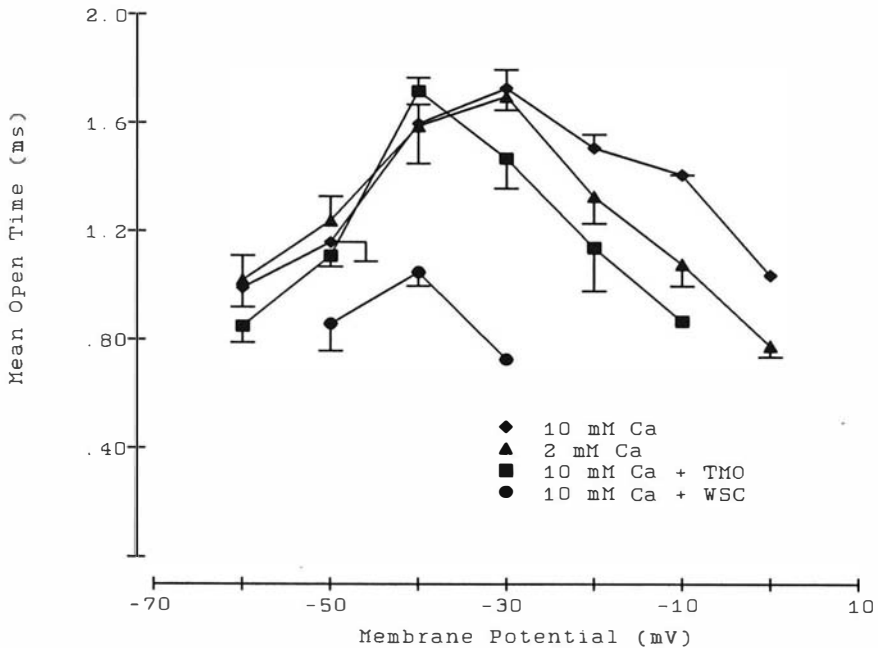


Figure 14. The effect of Ca^{2+} and carboxyl reagents on the mean open time-voltage relationship. At depolarized potentials, pretreatment with TMO affected the MOT-voltage relationship in an opposite manner from elevations in Ca^{2+} alone. However, neither changes in Ca^{2+} nor TMO-treatment altered MOT at more negative potentials. By itself, increasing Ca^{2+} from 2 mM (\blacktriangle) to 10 mM (\blacklozenge) resulted in a prolongation of the MOT at potentials positive to -30 mV. In high Ca^{2+} , pretreatment with TMO (\blacksquare) resulted in a decreased MOT at potentials positive to \sim -35 mV. In contrast to the lack of effect of TMO pretreatment or Ca^{2+} elevation on MOT at negative potentials, WSC altered channel gating near threshold. With 10 mM Ca^{2+} in the pipette, WSC exposure resulted in a decreased MOT at all potentials tested (\bullet).

TMO pretreatment seemed to decrease MOT even at more negative potentials (see Figure 13) while MOT at the higher Ca^{2+} was unaffected at potentials negative to -40 mV by TMO. In contrast to the lack of effect of TMO pretreatment or Ca^{2+} elevation on MOT at negative potentials, WSC altered channel gating near threshold. With 10 mM Ca^{2+} in the pipette, WSC exposure resulted in a decreased MOT at all potentials tested (●).

To investigate the basis of the changes in gating, the kinetics of transitions away from the open state were modeled by open to close state (O→C) and open to inactivated state (O→I) transitions which have opposite exponential dependencies on voltage (e.g., Scanley et al., 1990). The rate constant of transition (K) away from the open state was fitted numerically by the Marquardt method to the sum of two voltage dependent rate constants using the equation:

$$\text{MOT}^{-1} = K = K_{oc} \exp(V/S_{oc}) + K_{oi} \exp(V/S_{oi})$$

where K_{oc} and K_{oi} are the O→C and O→I transition rate constants at 0 mV, S_{oc} and S_{oi} are the slope factors reflecting the voltage sensitivities of the transitions, and V is the test potential.

The major effect of both TMO pretreatment and Ca^{2+} elevation appeared to be in the voltage range where closings to the inactivated state predominate over those to the closed state. Figure 15 shows the nonlinear least squares estimation of the observed K's under conditions of 2 mM Ca^{2+} (panel A), 10 mM Ca^{2+} (panel B), and 10 mM Ca^{2+} after TMO-treatment (panel C). In panel A, the parameters describing the curve and their asymptotic standard errors are $0.10 \pm 0.06 \text{ ms}^{-1}$, -27.3 ± 7.1 mV, $1.19 \pm 0.07 \text{ ms}^{-1}$, and 23.7 ± 4.9 mV for K_{oc} , S_{oc} , K_{oi} , and S_{oi} respectively. The parameters from Figure 15A imply that the O→C transition is relatively insensitive to the transmembrane voltage in 2 mM Ca^{2+} . S_{oc} is -27.3 mV, which is equivalent to 1.1 charges moving through the entire transmembrane field. Increasing Ca^{2+} from 2 to 10 mM caused little change in the O→C rate constant, K_{oc} (panel B). On the other hand, the O→I rate constant (K_{oi}), which dominates the rate of closing at depolarized potentials, was slowed by 10 mM Ca^{2+} . The voltage sensitivity of this

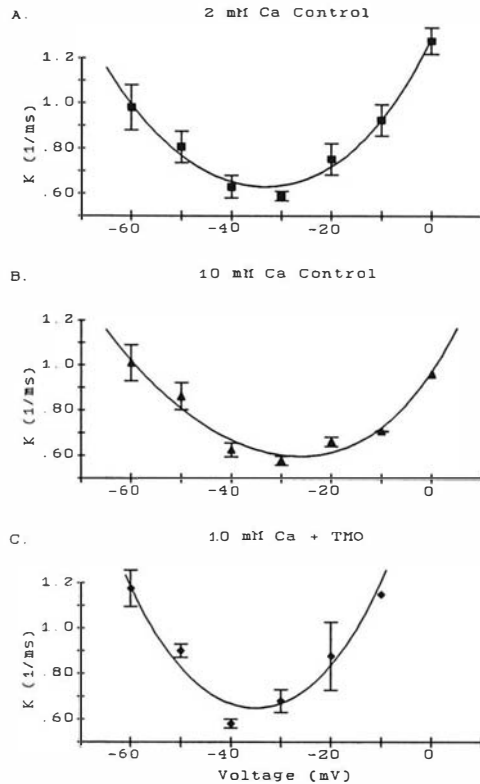


Figure 15. Transition rate constant (K) for leaving the open state - voltage relationships in 2 mM Ca^{2+} (panel A), 10 mM Ca^{2+} (panel B), and 10 mM Ca^{2+} after TMO-treatment (panel C). The weighted mean K 's were fitted numerically by the Marquardt method (SAS PROC NLIN; SAS Institute, Cary, NC) to the sum of two voltage dependent rate constants:

$$\text{MOT}^{-1} = K = K_{oc} \exp(V/S_{oc}) + K_{oi} \exp(V/S_{oi})$$

where K_{oc} and K_{oi} are the $\text{O} \rightarrow \text{C}$ and $\text{O} \rightarrow \text{I}$ transition rate constants at 0 mV, S_{oc} and S_{oi} are the slope factors, and V is the test potential. The major effect of both TMO pretreatment and Ca^{2+} elevation was in the voltage range where closings to the inactivated state predominate over those to the closed state. In 2 mM Ca^{2+} (panel A), the parameters of the fit were $0.10 \pm 0.06 \text{ ms}^{-1}$, $-27.3 \pm 7.1 \text{ mV}$, $1.19 \pm 0.07 \text{ ms}^{-1}$, and $23.7 \pm 4.9 \text{ mV}$ for K_{oc} , S_{oc} , K_{oi} , and S_{oi} , respectively. Increasing Ca^{2+} from 2 to 10 mM (panel B) caused little change in the $\text{O} \rightarrow \text{C}$ rate constant, K_{oc} . On the other hand, the $\text{O} \rightarrow \text{I}$ rate constant (K_{oi}), which dominates the rate of closing at depolarized potentials, was slowed by 10 mM Ca^{2+} . The voltage sensitivity of this step (S_{oi}) was unaffected by elevating Ca^{2+} . The estimated parameters in 10 mM Ca^{2+} were $0.18 \pm 0.12 \text{ ms}^{-1}$, $-35.5 \pm 12.7 \text{ mV}$, $0.79 \pm 0.13 \text{ ms}^{-1}$, and $20.5 \pm 10.5 \text{ mV}$ for K_{oc} , S_{oc} , K_{oi} , and S_{oi} , respectively. TMO pretreatment dramatically accelerated K_{oi} without significantly altering its voltage sensitivity, S_{oi} (panel C). Again, the parameters reflecting $\text{O} \rightarrow \text{C}$ transitions were relatively unaffected. The parameters in 10 mM Ca^{2+} after TMO pretreatment were $0.06 \pm 0.09 \text{ ms}^{-1}$, $-20.7 \pm 10.0 \text{ mV}$, $1.82 \pm 0.61 \text{ ms}^{-1}$, and $20.3 \pm 11.6 \text{ mV}$ for K_{oc} , S_{oc} , K_{oi} , and S_{oi} , respectively. Parameters are reported as the best estimate \pm the asymptotic standard error.

step (S_{oi}) was unaffected by elevating Ca^{2+} . The estimated parameters for the curve in 10 mM Ca^{2+} are $0.18 \pm 0.12 \text{ ms}^{-1}$, $-35.5 \pm 12.7 \text{ mV}$, $0.79 \pm 0.13 \text{ ms}^{-1}$, and $20.5 \pm 10.5 \text{ mV}$ for K_{oc} , S_{oc} , K_{oi} , and S_{oi} respectively. The changes in kinetics from panels B to C should reflect changes in gating as a result of TMO since the data were acquired under otherwise identical conditions. TMO pretreatment dramatically accelerated K_{oi} without significantly altering its voltage sensitivity, S_{oi} (panel C). Again, the parameters reflecting O→C transitions were relatively unaffected. The parameters for the curve in 10 mM Ca^{2+} after TMO pretreatment are $0.06 \pm 0.09 \text{ ms}^{-1}$, $-20.7 \pm 10.0 \text{ mV}$, $1.82 \pm 0.61 \text{ ms}^{-1}$, and $20.3 \pm 11.6 \text{ mV}$ for K_{oc} , S_{oc} , K_{oi} , and S_{oi} respectively.

The Na^+ channel gating characteristics described above bear a striking similarity with previously reported kinetic analyses. Our results showed that MOT was a biphasic function of voltage with a peak at $\sim -40 \text{ mV}$. This relationship has been seen by other investigators as well (Grant and Starmer 1987, Kirsch and Brown, 1989, Scanley et al., 1990). Also, our calculated rate constants and voltage sensitivities for the O→C and O→I transitions from averaged multi-channel patches are comparable to the rates reported for a single channel patch by Scanley et al. (1990). Extrapolating to 0 mV, their K_{oi} and K_{oc} are about 1.50 and 0.1 ms^{-1} , and the slope factors for these transitions are 27 ± 4 and $-30 \pm 4 \text{ mV}$, respectively. These rates and voltage sensitivities are statistically indistinguishable from our results. Our data also confirms the observation that inactivation from the open state is slightly voltage dependent. Further, both TMO pretreatment and elevations in Ca^{2+} should have altered the surface potential and the transmembrane voltage gradient, but neither intervention affected K_{oc} . This suggests that K_{oc} may be only secondarily voltage sensitive and that a large part of the voltage sensitivity of Na^+ channel opening may reside at an earlier C→C transition.

Because transitions between C→O and C→C states also might have been altered by TMO, ensemble averages were evaluated at -30 mV . Comparing ensemble averages in low Ca^{2+} from patches with or without TMO pretreatment revealed changes in macroscopic

kinetics with TMO (Figure 16). As the decay of the ensemble averages were linear to the level of the noise on semilogarithmic plots, the macroscopic rate of current decay was estimated by a least squares fit to a single exponential. In general, TMO-treated patches exhibited an earlier time to peak and a faster macroscopic inactivation. Before TMO, the time to peak current and the decay rate were 3.8 ± 0.5 ms and 4.7 ± 0.9 ms ($n = 5$), respectively. After pretreatment with TMO, the time to peak current and the decay rate were 2.2 ± 0.1 ms and 2.6 ± 0.2 ms ($n = 3$), respectively. *A priori* comparisons of means were performed by a Fisher's protected least significant difference test, and the reduction in both parameters was significant ($p < 0.05$). Although a decrease in MOT is expected to shorten the time to peak, the more rapid current decay may reflect alterations in the latency before channels open. Also implying a change in channel latency, a reduction in the time to peak current should be approximately equal to any decrease in MOT. However, I observed a larger decrease in the time to peak than in the MOT. This suggests that the rate constants for C→C or C→O transitions change with TMO preincubation. This inference is consistent with an acceleration of the macroscopic current decay since it is influenced by channel latency to opening (Aldrich et al., 1983; Scanley et al., 1990).

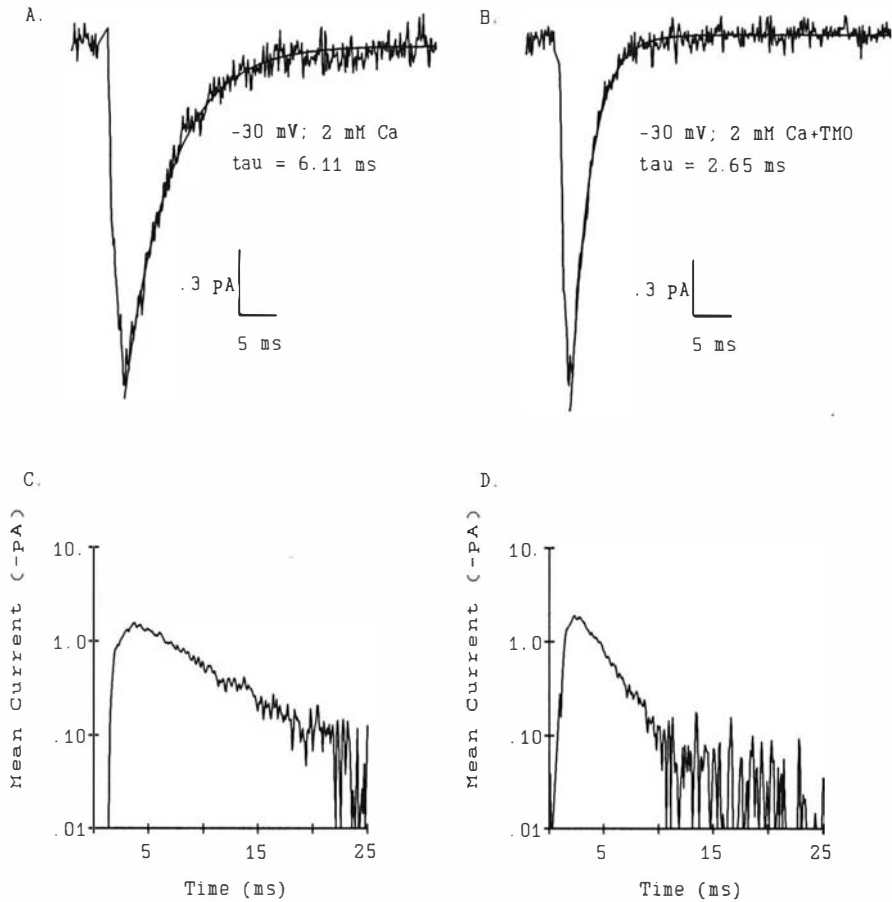


Figure 16. Ensemble averages at -30 mV in 2 mM Ca^{2+} from control (panels A and C, 150 sweeps) and TMO-treated (panels B and D, 168 sweeps) patches. The decays are well-described by single exponentials with time constants (τ) of 6.11 ms and 2.65 ms, respectively. Ensemble averages from TMO-treated patches show an earlier time to peak current and a more rapid current decay. The linearity of current decay in semilogarithmic plots confirms that the decays are monoexponential. Although the macroscopic current decay is often modeled as the sum of two exponentials, Grant and Starmer (1987) found that in at least 50% of patches from rabbit ventricle the ensemble current decay was well described at all potentials using a single exponential.

DISCUSSION

Na⁺ channels in nerve, heart, and skeletal muscle are blocked by a number of divalent cations including Ca²⁺ (Woodhull, 1973; Yamamoto et al., 1985; Weiss and Horn, 1986a and b; Sheets et al., 1987; Nilius, 1988a). Since this block is relieved by carboxyl modification, Ca²⁺ affinity in nerve Na⁺ channels has been attributed to a carboxyl group (Worley et al., 1986). Contrary to the result of Worley et al. (1986) on reconstituted rat brain Na⁺ channels, block of cardiac Na⁺ channels by 10 mM extracellular Ca²⁺ was not prevented after preincubation of isolated myocytes with either 50 mM TMO or 50 mM WSC, reagents that covalently modify external carboxyl groups and eliminate their negative charge. Rather than increasing unitary Na⁺ currents, as would be expected with the relief of Ca²⁺ block, TMO had no effect on the amplitude of openings in 10 mM Ca²⁺, and WSC decreased the unitary current amplitude. Although exposure to carboxyl modifiers failed to alter cardiac Na⁺ channel properties in 10 mM Ca²⁺, the effect of TMO was obvious at physiological Ca²⁺ levels. In 2 mM Ca²⁺, TMO decreased mean open time and resulted in openings to 3 distinct levels. Our finding of multiple conductance states after carboxyl modification of cardiac Na⁺ channels is consistent with brief reports that demonstrate multiple opening levels in batrachotoxin (BTX)-treated nerve channels exposed to either TMO (Cherbavaz, 1990) or two forms of WSC (Chabala et al., 1986).

Why are carboxyl reagents ineffective in preventing Ca²⁺ block of cardiac Na⁺ channels?

The failure of carboxyl reagents to prevent Ca²⁺ block of cardiac Na⁺ channels may arise from either of two possibilities. Modifiers could fail to react with the site that prevents Ca²⁺ block, or modifiers could continue to react but fail to induce the conformational change necessary to relieve Ca²⁺ block. Both possibilities require a difference in the primary amino acid sequence of the two channels. Analysis of a neonatal rat cardiac Na⁺ channel clone (rat heart I) confirms that the cardiac and nerve Na⁺ channels are distinct isoforms (Rogart et al., 1989). Changes in the amino acid sequence of the cardiac channel that could prevent

modification include a deletion of or substitution for a reactive carboxyl. Alternatively, the reactivity of the carboxyl group could be reduced by alterations to adjacent amino acids that hinder access by occupying space or altering the local electric field.

Several lines of evidence suggest that the differences in channel reactivity to carboxyl modifiers may arise from a single amino acid modification. In nerve Na^+ channels, carboxyl-specific modifying reagents not only prevent voltage-dependent Ca^{2+} block (Worley et al., 1986) but also reduce guanidinium toxin binding affinity (Shrager and Profera, 1973; Baker and Rubinson, 1975,1977; D'Arrigo, 1975; Reed and Raftery, 1976; Spalding, 1980; Gülden and Vogel, 1985; Krueger et al., 1986; Worley et al., 1986) and decrease single channel conductance when Ca^{2+} is omitted (Sigworth and Spalding, 1980; Chabala et al., 1986; Krueger et al., 1986; Worley et al., 1986; Cherbavaz, 1990). Because these three effects occurred concurrently in an all-or-none fashion in their experiments, Worley et al. (1986) proposed the *one hit* hypothesis in which carboxyl reagents modify a single group that is responsible for all three observations. Therefore, a single, naturally occurring amino acid change in the cardiac channel could explain the lower affinity for guanidinium toxins (e.g., Moczydlowski et al., 1986b) and the lower unitary conductance under identical conditions (Baumgarten et al., 1991).

Results from Stühmer and coworkers (Noda et al., 1989) also suggest that the failure of carboxyl agents to relieve Ca^{2+} block of the cardiac Na^+ channel may result from a single amino acid change. They found that a point mutation of glutamate-387 to glutamine (E387Q) renders the rat brain II channel insensitive to TTX and STX and lowers macroscopic current. They suggest that glutamate-387 may be the carboxyl group modified in nerve channels which inhibits guanidinium toxin binding, lowers unitary current, and relieves Ca^{2+} block. As pointed out by Noda et al. (1989), the corresponding glutamate in the rat heart I channel (amino acid 376) is conserved, but a positively charged arginine replaces a neutral asparagine as the adjacent residue. Such a substitution might be expected to reduce the affinity of both

guanidinium toxins and carboxyl modification reagents. Although it is tempting to think that this site may form part of the binding pocket for both TTX and divalent cations, one cannot exclude the possibility that a particular substitution alters binding at a distant site by inducing a conformational change.

Comparison of the primary sequences of the α subunit of rat heart I (Rogart et al., 1989) and rat brain II (Noda et al., 1986) reveals a number of amino acid alterations that might account for the ineffectiveness of carboxyl modification to relieve Ca^{2+} block in heart (see Table I). There are 104 instances where carboxyl residues (aspartate or glutamate) in nerve are not conserved or would be likely to have decreased reactivity because of substitutions that alter the charge on the adjacent amino acid (i.e., neutral to positive or negative to neutral). None of the modified sites are in the putative membrane spanning segments, and only 23 are tentatively assigned to extracellular positions (Noda et al., 1984; Noda et al., 1986; Guy and Conti, 1990), including 18 in the S5-S6 linker region. Evidence implicates part of the S5-S6 linker as the pore-forming sequence in K^+ channels (for review, see Stevens, 1991). Two affected carboxyls are included in the SS1 and SS2 segments of this linker.

Another property, the sensitivity of cardiac Na^+ channels to block by transition metals (DiFrancesco et al., 1985; Frelin et al., 1986; Sheets et al., 1988; Tanguy and Yeh, 1988; Baumgarten and Fozzard, 1989; Visentin et al., 1990), is also relevant. High affinity for group IIb metals cannot be explained readily by a substitution of a positively charged amino acid in rat heart I adjacent to the putative TMO reaction site proposed by Noda et al. (1989). However, a histidine or cysteine substitution could account for both the high affinity of cardiac Na^+ channels for Cd^{2+} and Zn^{2+} and the ineffectiveness of TMO and WSC. It is noteworthy that sensitivity to transition metals and TTX resistance occur together both in heart and in several atypical nerve Na^+ channels (Bossu and Feltz, 1984; Ikeda and Schofield, 1987; Jones, 1987).

Table I. Selected non-conservative substitutions related to carboxyl-reagents and group IIb metal sensitivity.

Putative Location	Substitutions		Adjacent Residues			
	Brain II	Heart I	Brain II	Heart I		
Substitutions for Carboxyl Groups in Nerve Channels						
I	S1-S2	Asp-153	Pro-156			
		S2-S3	Glu-182	His-185		
	S5-S6		Asp-183	Ala-186	Glu-182	His-185
			Asp-284	...		
			Glu-289	...		
			Asp-301	Gly-290		
			Asp-317	Asp-306	Glu-318	Val-307
			Glu-318	Val-307		
			Glu-321	Asn-310		
			Asp-322	Asp-311	Glu-321	Asn-310
			Glu-330	Asn-319		
	SS2{ Glu-387	Glu-376	Asn-388	Arg-377		
II	S1-S2	Glu-785	Ala-744			
	S2-S3	Asp-821	Gln-780			
	S3-S4	Glu-844	Gly-803			
	S5-S6		Asp-917	Ser-876		
			Glu-919	Leu-878		
III	S5-S6	Asp-1376	Asn-1376			
		Glu-1391	Val-1391			
IV	S1-S2	Glu-1558	Glu-1557	Met-1559	Lys-1558	
	S3-S4	Glu-1616	Gln-1615			
	S5-S6	SS1{	Glu-1698	Gln-1697		
			Asp-1730	Tyr-1729		
			Glu-1734	Asn-1733		
			Asp-1736	Pro-1735		
		Asp-1745	Asn-1743			
Substitutions to His and Cys in Cardiac Channels						
I	S1-S2	Asn-149	His-152			
	S2-S3	Glu-182	His-185			
	S5-S6		Asn-276	His-279		
			Try-362	His-351		
			SS2{ Phe-385	Cys-374		
II	S5-S6	Cys-912	His-871			

Corresponding amino acids in the linkers between the membrane spanning segments of rat heart I and rat brain II Na⁺ channels. Substitutions in the amino and carboxyl termini and the linkers between repeats are omitted because of their suspected intracellular location. ..., deletion of amino acid in heart. Standard three letter amino acid abbreviations are used.

Comparison of the sequences of the α subunit of rat heart I (Rogart et al., 1989) and rat brain II (Noda et al., 1986) shows that there are 17 histidines and 8 cysteines replacing other nerve channel residues, but only 5 substitutions are thought to face the extracellular space. One of these, rat heart I histidine-871, is unlikely to be the cause of enhanced affinity for group IIb metals because the histidine replaces a cysteine and a positively charged arginine replaces a neutral adjacent amino acid. It is striking that the remaining 4 substitution sites are clustered in repeat I (3 in the S5-S6 linker) and that none of the 25 sites is found in the putative transmembrane segments. Cardiac cysteine-374, replacing phenylalanine, is just two residues from the TMO reaction site proposed by Noda et al. (1989) and notably is in the SS2 segment. Despite tentative assignment to the inner face of the membrane, cardiac histidine-185 and histidine-570 also may deserve consideration because they are the only instances in which a histidine or cysteine in heart replaces aspartate or glutamate in nerve.

The suggestion that a single amino acid substitution may explain the lower guanidinium toxin binding affinity and the failure of modification to relieve Ca^{2+} block of cardiac Na^+ channels may be an oversimplification. Our experiments showed that the Ca^{2+} binding site was unaltered by exposure to carboxyl modifiers, yet TTX and STX binding is reduced upon exposure of neonatal rat heart homogenates to TMO (Doyle, D. unpublished). Taken together, these chemical modification data suggest a dissociation of the guanidinium binding site and the site responsible for Ca^{2+} block. This conclusion is supported by other evidence. The guanidinium toxin binding site is not in the electrical field (Ulbricht and Wagner, 1975; Wagner and Ulbricht, 1975; Krueger et al., 1979; Kao and Walker, 1982; Rando and Strichartz, 1986), and the voltage dependence of binding seen in BTX-treated channels is the result of state dependence (Moczydlowski et al., 1984; Moczydlowski et al., 1986c; French et al., 1984; Green et al., 1987b). On the other hand, electrical measurements suggest that Ca^{2+} enters and is affected by 25-30% of the transmembrane electrical field (Woodhull, 1973; Yamamoto et al., 1985; Weiss and Horn, 1986a and b; Sheets et al., 1987). Furthermore,

measurements have failed to demonstrate any interaction between the toxin binding and the Ca^{2+} blocking sites (Green et al., 1987b) except at very high Ca^{2+} concentrations (Salgado et al., 1986).

Several studies on nerve Na^+ channels have demonstrated that the modification of the guanidinium toxin binding site can be separated from a reduction in current. Rack and Woll (1984) were the first to show that the highly carboxyl specific reagent N-ethoxy-carbonyl-2-ethoxy-1,2-dihydroquinoline (EEDQ) reduced the whole cell Na^+ current without affecting TTX binding. Later, Gülden and Vogel (1985) showed that exposure of the toad node of Ranvier to TMO resulted in a decrease in TTX affinity, a decrease in macroscopic I_{Na} , and a slower inactivation time constant. However, simultaneous exposure of channels to TTX and TMO reduced I_{Na} and the inactivation rate but failed to reduce the TTX binding affinity. Removal of the TTX followed by reexposure to TMO lowered the current further and reduced the TTX binding affinity without further changes in the inactivation rate. The ability to dissociate these effects implies that multiple carboxyl groups are modified. Further, Chabala et al. (1986) were able to demonstrate two discrete conductance decreases without modification of TTX affinity suggesting that there are at least three carboxyl groups accessible to modification. In our results, the finding of two lower γ_{Na} implies that TMO caused two distinct modifications of the cardiac Na^+ channel.

Low Amplitude Openings

TMO-treated myocytes exhibited openings to three unitary current levels within a single patch exposed to 2 mM Ca^{2+} . The levels were 55, 86, and 95% of the control unitary current at -50 mV. Our results are consistent with brief reports on reconstituted, BTX-treated nerve Na^+ channels in which TMO (Cherbavaz, 1990) and WSC (Chabala et al., 1986) cause at least two reductions in γ_{Na} in the absence of Ca^{2+} . In contrast, low amplitude events were undetected when pipette Ca^{2+} was elevated to 10 mM. One possible explanation is that

high Ca^{2+} might preferentially reduce the rate of opening to the lower current levels. However, the enhanced Ca^{2+} block reduces the signal-to-noise ratio making the detection of low amplitude events more difficult. If the ratio of current amplitudes remained the same in 10 mM as in 2 mM Ca^{2+} , the signal-to-noise ratio should have been sufficient to allow detection of low amplitude events, at least at more negative potentials. Alternatively, low amplitude events in 2 mM Ca^{2+} could occur because Ca^{2+} block is *enhanced* in modified channels. In that case, unitary currents might be too small to detect in 10 mM Ca^{2+} .

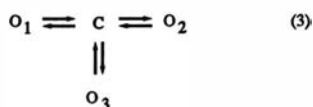
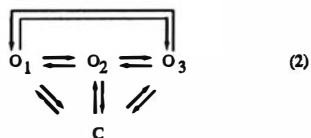
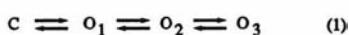
It is unlikely that the subconductance states seen in our experiments can be explained by previously described subconductance levels. In our experiments, low amplitude events were considerably more common than those reported previously and clearly had a shorter MOT than control channels. Furthermore, only two levels of unitary current have been reported in unmodified cardiac (Cachelin et al., 1983; Kunze et al., 1985; Scanley and Fozzard, 1987; Patlak, 1988) and skeletal muscle (DeCino and Kidokoro, 1985) Na^+ channels in their native membranes. Although the rarity of low amplitude events precluded complete analysis, the spontaneously occurring second current level is 60% of the more common level in neonatal rat ventricle, and the MOT is the same or less than that of the more common event (Cachelin et al., 1983; Kunze et al., 1985). In dog Purkinje fibers, the smaller unitary current is 33% of the more common level, and based on limited analysis, the kinetics of the two states appear similar (Scanley and Fozzard, 1987). Cultured neuroblastoma cells show openings to 80% and 50% of the most commonly observed level (Nagy et al., 1983). The smallest openings are exceedingly rare, and the middle level varies considerably from patch to patch. In contrast to the rarity of low amplitude openings in unmodified channels, openings to multiple levels occur frequently in Na^+ channels treated with agents that inhibit inactivation (Chinn and Narahashi, 1986; Garber and Miller, 1987; Green et al., 1987a; Nagy, 1987a and b; Urban et al., 1987; Chinn, 1988; Nilius et al., 1989; Schreibmayer et al., 1989).

Our results also are unlikely to be explained by an observation of Patlak (1990), who noticed slowly developing multiple amplitude events when the cytoplasm of ventricular myocytes was acidified for 10 - 15 min. Although TMO liberates protons on hydrolysis, the reaction solution initially was pH 8, was buffered by 100 mM HEPES, and the pH fell to only 7.3 during the reaction. Furthermore, the cells were washed after a 10 min exposure to TMO, resuspended in pH 7.4 media, and incubated for at least one hour prior to use.

Are multiple unitary current levels substates or unique populations of modified channels?

Because there was more than one Na⁺ channel in each of the patches studied, multiple opening levels after modification can be explained either by the opening of individual channels to multiple substates or by modifications that create several populations of channels each opening to a distinct current level. Transitions between higher and lower conductance states have been advanced as one method of identifying substates.

For purposes of illustration of substate behavior, consider a model with only one closed state and three open states. Several classes of kinetic schemes can be drawn:



where C is the closed state and O₁, O₂, and O₃ represent open states with different current levels. If rate constants for the transitions are stable, all three schemes predict a constant proportion of O₁, O₂, and O₃ from patch to patch. Recorded with a sufficient bandwidth, scheme 1 predicts that openings to O₁ would always precede and follow sojourns in O₂ and

O₃. In scheme 2, the channel can open to and close from any current level. Again, transitions between states would be detected. Meves and Nagy (1989) point out that there is evidence for schemes analogous to 1 and 2 with only two open states in Na⁺ channels exposed to agents which inhibit inactivation. The absence of transitions between open states may not rule out the existence of substates, however. In contrast to schemes 1 and 2, transitions between substates are absent in scheme 3.

I never detected transitions among the three open current levels in TMO-treated patches despite the fact that the mean dwell times in each open state were long enough to resolve clearly. This strongly argues against substates arranged as schemes 1 and 2 but does not rule out scheme 3. On the other hand, the proportion of openings to each current level varied greatly from patch to patch (see Figure 11). Such variability is incompatible with all three classes of models. Consequently, it seems reasonable to suggest that the three levels of openings represent different populations of channels. The lower conductance states may represent either sequential modifications of the same channel or two entirely different modifications of separate channels.

Carboxyl Reagents' Mechanism of Action

Contrary to the conclusions of Worley et al. (1986), our results indicate that changes in the surface potential cannot explain all of the effects of carboxyl modification. Elevation of Ca²⁺ and the elimination of surface charge with modification should have analogous effects on the transmembrane potential gradient, yet the two experimental manipulations resulted in opposing changes in the rate of O→I transitions at depolarized potentials (see Figure 14). One can infer from this divergence that the effect of modification on gating is likely to result at least in part from a conformational change. A conformational change of the Ca²⁺ binding site in relation to the selectivity filter carboxyl group could explain the pK_a shift seen by Spalding (1980) without invoking the hypothesis that TMO directly modifies a carboxyl group in the

ion permeation pathway. Conformational changes in the Na^+ channel may also explain the correlation in nerve between TTX affinity and Ca^{2+} block (Salgado et al., 1986; Worley et al., 1986) and TTX affinity and γ_{Na} (Noda et al., 1989).

Are decreases in conductance also the result of allosteric effects? Although both TMO and WSC must have eliminated negative charges, a reduction of γ_{Na} in 10 mM Ca^{2+} was noted in channels pretreated with WSC, but γ_{Na} was unaffected by TMO. Assuming the same carboxyl groups are modified, this suggests that a reduction in the local potential is insufficient to decrease γ_{Na} and that WSC also must induce a conformation change. Divergence of the effects of these agents on γ_{Na} also may result from the propensity of WSC to induce crosslinking (Baker and Rubinson, 1975). Cherbavaz (1990) also suggested that a reduction in surface potential cannot explain the TMO-induced decrease in γ_{Na} . She found that the ratio of γ_{Na} at different Na^+ concentrations and ionic strengths was unaffected by TMO. In contrast, an agent that reduces γ_{Na} only by altering the surface potential should have a smaller effect at higher ionic strengths because of shielding.

In summary, I have observed that the effects of carboxyl modification of cardiac Na^+ channels is different from that of nerve Na^+ channels. This difference, along with the other known biophysical and amino acid sequence differences, should help to refine structural models of various Na^+ channels. Furthermore, the results of group-specific modification suggest future directions for site-directed mutagenesis experiments.

CHAPTER 3

ACUTE EXPOSURE TO 3,5,3'-TRIIODO-L-THYRONINE INCREASES BURSTING OF CARDIAC SODIUM CHANNELS

ABSTRACT

Burst mode gating of single cardiac Na⁺ channels contributes to the slowly inactivating macroscopic Na⁺ current (I_{Na}) and to a prolongation of the action potential, yet under normal conditions, bursts carry only a modest amount of the total I_{Na} . In single channel recordings from isolated rabbit ventricular myocytes, physiological concentrations of 3,5,3'-triiodo-L-thyronine (T_3) increased bursting as measured by the ratio of long events (LE) to the total number of events. A long event was defined as a set of openings with a total duration of $\geq 5 \times$ the control mean open time (MOT) for cell-attached patches and with no intervening closings $> 250 \mu s$. In the cell-attached patch configuration, addition of 5 nM T_3 to the pipette increased the %LE at all potentials examined. The increase had a biphasic voltage-dependence and peaked at -50 mV, although the largest percentage change from control occurred between -30 and -40 mV. A similar increase in the %LE occurred with 50 nM T_3 suggesting saturation at ≤ 5 nM. There was no evidence of a change in unitary conductance or MOT with the increase in bursting. Long events sometimes were grouped into runs, but the more usual pattern suggested that modal shifts occurred in ~ 1 s. To investigate the possible involvement of a second messenger, cell-attached recordings were made with and without T_3 added to the bath. Addition of either 50 or 100 nM T_3 to the bath failed to alter the MOT, unitary current, or %LE. Na⁺ channel gating also was unaffected by patch excision or by addition of 50 nM T_3 to the cytoplasmic face of inside-out patches. Nevertheless, with 5 nM T_3 in the pipette, patch excision to the inside-out configuration caused a dramatic increase in the %LE, especially near the threshold potential, and an increase in the MOT. A shift in the current-voltage relationship (i/V), without a change in the single Na⁺ channel conductance (γ_{Na}), accompanied the increase in bursts with excision. These results suggested that T_3 was not membrane permeable during the time scale of the experiments (~ 15 min) and that T_3 's action required close proximity to the extracellular face of the Na⁺ channel. T_3 -

induced bursting may have been caused by direct binding to the channel, receptor-mediation, or a generalized sarcolemmal membrane disruption. A shift toward prolonged openings may contribute to the propensity for arrhythmias in hyperthyroidism.

INTRODUCTION

For some time, thyroid hormone has been known to modulate cardiac electrophysiological properties. Chronic hyperthyroidism shortens the action potential duration (Freedberg et al., 1970; Johnson et al., 1973; Sharp et al., 1985) and increases the whole cell Ca^{2+} and K^{+} currents (Binah et al., 1987). These effects seem to be independent of the modulation of the autonomic nervous system by hyperthyroidism (Margolius and Gaffney, 1965; Cairoli and Crout, 1967; Aoki et al., 1972; Johnson et al., 1973, El Shahawy et al., 1975). Thyroid hormone's action generally is thought to require protein synthesis. However, recent evidence suggests that 3,5,3'-triiodo-L-thyronine (T_3) has specific cardiac membrane binding sites and can immediately influence the sarcolemmal calcium-ATPase (Rudinger et al., 1984), adenylate cyclase (Levey and Epstein, 1969; Will-Shahab et al., 1976), the number of β - and α -adrenergic receptors (Chang and Kunos, 1981), and 2-deoxyglucose transport (Segal, 1989b; Segal, 1989c; Segal, 1990a; Segal, 1990b). Studies on plasma membrane T_3 receptors and the extranuclear effects of T_3 were reviewed recently by Segal (1989a).

Evidence is accumulating that Na^{+} channels are modulated by a number of hormones and other endogenous substances. The best studied example is that of adrenergic agonists. In whole cell recordings, β -receptor stimulation alters the peak macroscopic Na^{+} current (I_{Na}) in cardiac preparations. There is considerable variability in the direction of the effect, however. Several investigators have seen an increase (Murray et al., 1990; Lee et al., 1990; Tytgat et al., 1990; Matsuda et al., 1991) while others have reported a decrease in the peak I_{Na} after application of isoproterenol (Hisatome et al., 1985; Ono et al., 1989; Schubert et al., 1989; Schubert et al., 1990; Sculptoreanu et al., 1991). These divergent results may depend on the holding potential (Schubert et al., 1989; Lee et al., 1990; Schubert et al., 1990), the internal Ca^{2+} concentration (Murray et al., 1990), or the basal level of Na^{+} channel phosphorylation (Matsuda et al., 1991). The soluble second messenger cyclic adenosine monophosphate

(cAMP) has been implicated in the regulation of cardiac Na⁺ currents. Forskolin, nonhydrolyzable analogs of cAMP, and cAMP phosphodiesterase inhibitors approximate the action of isoproterenol. In addition to an indirect effect on the Na⁺ channel through cAMP, Brown and his coworkers (Schubert et al., 1989; Schubert et al., 1990) have proposed that the G protein, G_β, directly inhibits rat heart Na⁺ channels by a membrane limited process. Another report has implicated at least two G proteins in the modulation of brain Na⁺ channels expressed in *Xenopus* oocytes (Cohen-Armon et al., 1989). Experiments with phorbol compounds and diacylglycerols have pointed to protein kinase C as another possible modulator of Na⁺ channels (Moorman et al., 1989; Numann et al., 1991).

A number of other endogenous substances affect Na⁺ channels. Angiotensin II increases the probability of single channel openings in neonatal rat ventricle (Moorman et al., 1989). Forskolin (Ono and Fozzard, 1991), lysophosphatidylcholine (Burnashev et al., 1989), a soluble diacylglycerol (Numann et al., 1991), and two glycolytic pathway metabolites (Kohlhardt et al., 1989) alter Na⁺ channels by inducing prolonged openings or bursts at the single channel level.

Here, I report that acute exposure to T₃ increased bursting by rabbit ventricular Na⁺ channels. Preliminary results have been reported elsewhere in abstract form (Dudley and Baumgarten, 1991b).

METHODS

Cell Isolation Procedure

Ventricular myocytes were isolated from New Zealand white rabbits (1.5-2.5 kg) by a collagenase-protease digestion procedure (Poole et al., 1989). After removal from the animal, hearts were perfused retrogradely on a Langendorff apparatus for 4 min with a warm (37°C) modified Tyrode's solution containing 0.75 mM CaCl₂. Tyrode's solutions consisted of (in mM): 130 NaCl, 20 taurine, 10 creatine, 5.4 KCl, 0.4 NaH₂PO₄, 3.5 MgCl₂, 5 N-2-hydroxyethylpiperazine-N'-2-ethanesulfonic acid (HEPES), 10 glucose, and CaCl₂ as noted (titrated to pH 7.25 with NaOH and bubbled with 100% O₂). After rinsing with a nominally Ca²⁺-free Tyrode's solution supplemented with 100 μM ethyleneglycol-bis-(β aminoethyl-ether) N,N,N',N'-tetraacetic acid (EGTA), a low Ca²⁺ Tyrode's solution containing 1 mg/ml collagenase (type II; Worthington Biomedical, Freehold, NJ), 0.1 mg/ml protease (pronase E, type XIV; Sigma, St. Louis, MO), and 80 μM added Ca²⁺ (total Ca²⁺ ~200 μM) was recirculated for 15 min. Then, the ventricles were isolated, cut into small pieces (~5 × 5 mm), and divided among three flasks containing 3 ml of the enzyme solution with the addition of 10% bovine serum albumin. The flasks were gently shaken for up to 15 min in a Dubnoff metabolic shaking incubator maintained at 37°C. Single myocytes were separated from the undigested material by filtration through nylon gauze (250 μm pore size). Isolated cells were washed twice and stored at room temperature in a Kraft-Bruhe solution containing (in mM): 88 KOH, 80 glutamic acid, 11 glucose, 10 taurine, 10 KH₂PO₄, 10 HEPES, 0.5 EGTA, 2.5 KCl, 1.8 MgSO₄ (titrated to pH 7.2 with 1 N KOH). This procedure consistently yielded >70% Ca²⁺-tolerant, rod-shaped cells.

Addition of T₃ and TAA

The standard pipette and bath solutions consisted of (in mM): 280 NaCl, 2 CaCl₂, 10 HEPES (pH = 7.4) and 140 K-aspartate, 10 EGTA, 5 HEPES (pH = 7.4), respectively. The

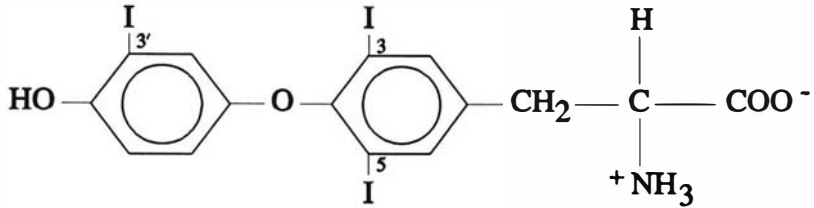
high Na^+ concentration in the pipette solution increased the signal-to-noise ratio and improved the resolution of channel openings and kinetics. The bath solution depolarized the cell membrane in series with the cell-attached patches to near 0 mV. A 10 μM stock solution of 3,5,3'-triiodo-L-thyronine (T_3 ; Sigma, St. Louis, MO; purity ~98%) was made fresh each day and stored at 4°C. T_3 was solubilized by addition of 3-4 drops of either 1 N NaOH or KOH depending on whether the stock solution was to be added to the pipette or bathing solutions. Either 5, 50, or 100 μl were added to 10 ml of pipette or bathing solution for a final concentration of 5, 50, or 100 nM T_3 . A 10 μM stock solution of triiodothyroacetic acid (TAA; Sigma; purity ~95%) was made in an analogous fashion to that of T_3 except that alkalization was not necessary. TAA was added to the pipette solution giving a final concentration of 50 nM. The chemical structure of T_3 and TAA are shown in Figure 17.

The experimental chamber was pretreated with 5 $\mu\text{g}/\text{ml}$ human fibronectin (Collaborative Research Inc., Bedford, MA) and 100 $\mu\text{g}/\text{ml}$ poly-L-lysine hydrobromide (Sigma; MW > 300,000) in order to affix cells to the chamber floor. Omission of fibronectin did not affect the results. Bathing solutions were cooled to $10 \pm 1^\circ\text{C}$ during passage through ~50 cm of polyethylene tubing embedded in an aluminum block attached to a Peltier device. Solution changes were effected by an electronically-controlled 4-way valve mounted on the microscope stage. The valve's output was directed at the test cell through a glass pipette, and the solution flow rate was ~1 ml/min. With this perfusion system, solution changes occurred within < 5 s. The bath volume was maintained at ~500 μl by aspiration.

Single Channel Recordings

Unitary Na^+ channel currents were measured with a List EPC-7 patch clamp amplifier in the cell-attached and inside-out patch configurations (Hamill et al., 1981). Experimental conditions which minimized the number of channels in a patch were employed. The patch electrodes were pulled from 7740 Corning Pyrex borosilicate glass (Glass Co. of America,

Triiodo-L-thyronine



Triiodothyroacetic Acid

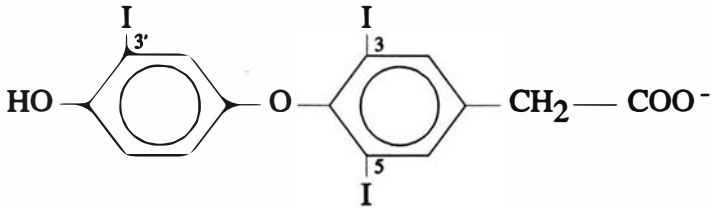


Figure 17. The chemical structures of triiodo-L-thyronine (T_3) and triiodothyroacetic acid (TAA). T_3 is amphipathic and zwitterionic at physiological pH. TAA also is amphipathic but is anionic at physiological pH.

Bargaintown, NJ), coated twice with Sylgard 184 (Dow Corning, Midland, MI) to improve their capacitive properties, and heat polished. Resultant electrode tip resistances were 5-10 M Ω when filled with the standard pipette solution. Patches made using these electrodes typically contained 2-4 channels.

Pulse protocols, data acquisition, and analysis were computer directed by programs written in ASYST (Keithley, Rochester, NY). In all but two patches, the holding potential was -130 mV, and step depolarizations 45 ms in duration were applied at 1 Hz. Current records were digitized at 10 kHz (12 bits) after filtering at 2 kHz (-3 dB, 8-pole Bessel). Capacity transients were canceled by a combination of analog circuitry and subtraction of averaged null sweeps. The baseline current was set to 0 pA sweep-by-sweep to adjust for any changes in the leak current. The half-amplitude threshold criterion was applied in assigning openings. To eliminate the effect of filtering ($t_{50-90} \approx 0.08$ ms) on unitary current determinations, open channel amplitude histograms were calculated after excluding the first and last points above threshold.

To quantify the increase in bursting seen with T₃, groups of openings separated by closing of ≤ 250 μ s were considered to be part of the same event. If the sum of the open and closed times of an event exceeded 5-times the mean open time (MOT) for control channel at the same voltage, the group was considered as a single long event (LE). Openings ≥ 5 -times the control MOT without apparent interruptions were also considered LEs. These openings may represent either a single sojourn in the open state or a burst of openings with intervening closings that were too brief to detect.

LEs were a relatively rare occurrence. Testing for significant nonrandom clustering of the sweeps containing similar gating was performed by a runs analysis (Horn et al., 1984; Grant and Starmer, 1987; Nilius, 1988b; Moorman et al., 1990). A group of uninterrupted,

sequential sweeps containing similar gating (i.e., LEs or no LEs) was considered as a run. A Z value was calculated based on the formula

$$Z = \frac{R_{\text{obs}} - R_{\text{pred}}}{\sigma} = \frac{R_{\text{obs}} - 2Np(1 - p)}{2\sqrt{N}p(1 - p)}$$

where R_{obs} is the observed number of runs, R_{pred} is the number of predicted runs based on a binomial probability of occurrence, σ is the standard deviation, N is the total number of sweeps, and p is the relative frequency of sweeps containing the property of interest (i.e., the number of sweeps with LEs / total number of sweeps). A Z value of < -1.64 indicated significant undermixing of sweeps with different types of gating at the 5% level (one-tail). Experiments with $R_{\text{obs}} < 10$ were excluded since the approximation to a normal distribution is untenable.

Statistical analyses of multiple, unpaired observations were carried out using two-way analyses of variance (ANOVA). Reported γ_{Na^+} s were based on weighted linear least squares fits and were compared by a Student's t test for homogeneity or by a one-way ANOVA and an F-ratio test. MOTs were based on a monoexponential least squares fit to the open time histograms. A paired t test was used to assess the effect of a treatment upon a single patch. *A priori* multiple comparisons of means were performed with a Fisher's protected least significant difference test. Nonlinear curves were fitted by the DUD method with PROC NLIN (SAS Institute, Cary, NC) or by the Marquardt method in ASYST. Measured values are reported as means \pm SE.

RESULTS

The Effect of T₃ on Na⁺ Channel Gating in Cell-Attached Patches

Cardiac Na⁺ channel gating was altered by the addition of T₃ to the pipette solution. Figure 18 compares typical, consecutive current records at steps to -50 mV from cell-attached patches with or without T₃ in the pipette. Panel A shows the typical unitary current and gating behavior for cardiac Na⁺ channels exposed to 280 mM Na⁺ and 2 mM Ca²⁺. Panel B displays sweeps recorded from a separate patch with 5 nM T₃ in the pipette solution. Channels exposed to T₃ typically exhibited two types of unitary events. One population of openings appeared like those in control patches, and a second population exhibited bursting (i.e., prolonged openings interrupted by brief closings). From the time of seal formation, the onset of bursting was consistently less than the time required to adjust the capacity compensation and initiate recording (i.e., <30 s). This modification of gating was considerably faster than the time required for appearance of the earliest DNA transcription product induced by T₃ (Oppenheimer, 1985), implying that the observed effects were independent of the hormone's nuclear effects. Once induced, bursting continued for the duration of the experiment (up to 30 min). Occasionally, however, channels exposed to extracellular T₃ failed to display any obvious change in gating behavior. Patch excision has been reported to increase bursting (Horn and Vandenberg, 1986; Nilius, 1988b; Kirsch and Brown, 1989). Therefore, I verified to the extent possible that patches remained cell-attached throughout the experiment by visual inspection upon withdrawing the electrode and by the lack of a characteristic shift in the *i/V* relationship upon excision (*vide infra*).

At times, the bursts induced by 5 nM T₃ in the pipette clustered together. Figure 19A shows consecutive traces recorded from steps to -30 mV in a cell-attached patch. In the first several traces of this multichannel patch, a single Na⁺ channel appears to remain open for tens of milliseconds after the initial collection of openings. Then, there is an intervening interval

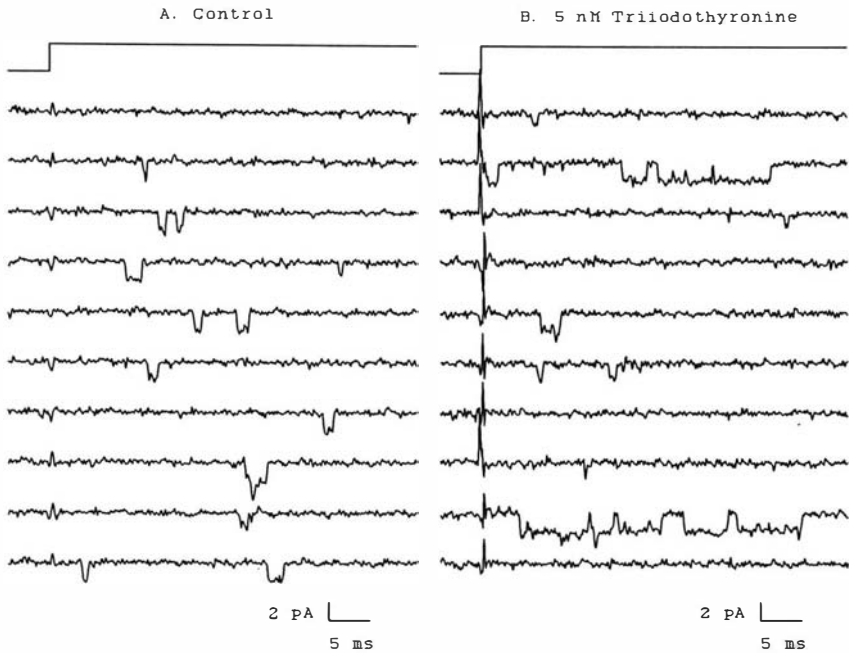


Figure 18. Consecutive current traces at -50 mV from cell-attached patches with and without 5 nM T_3 in the pipette solution. *Panel A:* Typical control recordings with a pipette solution containing 280 mM Na^+ and 2 mM Ca^{2+} . *Panel B:* T_3 resulted in a second population of long openings with burst mode gating behavior (sweeps 2 and 9). The induction of bursting occurred as fast as recording could be initiated, within ~ 30 s of seal formation. Depolarizing steps 45 ms in duration were applied at 1 Hz. The step function above each set of sweeps indicates the timing of the voltage step.

showing the usual gating pattern followed by one channel returning to the burst mode. The tendency for bursts to cluster is consistent with past observations on unmodified patches (Grant and Starmer, 1987; Nilius, 1988b; Kirsch and Brown, 1989; Moorman et al., 1990). In the presence of T_3 , the grouping of bursts was relatively uncommon, and the rapid switching of gating modes shown in Figure 18B predominated. To determine if the clustering trend was significant, I performed a runs analysis (Horn et al., 1984; Grant and Starmer, 1987; Nilius, 1988b; Moorman et al., 1990). Sweeps were divided into two classes, records containing at least one LE and records without any LEs. Sweeps without a LE included records without openings and records containing openings or bursts with a duration of < 5 control MOTs. In unmodified cell-attached patches, 0 of 17 experiments showed statistically significant clustering of sweeps containing LEs whereas 7 of 12 experiments showed clustering with 5 nM T_3 in the pipette. When pipette T_3 was increased to 50 nM, only 1 of 8 experiments demonstrated clustering. The decrease in clustering at higher T_3 concentrations may reflect experimental variability, an acceleration of modal shifts beyond the frequency detectable in our experiments, or a tendency toward a diminution of T_3 's immediate effects at high concentrations (Segal, 1989a). Since I recorded traces at 1 Hz, the moderate level of clustering with 5 nM T_3 suggested that the duration of the bursting mode usually was ~ 1 s.

Another feature demonstrated by the records in Figure 19A is the transition from the typical unitary current to a lower level within a burst. The smaller current level was a sporadic finding. I infrequently observed openings to or closings from this state, and I did not observe this current level outside a burst. This suggests that the lower current level represents a substate closely associated with burst mode gating. The relative rarity of the low amplitude events precluded quantitative analysis. A substate during bursting also can be seen in recordings from unmodified Na^+ channels (Kohlhardt et al., 1987; Nilius, 1988b) and has been reported to constitute $\leq 5\%$ of the burst duration (Patlak and Ortiz, 1989).

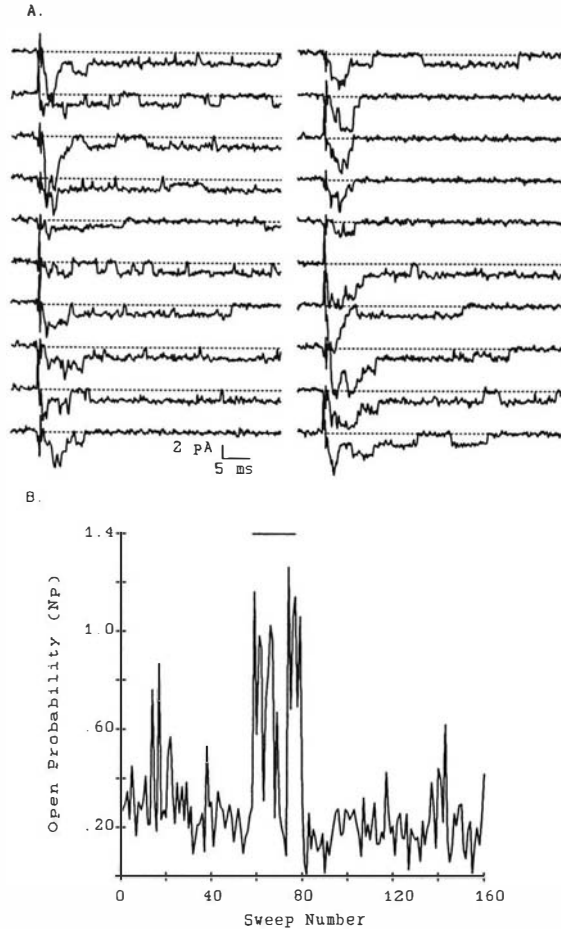


Figure 19. Current traces and open probability diary showing runs of bursts in the presence of 5 nM T_3 . *Panel A:* Twenty consecutive traces recorded at -30 mV from a cell-attached patch show grouping of bursts. In this multichannel patch, a single Na^+ channel remained open for tens of milliseconds. Normal gating (sweeps 12-15) intervened between runs of bursts (sweeps 1-11 and 16-20). The dotted line represents the closed, zero current level. Long runs were relatively uncommon, however, and rapid shifts of gating modes as in Figure 18A were more typical of the effect of T_3 . Also, note the occurrence of transitions between the main conductance level and a lower conductance state in sweeps 4 and 8. *Panel B:* Open probability multiplied by the number of channels in the patch (Np) per sweep as a function of the sweep number for the same patch as panel A. Between sweeps 11-22 and 59-79, Np was markedly elevated. The horizontal line demarcates the sweeps shown in panel A.

In Figure 19B, the open probability per sweep is shown for the same patch illustrated in panel A. The open probability (Np) was defined as the time channels were open as a fraction of the test pulse duration (45 ms) and was equivalent to the number of channels in a patch (N) multiplied by the open probability of a single channel (p). Since the patch shown had multiple channels, Np occasionally exceeded unity. Consistent with a grouping of bursts, the Np shows a marked elevation between sweeps 50 and 79 and a less impressive grouping between sweeps 11 and 22.

The effect of T_3 on unitary conductance also was evaluated. Open channel amplitude histograms were well fitted by a single Gaussian function in control patches as well as patches exposed to 5 or 50 nM T_3 in the pipette. Figure 20A shows the i/V relationships constructed from the amplitude histograms. Channels exposed to T_3 exhibited no change in γ_{Na} or reversal potential (E_{rev}) from control values. The γ_{Na} s were 18.5 ± 0.9 pS, 15.5 ± 1.0 pS, and 17.5 ± 2.0 pS in control patches (\blacklozenge) and patches exposed to 5 (\blacktriangle) or 50 nM T_3 (\blacksquare), respectively. As compared with control, there was no significant effect on γ_{Na} of 5 ($p = 0.26$) or 50 nM T_3 ($p = 0.67$). Extrapolated E_{rev} s of 81.3 ± 8.2 mV ($p = 0.16$) and 66.3 ± 10.9 mV ($p = 0.70$) for channels exposed to 5 or 50 nM T_3 , respectively, also were not statistically different from an E_{rev} of 59.6 ± 7.8 mV for control channels. Thus, T_3 -modified channels appeared to have the same conductance properties as control channels.

Figure 20B depicts the voltage-dependence of the dwell time in the open state. The biphasic MOT-voltage relationship of control cardiac Na^+ channels (\blacklozenge ; Kirsch and Brown, 1989; Scanley et al., 1990; Dudley and Baumgarten, 1991a) remained unchanged in cell-attached patches exposed to either 5 (\blacktriangle ; $p = 0.82$) or 50 nM T_3 (\blacksquare ; $p = 0.22$). Even in the presence of bursting, I found that a single exponential was sufficient to describe the open time distribution for openings < 10 ms in duration. Too few longer events were detected for a reliable biexponential fit to the data over a wider range. A monoexponential open time distribution is consistent with other reports from unmodified cell-attached patches in the

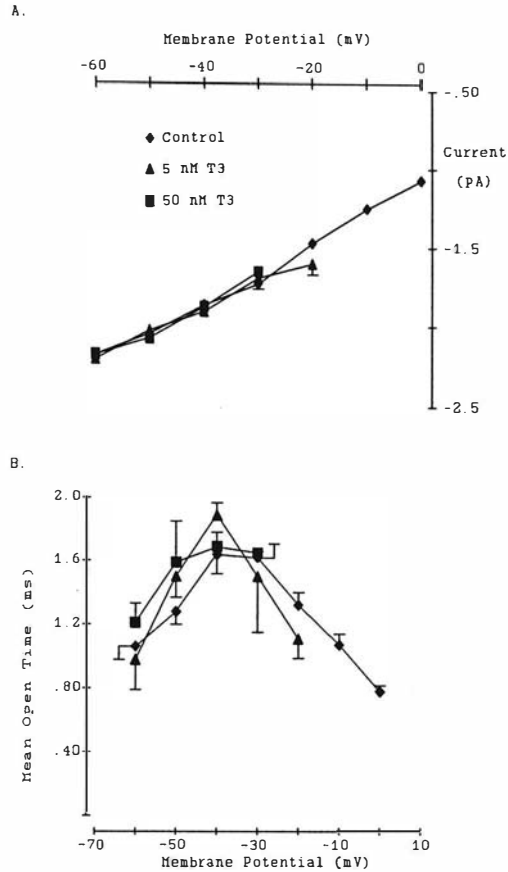


Figure 20. The effect of T₃ in the patch pipette on unitary current and mean open time (MOT) in cell-attached patches. Panel A shows the unitary current-voltage relationship in cell-attached patches under control conditions (◆) and with either 5 (▲) or 50 nM (■) T₃ in the pipette solution. As compared with control, there was no statistically significant effect on unitary current of either 5 ($p = 0.26$) or 50 nM T₃ ($p = 0.67$). The unitary conductance of control Na⁺ channels was 18.5 ± 0.9 pS and was 15.5 ± 1.0 pS and 17.5 ± 2.0 pS in patches exposed to 5 or 50 nM T₃, respectively. As shown in panel B, neither 5 (▲; $p = 0.92$) nor 50 nM T₃ (■; $p = 0.22$) significantly altered the biphasic MOT-voltage relationship as compared with control. Therefore, the MOT was unaffected by the number of bursts induced by T₃. In both panels, data points represent the means of up to 18 experiments, and error bars (\pm SE) are shown when they exceed the symbol size.

presence of bursts (Kunze et al., 1985; Patlak et al., 1986; Grant and Starmer, 1987; Kiyosue and Arita, 1989; Nilius, 1988b; Moorman et al., 1990). Some investigators, however, have found evidence for a biexponential open time distribution in unmodified cell-attached (Patlak and Ortiz, 1986; Kirsch and Brown, 1989) or excised patches (Nilius, 1988b; Josephson and Sperelakis, 1989) displaying bursts. Figure 20B also suggests that the MOT calculated from all of the openings in a patch is relatively insensitive to the number of bursts. However, when analyzed separately, openings within bursts in unmodified channels usually have longer MOTs than openings outside bursts (see Discussion; Patlak and Ortiz, 1985; Patlak and Ortiz, 1986; Grant and Starmer, 1987; Kohlhardt et al., 1987; Kiyosue and Arita, 1989; Moorman et al., 1990).

The effect of 5 (▲) or 50 nM T_3 (■) in the pipette on the %LE (long events/total number of events \times 100) as a function of voltage in cell-attached patches is shown in Figure 21. Assuming that the control open time distribution was monoexponential, the predicted number of %LE is $\exp(-5 \cdot \text{MOT}/\text{MOT})$ or 0.67%. The actual %LE observed in control patches was 2.5% at -60 mV and decreased to 1.2% at -10 mV. The discrepancy probably resulted from missed closings, inclusion of openings and closings of separate channels in close proximity, and occasional bursting in control records. Using a similar definition for a burst, Nilius (1988b) reported 2.8% of depolarizations of unmodified patches in the cell-attached mode elicited bursts. As compared with control, addition of either 5 ($p < 0.01$) or 50 nM T_3 ($p < 0.01$) resulted in an abrupt increase in the %LE. There was no difference in the effect of 5 or 50 nM T_3 ($p = 0.97$), and therefore, the response to T_3 appeared to saturate at < 5 nM. This saturation level is consistent with a maximal acute increase in 2-deoxyglucose uptake at 1 nM T_3 (Segal, 1989b; Segal, 1990a; Segal and Ingbar, 1989) and a maximal acute stimulation of the rabbit cardiac sarcolemmal calcium-ATPase activity at 100 pM (Rudinger et al., 1984). While the largest %LE with T_3 occurred near threshold, the greatest increase from controls occurred at -30 to -40 mV. Consequently, there

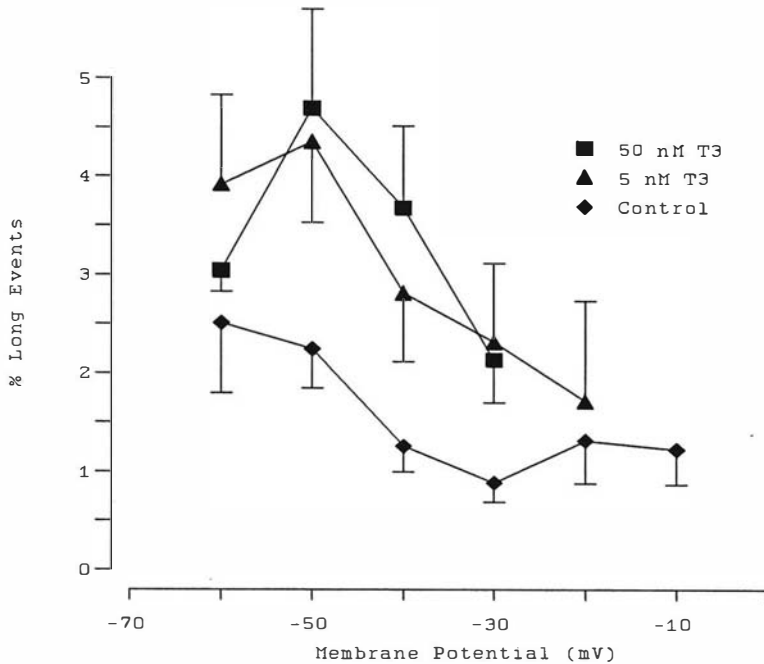


Figure 21. Effect of T_3 in the pipette on percent long events (%LE) as a function of voltage in cell-attached patches. Events were defined as a group of openings with intervening closed intervals $\leq 250 \mu s$. To be considered as a LE, the total duration of a single opening or an event must exceed $5 \times$ the MOT for control channels at the same voltage. The %LE was calculated as the ratio of LEs to the total number of events multiplied by 100. The %LE was significantly greater than in control with either 5 (\blacktriangle ; $p < 0.01$) or 50 nM T_3 (\blacksquare ; $p < 0.01$) in the pipette. The effects of 5 and 50 nM T_3 on %LE were statistically indistinguishable ($p = 0.97$) indicating saturation at ≤ 5 nM. While the largest value of %LE occurred near threshold, the largest deviations from control were at -30 to -40 mV.

was a striking difference in the voltage dependence of the %LE between control channels and channels exposed to extracellular T_3 . With T_3 in the pipette, the %LE was biphasic and reached a maximum at -50 mV while the %LE of control patches seemed to decrease from -60 to -40 mV and remain unchanged at more positive potentials.

Extracellular TAA, an analog of T_3 which does not induce DNA transcription (DeNayer, 1987), also increased the %LE in a manner similar to T_3 . The voltage dependence of the %LE with 50 nM TAA (\blacktriangledown) in pipette is shown in Figure 22 and is comparable to that of 50 nM T_3 (\blacksquare). There was considerable variability in the effect of TAA, however. Therefore, only the %LE at -40 mV was significantly different from that of control channels (\blacklozenge ; $p < 0.05$). The fact that TAA induced bursting also suggests that this behavior is independent of the cell's nucleus.

There are many reports suggesting a slowly inactivating component of the cardiac macroscopic I_{Na} (Reuter, 1968; Brown et al., 1981; Patlak, 1984; Carmeliet, 1987; Follmer et al., 1987). Single channel studies have correlated the late Na^+ current with late reopenings which come in two forms, brief background openings and bursts (Kunze et al., 1985; Patlak and Ortiz, 1985; Patlak and Ortiz, 1986; Grant and Starmer, 1987; Kohlhardt et al., 1987; Kiyosue and Arita, 1989; Josephson and Sperelakis, 1989; Moorman et al., 1990). Bursts contribute up to 85% of the slowly inactivating I_{Na} (Patlak and Ortiz, 1986). As might be expected with an increase in bursting, ensemble average current decays with T_3 in the pipette showed a second, slow decay rate. Figure 23A shows a typical ensemble average at -30 mV from a patch exposed to T_3 in the pipette. The dashed line represents the least squares fit to a single exponential. The current decay is better described by the sum of two exponentials as shown by the solid line. The time constants of this decay were 3.7 ± 0.1 ms and 21.5 ± 2.7 ms. The presence of two components of the decay was confirmed by the bend in the semilogarithmic plot of the ensemble (panel B). In this example, the amplitude of the slower component was only 2.5% of that of the faster component. A second, slow component

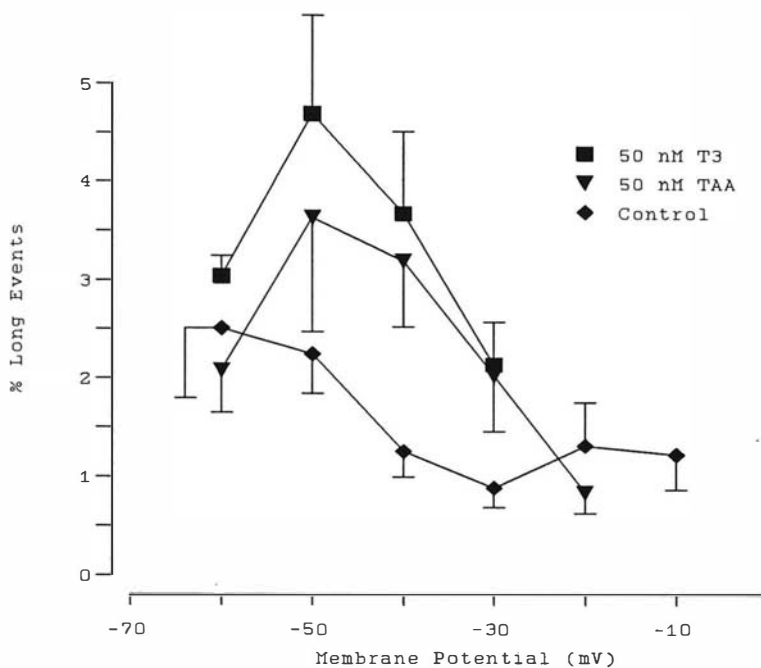


Figure 22. Effect of triiodothyroacetic acid (TAA) in the pipette on the %LE as a function of voltage in cell-attached patches. The %LE for control (◆) and the 50 nM T₃ (■) are repeated from Figure 21. TAA is an analog of T₃ that does not stimulate DNA transcription. Addition of 50 nM TAA (▼) to the extracellular face of the Na⁺ channel increased the %LE. Because of the high degree of variability in the effect of TAA, only the value at -40 mV was significantly different from control ($p < 0.05$). The increase in %LE with thyroid hormones does not appear to have the same specificity as the nuclear thyroid hormone receptor.

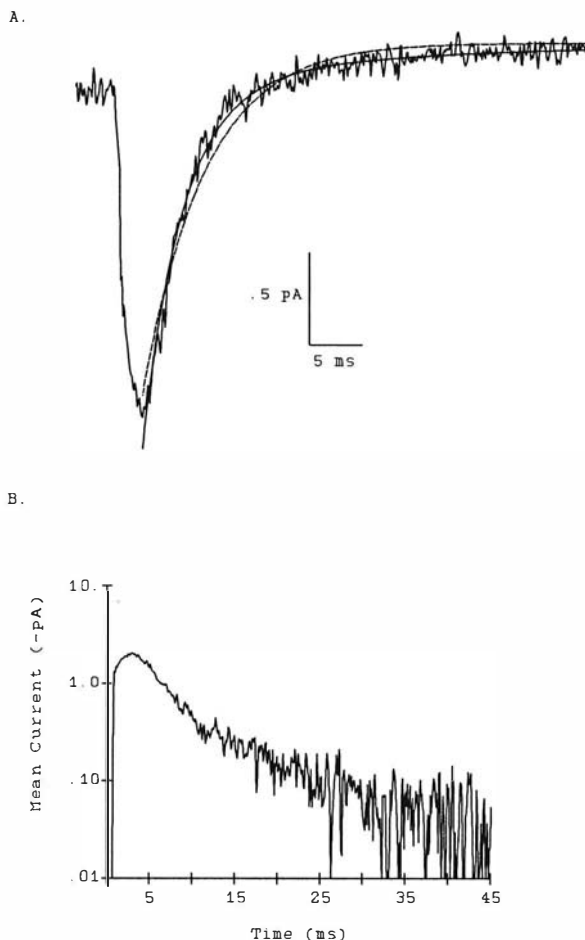


Figure 23. Ensemble average of single channel currents from a cell-attached patch with 5 nM T_3 in the pipette. *Panel A:* Ensemble at -30 mV. The dashed line illustrates a mono-exponential least squares fit to the current decay. The current decay is better fitted by the sum of two exponentials (solid line) with time constants of 3.7 ± 0.1 ms and 21.5 ± 2.7 ms and amplitudes of -16.2 ± 0.9 pA and -0.4 ± 0.1 pA, respectively. The amplitude of the slow component was only 2.5% of the fast component. *Panel B:* The bend in the semilogarithmic plot of the same ensemble confirms the existence of two components of the current decay. A second component could not be identified in some ensembles from records with bursts. The time a Na^+ channel spends in the burst mode is a small percentage of the total open time, and thus, the amplitude of the slow component is expected to be small.

of inactivation could be detected approximately half the time with T_3 in the pipette. Failure to detect a second component in ensembles from some patches despite evidence of bursts in the sweeps probably results from the small amplitude of the slow component. Under our conditions which were optimized for analyzing single channel kinetics by limiting the number of channels in a patch, ensembles from control patches were well fitted by a monoexponential inactivation rate (Dudley and Baumgarten, 1991a).

The Role of Second Messengers in the Effect of T_3

Table II shows the effects on the %LE of T_3 added to the bath with patches in the cell-attached or inside-out configurations. All experiments were performed at -50 mV because the greatest change in the %LE occurred at this voltage when T_3 was added to the pipette. The %LE before and after the addition of T_3 to the bath were compared by paired t tests. In seven paired experiments on cell-attached patches, neither 50 or 100 nM T_3 increased the %LE. The lack of an increase in the %LE at concentrations > 20 times a saturating dose for T_3 added to the pipette implies that T_3 did not permeate the membrane during the time course of our experiments (~15 min). If the effect of T_3 had been mediated by a soluble second messenger, the messenger should have been able to diffuse through the cytoplasm from sites of production outside the patch to the channels within the patch. The failure to observe gating changes when the electrode isolated the Na^+ channels in the patch implies that the effect of T_3 on gating is not mediated by a soluble second messenger.

To further identify the site of action of T_3 , the hormone also was applied to excised, inside-out patches. The %LE in seven paired experiments was indistinguishable before and after addition of 50 nM T_3 to the cytoplasmic side of the Na^+ channel. Contrary to some reports (Horn and Vandenberg, 1986; Nilius, 1988b; Kirsch and Brown, 1989), excision alone did not increase bursting in our experiments. Our results were more consistent with those of Burnashev et al. (1989) who saw only rare bursts of control channels in the inside-out

Table II. T_3 requires access to the Na^+ channel's extracellular face to induce long events.

Condition	Change in Long Events with T_3		p
	Control %LE	Δ %LE	
50 nM T_3 (in bath, cell-attached)	0.97 ± 0.60 (3)*	0.1 ± 0.2 (4)†	0.33
100 nM T_3 (in bath, cell-attached)	2.85 ± 0.42 (3)	0.8 ± 1.1 (3)	0.27
50 nM T_3 (in bath, inside-out)	2.72 ± 0.96 (4)	0.1 ± 0.4 (7)	0.41

* number of experiments

† number of paired comparisons including washout

configuration. There was considerable variability in the %LE from patch to patch in the absence of T_3 , probably reflecting variable rates of bursting. Taken together, the ineffectiveness of T_3 applied to the cytoplasmic face of inside-out patches and to the cell when the channels studied were isolated by the patch electrode suggests that T_3 requires access to the extracellular face of the Na^+ channel or to adjacent structures in order to cause a change in gating.

Patch Excision in the Presence of Pipette T_3 Increases Bursting

In the absence of T_3 , I did not find an increase in the %LE with excision to the inside-out configuration (see Table II). However, with T_3 added to the pipette, excision resulted in a dramatic rise in the %LE. Figure 24A shows consecutive current records at -40 mV with 5 nM T_3 in the pipette from a patch before and after excision. In the cell-attached mode, current records showed several long events. With excision to the inside-out configuration, there was a marked increase in prolonged openings. Panels B and C show diaries of the open channel probabilities per sweep (N_p) for the cell-attached and inside-out configurations, respectively. As compared to channel behavior in the cell-attached configuration, patch excision to the inside-out configuration induced an increase in N_p and a number of instances where a channel was open for most of the 45 ms depolarizing epoch.

Figure 25 demonstrates the effect of excision in the presence of pipette 5 nM T_3 on the unitary current, MOT, and %LE. In panel A, the i/V curve is shifted upward upon excision without a change in conductance. The γ_{Na} of cell-attached patches (\blacksquare) was 15.5 ± 1.0 pS and was 15.0 ± 0.7 pS after excision (\blacktriangle ; $p = 0.82$). The lack of change in the γ_{Na} suggested that the observed difference in unitary current resulted from a shift in the E_{rev} or, more likely, that the membrane potential in series with the cell-attached patch was not exactly 0 mV. Consistent with the analyses of other investigators (Kohlhardt et al., 1987; Kirsch and Brown, 1989), I found that the open time histogram of all openings in excised patches was

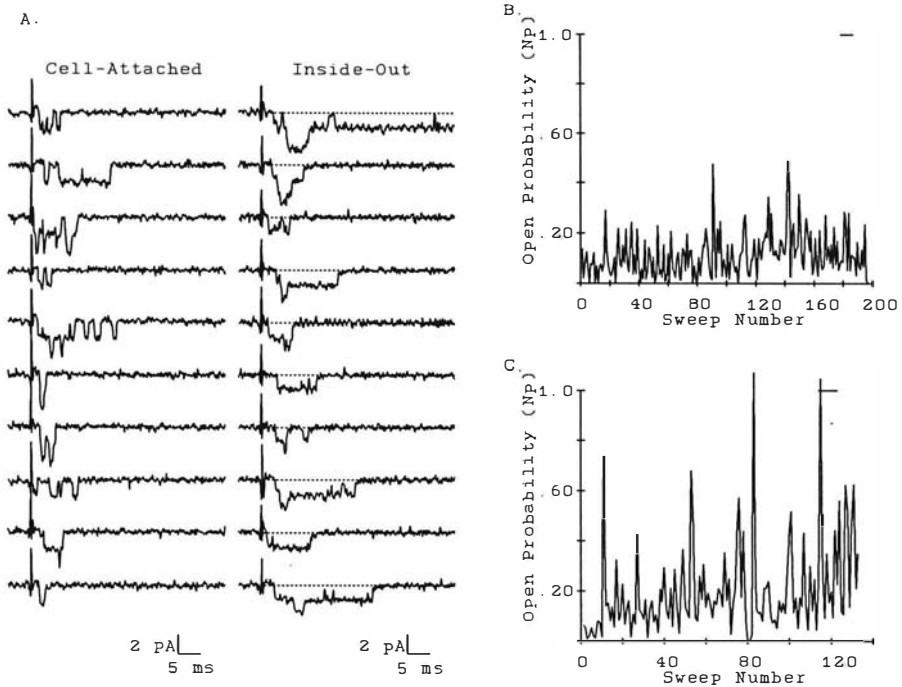


Figure 24. The effect of patch excision with 5 nM T_3 in the pipette. Panel A presents consecutive sweeps recorded at -40 mV from the same patch before (cell-attached) and after patch excision (inside-out). In the cell-attached configuration, the Na^+ channels exposed to T_3 show occasional LEs. The number of LEs increased in the inside-out configuration. The dotted line represents the closed, zero current level. Panel B and C are the open channel probability (Np) diaries for the cell-attached and inside-out configurations, respectively. Excision in the presence of T_3 resulted in a considerable increase the channel open probability. The horizontal lines demarcate the sweeps displayed in panel A.

well fitted by a single exponential distribution. On the other hand, Nilius (1988b) and Josephson and Sperelakis (1989) reported a biexponential open time distribution in excised patches showing bursts.

As demonstrated in Figure 25B, the MOT of channels exposed to T_3 on their cytoplasmic face was greater for inside-out (\blacktriangle) than for cell-attached patches (\blacksquare ; $p < 0.01$). The increase in MOT upon excision was particularly dramatic near the threshold potential. The voltage dependencies of MOT in both configurations were similar to those reported by Kirsch and Brown (1989) for rat ventricular Na^+ channels, but our MOTs were consistently shorter. The difference in MOTs may represent species variations in the response to excision. On the contrary, Nilius (1988b) found that excision of patches from guinea pig ventricle resulted in a biexponential open time distribution. The component with a shorter MOT had a similar MOT to that of his cell-attached patches and was voltage independent. The second component, present only after excision, had a longer MOT which increased linearly with depolarization. This second component ranged from 0.48 ms at -80 mV to 2.87 ms at -20 mV.

The %LE-voltage relationships with 5 nM T_3 in the pipette before and after excision are shown in Figure 25C. The increase in the %LE in the inside-out configuration (\blacktriangle) was significantly greater than that observed in the cell-attached mode (\blacksquare ; $p < 0.01$). For example, the %LE in the cell-attached position was 3.9 ± 0.9 at -60 mV before excision and was 13.3 ± 1.8 after excision. The %LE-voltage relationship appeared to have a similar voltage sensitivity to that in cell-attached patches, but the curve was shifted about 10 mV in the hyperpolarizing direction. The magnitude and direction of this shift with patch excision is consistent with other reports (Cachelin et al., 1983; Grant et al., 1983; Nagy et al., 1983; Fernandez et al., 1984; Kunze et al., 1985; Kirsch and Brown, 1989). The increase in the MOT and %LE as well as the decrease in unitary current required the presence of T_3 in the pipette; neither patch excision alone nor the subsequent addition of 50 nM T_3 to the cytoplasmic face of the channel altered these parameters.

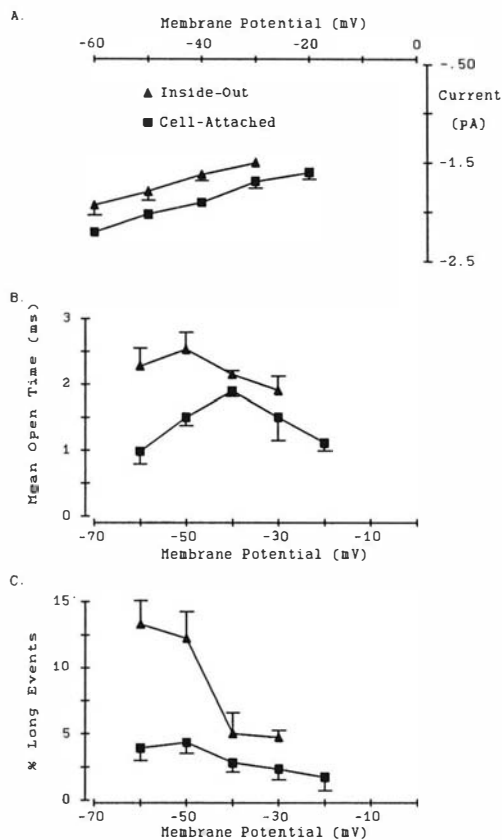


Figure 25. The effect of patch excision in the presence of 5 nM T_3 on the unitary current, MOT, and %LE. *Panel A:* Patch excision to the inside-out configuration resulted in a shift in the i/V curve. The unitary conductance (γ_{Na}) in the cell-attached configuration (■) was 15.5 ± 1.0 pS and was 15.0 ± 0.7 pS after excision (▲). The two values of γ_{Na} were statistically indistinguishable ($p = 0.82$). This suggests that the change in unitary current results from a shift in the E_{rev} or that the membrane potential in series with the cell-attached patch was not exactly 0 mV. *Panel B:* Excision (▲) increased the MOT as compared with the cell-attached configuration (■) especially near threshold ($p < 0.01$). The increase in MOT may reflect the substantial increase in %LE at threshold voltages with excision. *Panel C:* %LE before (■) and after (▲) excision. The decrease in unitary current as well as the increase in the MOT and %LE required the presence of T_3 in the pipette. Neither patch excision alone nor subsequent addition of 50 nM T_3 to the cytoplasmic face of the channel altered these parameters. All data points represent means, and error bars (\pm SE) are shown when they exceeded the symbol size.

DISCUSSION

Our results showed that T_3 can modulate cardiac Na^+ channels by increasing the propensity for channels to enter a gating mode characterized by bursts, and the frequency of bursting was assessed as %LE. This action of T_3 was independent of nuclear transduction. Bursts were noted as soon as recording began (~30 s from the time of seal formation), far too rapidly to have resulted from the chain of events initiated by T_3 binding to its nuclear receptor. Burst mode gating also was stimulated by TAA, which is inactive at the thyroid hormone nuclear receptor (DeNayer, 1987). T_3 required access to the extracellular side of the Na^+ channel to bring about bursting. Bursting was enhanced when T_3 or TAA were included in the patch pipette, and the %LE dramatically increased when inside-out patches were made with T_3 in the pipette. In contrast, adding T_3 to the bath while channels in cell-attached patches were exposed to a T_3 -free pipette solution or applying T_3 to the cytoplasmic face of inside-out patches failed to increase the %LE. These data suggest that T_3 does not cross the membrane within the time course of our single channel studies and that induction of bursting does not involve a soluble intracellular second messenger. The modification of single channel gating by T_3 was shown to give rise to a second, slow component of the current decay in ensemble averages and would contribute to a slowing of the overall rate of macroscopic inactivation. A brief report by Craelius et al. (1990) previously suggested that acute exposure to T_3 slows inactivation of macroscopic Na^+ currents in neonatal rat heart.

Nilius (1988b) proposed three criteria to establish the existence of modal kinetics. The criteria are: 1) coexistence of distinct kinetic schemes, 2) a tool that can shift gating between schemes, and 3) slow transitions between schemes resulting in clustering of records with similar gating. All three of these criteria were met. Some sweeps contained bursts while others did not. Addition of T_3 to the pipette increased the number of LEs. Finally, as demonstrated by a runs analysis, the sweeps with LEs tended to cluster together. The modal

gating behavior in the presence of extracellular T_3 is consistent with previous reports on bursting of native Na^+ channels (Horn et al., 1984; Grant and Starmer, 1987; Nilius, 1988b; Moorman et al., 1990). Besides the present results with T_3 , forskolin (Ono and Fozzard, 1991), lysophosphatidylcholine (Burnashev et al., 1989), a soluble diacylglycerol (Numann et al., 1991), and two glycolytic pathway metabolites (Kohlhardt et al., 1989) also induce bursts. This suggests that alterations in gating may be a common method of modulation of Na^+ channels. Modes are also a feature of the L-type Ca^{2+} channels (Hess et al., 1984) and Ca^{2+} -activated K^+ channels (McManus and Magleby, 1988).

The Origin of Bursts

Several lines of evidence suggest that burst mode gating is an intrinsic property of native Na^+ channels and not the result of separate populations of channels within a patch. Bursting has been observed in Na^+ channels from a number of tissues including heart (Patlak and Ortiz, 1985; Grant and Starmer, 1987; Kohlhardt et al., 1987; Kiyosue and Arita, 1989; Nilius, 1988b; Burnashev et al., 1989; Josephson and Sperelakis, 1989; Kirsch and Brown, 1989), skeletal muscle (Patlak and Ortiz, 1986; Patlak et al., 1986; Patlak and Ortiz 1989; Zhou et al., 1991), brain (Moorman et al., 1990), and the GH_3 cell line derived from rat pituitary gland (Horn et al., 1984, Horn and Vandenberg, 1986). Because of the variety of temperature, ionic conditions, and patch configurations in these experiments, bursts are unlikely to result from a particular experimental maneuver. Using a number of protease inhibitors, Horn and Vandenberg (1986) confirmed that residual enzymes from the cell isolation procedure were not creating distinct channel populations. Patlak et al. (1986) and Patlak and Ortiz (1989) have described changes in gating within a burst, which they called dynamic heterogeneity. Different gating patterns within a burst suggests that individual channels are capable of switching kinetic schemes. Finally, Moorman et al. (1990) observed two gating modes when the rat brain III Na^+ channel mRNA was injected into *Xenopus* oocytes. This suggests that

bursting arises from a single type of channel, although posttranslational modification of some of the channels cannot be ruled out.

I confirmed bursting in cell-attached patches is a rare but consistent feature of native Na^+ channel behavior. In our experiments using the cell-attached patch configuration, γ_{Na} , E_{rev} , and MOT were not altered when T_3 in the pipette increased the number of bursts. In all cases, the open channel amplitude histograms were well described by a single Gaussian function, and the open time histograms were monoexponential. Therefore, I found no evidence for multiple conductance or open states. Also, the increase in bursting upon excision with T_3 in the pipette is most simply explained by the alteration of channel kinetics rather than by the induction of a new population of channels.

Several investigators have reported an increase in bursting of cardiac Na^+ channels with patch excision in acutely isolated guinea pig ventricle (Nilius, 1988b) and cultured rat heart (Kirsch and Brown, 1989). A number of studies suggest that bursting or its macroscopic consequence, slowing of inactivation, may result from changes in the cytoplasmic constituents (Chandler and Meves, 1970; Schauf, 1983; Oxford and Yeh, 1985; Horn and Vandenberg, 1986). It is unlikely that changes in ionic constituents alone can account for the gating shifts in the present experiments. I did not observe any increase in %LEs or prolonged openings when patches were excised to the inside-out configuration in the absence of pipette T_3 . Patch excision also fails to increase bursting in rat ventricular (Burnashev et al., 1989) and rat brain Na^+ channels (Kirsch and Brown, 1989). Nevertheless, one element of our findings argues that a cytoplasmic factor may moderate shifts between conventional kinetics and the burst mode. While the %LEs were indistinguishable in cell-attached and excised inside-out patches with control solution, bursting was significantly enhanced by excision when 5 nM T_3 was included in the pipette solution. Comparing the maximums, 4.4 ± 0.8 % of openings were LEs in cell-attached patches with T_3 in the pipette, but the %LE increased to 13.3 ± 1.8 % after excision. A comparison of the maximum values excludes the possibility that the change in the

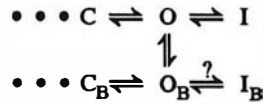
%LE with excision results from a shift of the %LE-voltage curve along the voltage axis. Rather, these data suggest that a cytoplasmic factor may stabilize channels in the conventional mode of gating. The lack of this postulated stabilizing factor may explain the unusually high number of bursts recorded in the cell-attached mode from rat skeletal muscle μI (Zhou et al., 1991) and rat brain III Na^+ channels (Moorman et al., 1990) expressed in *Xenopus* oocytes.

Kinetic Schemes

Several investigators have proposed that Na^+ channel bursting may result from a reversible failure of inactivation (Horn and Vandenberg, 1986; Grant and Starmer, 1987). In this model, bursts result from repeated transitions between the open and closed states. At more positive potentials, the rate of closing decreases, so the MOT of openings within a burst should increase. On the other hand, the inactivation rate is slow near threshold, and its contribution to the rate of channel closure is small. Therefore, the MOT of openings within a burst should not differ significantly from the MOT of control openings.

Although this theory explains the origin of bursts simply, several experimental findings suggest that the model is incomplete. The MOT of openings within bursts in native channels is considerably longer than the control MOT (Patlak and Ortiz, 1985; Patlak and Ortiz, 1986; Grant and Starmer, 1987; Kohlhardt et al., 1987; Kiyosue and Arita, 1989). For example, Kiyosue and Arita (1989) found that the MOT in a burst was 5-times that of the background openings when measured 10 mV positive to the resting potential. In excised patches with T_3 in the pipette, I saw a more modest increase in the MOT of all openings near threshold. However, Figure 21 indicates that bursting induced by extracellular T_3 is most marked between -50 and -30 mV and is less prominent outside of this range. A simple model in which bursting arises from a reversible failure of inactivation does not predict a decrease in the frequency of bursts at depolarized potentials.

I propose the following Markov chain model of Na⁺ channel bursting induced by T₃.



C, O, and I are the conventional closed, open, and inactivated states, and C_B, O_B, and I_B represent the parallel burst mode closed, open, and inactivated states, respectively. The model postulates that the burst mode is entered predominately from the open state rather than the closed state because the biphasic voltage-dependence of bursting parallels the biphasic voltage-dependence of MOT in control channels (Kirsch and Brown, 1989; Scanley et al., 1990; Dudley and Baumgarten, 1991a). The I_B state is not required by the present data but was included on the assumption that T₃ modulates transition kinetics rather than preventing transitions. Entry into the burst mode from the open state predicts that the number of bursts should be correlated with the number and duration of openings. In unmodified channels, Patlak and Ortiz (1986) showed the number of bursts is correlated with the number of openings.

T₃'s Mechanism of Action

Our experiments showed an increase in bursting only when T₃ was applied to the extracellular face of the cardiac Na⁺ channel. T₃ could act by binding to another receptor, by binding directly to the extracellular side of the channel, or by perturbing the membrane outer leaflet. Specific membrane binding sites for T₃ exist in the heart and mediate extra-nuclear effects such as an increase in the sarcolemmal calcium ATPase activity (Rudinger et al., 1984), an increase in adenylate cyclase activity (Levey and Epstein, 1969; Will-Shahab et

al., 1976), an alteration in the number of α - and β -adrenergic binding sites (Chang and Kunos, 1981), and a stimulation of 2-deoxyglucose transport (Segal, 1989a). Modulation of the sugar uptake rate is one of the most thoroughly investigated actions of T_3 at the plasma membrane level. Nanomolar concentrations of T_3 cause an immediate enhancement of the 2-deoxyglucose transport in rat heart and other tissues. The effect occurs within minutes, is independent of protein synthesis, is maximal at 1 nM, and requires a Ca^{2+} influx for initiation. This Ca^{2+} influx stimulates adenylate cyclase via a calmodulin dependent event mediated by a G protein. The resultant increase in cAMP is responsible for stimulating sugar transport (for review see Segal, 1989a). Our failure to observe an increase in %LE with T_3 added to the bath rules out the participation of a soluble mediator other than Ca^{2+} . Although a role for Ca^{2+} seems unlikely in enhancing Na^+ channel bursts, it cannot be excluded. A high EGTA concentration in our standard bath solution should have helped buffer internal Ca^{2+} minimizing any local charges as the result of Ca^{2+} fluxes through the patch. Furthermore, Vandenberg and Horn (1986), saw no effect of ATP on the rate of bursting in GH_3 cells.

A G protein dependent modulation of bursting could explain the requirement for T_3 in the pipette. G proteins are present in heart (Scherer et al. 1987, Halvorsen and Nathanson, 1984) and affect at least six classes of ion channels by a membrane limited process. Muscarinic, β -adrenergic, and purinergic receptors are known to affect cardiac channels via direct G protein pathways (Birnbaumer et al., 1990; Brown and Birnbaumer, 1990). Reports have demonstrated the involvement of G proteins in the regulation of Na^+ channel gating by direct (Schubert et al., 1989; Schubert et al., 1990) and indirect pathways (Schubert et al., 1989; Schubert et al., 1990; Matsuda et al., 1991). One report has implicated at least two G proteins in the modulation of rat brain Na^+ channels expressed in *Xenopus* oocytes. (Cohen-Armon et al., 1989). The absence of the T_3 receptor or a G protein would explain the sporadic failure to see bursts in patches exposed to extracellular T_3 . In our experiments T_3

stimulated Na^+ channel openings, but three out of four reports have indicated an inhibition of the macroscopic peak I_{Na} (Cohen-Armon et al., 1989; Schubert et al., 1989; Schubert et al., 1990) or the single channel probability of opening (Schubert et al., 1989; Schubert et al., 1990).

The bursting caused by T_3 may result from perturbations in the plasma membrane which affect the stability of Na^+ configurations. T_3 is lipophilic (Lein and Dowben, 1961) and has acute and chronic effects on the lipid structure of rat liver cell membranes (Schroeder, 1982). A spin labeled derivative of T_3 shows significant association with multilamellar vesicles (Lai and Cheng, 1984). Our finding that T_3 added to the bath could not induce bursting in cell-attached patches, along with reports of hypothyroidism associated with the failure of carrier mediated transport (Wortsman et al. 1983), suggest that T_3 is not freely membrane permeable. This concept is consistent with reports of carrier mediated transport at the level of the plasma membrane (for review see Rao, 1981). Furthermore, the effect of T_3 on Na^+ channel gating is similar to that reported for other lipid soluble substances such as lysophosphatidylcholine (Burnashev et al., 1989), diacylglycerols (Numann et al., 1991), and a number of lipid soluble Na^+ channel toxins such as the alkaloids, pyrethroids, and brevitoxins (Strichartz et al., 1987). On the other hand, the effects of these toxins are not completely analogous with those of T_3 since the toxins alter ionic selectivity and are equally effective when added to either side of the membrane.

Finally, T_3 may bind directly to the external face of the Na^+ channel. Presumably, this binding would stabilize an open conformation and delay the onset of inactivation. This mechanism is similar to that described for Na^+ channel peptide toxins from scorpions, sea anemones, and cone snails. These toxins may have some structural similarity to T_3 since they are structurally compact (Fontecilla-Camps et al., 1980). The smallest toxin, μ -conotoxin, is comprised of only 22 amino acids (Olivera et al., 1985). A number of toxins bind sites on the external face of the channel and alter gating without affecting ion selectivity.

In summary, I observed an acute increase in burst mode gating of cardiac Na⁺ channels with T₃ in proximity to the extracellular face of the channel. Three possible mechanisms by which T₃ delays channel inactivation include receptor mediation, direct binding to the channel, and a perturbation of the sarcolemma. The increase in bursts may contribute to the proclivity for arrhythmias seen in hyperthyroidism (Olshausen et al., 1989).

BIBLIOGRAPHY

Bibliography

- Aldrich RW, Corey DP, Stevens CF: A Reinterpretation of Mammalian Sodium Channel Gating Based on Single Channel Recording. *Nature* 1983; 306:436-441.
- Aldrich RW, Yellen, G: Analysis of Nonstationary Channel Kinetics. *In* Single Channel Recording. B. Sakmann and E. Neher, editors. Plenum Press. New York. 1983; 287-299.
- Aoki VS, Wilson WR, Thielen EO: Studies of the Reputed Augmentation of the Cardiovascular Effects of Catecholamines in Patients With Spontaneous Hyperthyroidism. *J. Pharmacol. Exp. Ther.* 1972; 181:362-368.
- Auld VJ, Goldin AL, Krafte DS, Marshall J, Dunn JM, Catterall WA, Lester HA, Davidson N, Dunn RJ. A Rat Brain Na⁺ Channel Alpha Subunit with Novel Gating Properties. *Neuron* 1988; 1:449-461.
- Baker PF, Rubinson KA: Chemical Modification of Crab Nerves Can Make Them Insensitive to the Local Anaesthetics Tetrodotoxin and Saxitoxin. *Nature* 1975; 257:412-414.
- Baker PF, Rubinson KA: TTX-Resistant Action Potentials in Crab Nerve after Treatment with Meerwein's Reagent. *J. Physiol. (London)* 1977; 266:3P.
- Barchi RL: Probing the Molecular Structure of the Voltage-Dependent Sodium Channel. *Ann. Rev. Neurosci.* 1988; 11:455-495.
- Baumgarten CM, Dudley SC, Rogart RB, Fozzard HA: Cardiac and Neuroblastoma Sodium Channels Have Different Unitary Conductances and Kinetics. *Biophys. J.* 1991; 59:69a.
- Baumgarten CM, Fozzard HA: Cd²⁺ and Zn²⁺ Block Unitary Na⁺ Currents in Purkinje and Ventricular Cells. *Biophys. J.* 1989; 55:313a.

- Binah O, Rubinstein I, Gilat E: Effects of Thyroid Hormone on the Action Potential and Membrane Currents of Guinea Pig Ventricular Myocytes. *Pflügers Arch.* 1987; 409:214-216.
- Birnbaumer L, Abramowitz J, Yatani A, Okabe K, Mattera R, Graf R, Sanford J, Codina J, Brown AM: Roles of G Proteins in Coupling of Receptors to Ionic Channels and Other Effector Systems. *Biochem. Mol. Biol.* 1990; 25:225-244.
- Bishop GH: My Life Among the Axons. *Ann. Rev. Physiol.* 1965; 27:1-8.
- Bossu J-L, Feltz A: Patch Clamp Study of Tetrodotoxin-Resistant Sodium Current in Group C Sensory Neurones. *Neurosci. Lett.* 1984; 51:241-246.
- Brodwick MS, Eaton DC: Chemical Modification of Excitable Membranes. In Proteins in the Nervous System: Structure and Function. B. Haber and R. Perez-Polo, editors. Alan R. Liss, Inc. New York. 1982; 51-72.
- Brown AM, Birnbaumer L: Ionic Channels and Their Regulation by G Protein Subunits. *Ann. Rev. Physiol.* 1990; 52:197-213.
- Brown AM, Lee KS, Powell T: Sodium Current in Single Rat Heart Muscle Cells. *J. Physiol. (London)* 1981; 318:479-500.
- Burnashev NA, Undrovinas AI, Fleidervish IA, Rosenshtraukh LV: Ischemic Poison Lyso-phosphatidylcholine Modifies Heart Sodium Channels Gating Inducing Long-Lasting Bursts of Openings. *Pflügers Arch.* 1989; 415:124-126.
- Cachelin AB, DePeyer JE, Kokubun S, Reuter H: Sodium Channels in Cultured Cardiac Cells. *J. Physiol. (London)* 1983; 340:389-401.
- Cairolì VJ, Crout JR: Role of the Autonomic Nervous System in the Resting Tachycardia of Experimental Hyperthyroidism. *J. Pharmacol. Exp. Ther.* 1967; 158:55-65.
- Carmeliet E: Slow Inactivation of the Sodium Current in Rabbit Cardiac Purkinje Fibres. *Pflügers Arch.* 1987; 408:18-26.
- Chabala LD, Green WN, Andersen OS: Covalent Modification of External Carboxyl Groups of Batrachotoxin-Modified Canine Forebrain Sodium Channels. *Biophys. J.* 1986; 49:40a.

- Chandler WK, Meves H: Evidence for Two Types of Sodium Conductance in Axons Perfused with Sodium Fluoride Solution. *J. Physiol. (London)* 1970; 211:653-678.
- Chang HY, Kunos G: Short Term Effects of Triiodothyronine on Rat Heart Adrenoceptors. *Biochem. Biophys. Res. Commun.* 1981; 100:313-320.
- Cherbavaz DB: TMO-Modification of Na⁺ Channels Does Not Remove Surface Charge Near the Conduction Pathway. *Biophys. J.* 1990; 57:300a.
- Chinn K: Substate and Kinetic Characteristics of Deltamethrin-Modified Sodium Channels. *Biophys. J.* 1988; 53:230a.
- Chinn K, Narahashi T: Stabilization of Sodium Channel States by Deltamethrin in Mouse Neuroblastoma Cells. *J. Physiol. (London)* 1986; 380:191-207.
- Cohen-Armon M, Sokolovsky M, Dascal N: Modulation of the Voltage-Dependent Sodium Channel by Agents Affecting G-Proteins: A Study in *Xenopus* Oocytes Injected With Brain RNA. *Brain Res.* 1989; 496:197-203.
- Colquhoun D, Hawkes AG: The Principles of the Stochastic Interpretation of Ion-Channel Mechanisms. *In* Single Channel Recording. B. Sakmann and E. Neher, editors. Plenum Press. New York. 1983; 135-175.
- Colquhoun D, Sigworth FJ: Fitting and Statistical Analysis of Single-Channel Records. *In* Single Channel Recording. B. Sakmann and E. Neher, editors. Plenum Press. New York. 1983; 191-263.
- Corey DP, Stevens CF: Science and Technology of Patch-Recording Electrodes. *In* Single Channel Recording. B. Sakmann and E. Neher, editors. Plenum Press. New York. 1983; 53-68.
- Craelius W, Harris D, Green W: Thyroid Hormone Enhances Slow Inactivation of Sodium Current in Cardiac Myocytes. *J. Mol. Cell. Cardiol.* 1990; 22:S14.
- D'Arrigo JS: Axonal Surface Charges: Evidence for Phosphate Structure. *J. Memb. Biol.* 1975; 22:255-263.
- DeCino P, Kidokoro Y: Development and Subsequent Neural Tube Effects on the Excitability of Cultured *Xenopus* Myocytes. *J. Neurosci.* 1985; 5:1471-1482.

- DeNayer P: Thyroid Hormone Action at the Cellular Level. *Hormone Res.* 1987; 26:48-57.
- DiFrancesco D, Ferroni A, Visentin S, Zaza A: Cadmium-Induced Blockade of the Fast Na⁺ Channels in Calf Purkinje Fibres. *Proc. Roy. Soc. London Ser. B* 1985; 223:475-484.
- Draper MH, Weidmann S: Cardiac Resting and Action Potentials Recorded with an Intracellular Electrode. *J. Physiol.* 1951; 115:74-94.
- Dudley SC, Baumgarten CM: Trimethyloxonium (TMO) Decreases Unitary Conductance and Mean Open Time of Cardiac Na⁺ Channels. *J. Mol. Cell. Cardiol.* 1990a; 22(Suppl. I):P38.
- Dudley SC, Baumgarten CM: Trimethyloxonium Fails to Prevent Ca²⁺ Block of Cardiac Na⁺ Channels. *Biophys. J.* 1990b; 57:106a.
- Dudley SC, Baumgarten CM: Carboxyl-Group Specific Modification of Cardiac Sodium Channels. *J. Gen. Physiol.* 1991a; submitted.
- Dudley SC, Baumgarten CM: Physiological Concentrations of Triiodo-L-thyronine Increase Bursting of Cardiac Na⁺ Channels. *Biophys. J.* 1991b; 59:98a.
- El Shahawy M, Stefadouros MA, Carr AA, Conti R: Direct Effect of Thyroid Hormone on Intracardiac Conduction in Acute and Chronic Hyperthyroid Animals. *Cardiovasc. Res.* 1975; 9:524-531.
- Fernandez JM, Fox AP, Krasne S: Membrane Patches and Whole-Cell Membranes: A Comparison of Electrical Properties in Rat Clonal Pituitary (GH₃) Cells. *J. Physiol. (London)* 1984; 356:565-585.
- Follmer CH, TenEick RE, Yeh JZ: Sodium Current Kinetics in Cat Atrial Myocytes. *J. Physiol. (London)* 1987; 384:169-197.
- Fontecilla-Camps JC, Almássay RJ, Suddath FL, Watt DD, Bugg CE: Three-Dimensional Structure of a Protein from Scorpion Venom: A New Structural Class of Neurotoxins. *Proc. Natl. Acad. Sci. USA* 1980; 77:6496-6500.
- Fozzard HA, Hanck DA: Sodium Channels. *In* The Heart and Cardiovascular System, Second Edition. H.A. Fozzard, E. Haber, R.B. Jennings, A.M. Katz, and H.E. Morgan, editors. Raven Press. New York. 1991; in press.

- Freedberg AS, Papp JG, Vaughan-Williams EM: The Effect of Altered Thyroid State on Atrial Intracellular Potentials. *J. Physiol. (London)* 1970; 207:357-369.
- Frelin C, Cognard C, Vigne P, Lazdunski M: Tetrodotoxin-Sensitive and Tetrodotoxin-Resistant Na⁺ Channels Differ in Their Sensitivity to Cd²⁺ and Zn²⁺. *Eur. J. Pharmacol.* 1986; 122:245-250.
- French RJ, Worley III JF, Bean BP: Voltage-Dependent Block by Saxitoxin of Sodium Channels Incorporated in Planar Lipid Bilayers. *Biophys. J.* 1984; 45:301-310.
- Garber SS, Miller C: Single Na⁺ Channels Activated by Veratridine and Batrachotoxin. *J. Gen. Physiol.* 1987; 89:459-480.
- Grant AO, Starmer CF: Mechanisms of Closure of Cardiac Sodium Channels in Rabbit Ventricular Myocytes: Single Channel Analysis. *Circ. Res.* 1987; 60:897-913.
- Grant AO, Starmer CF, Strauss HC: Unitary Sodium Channels in Isolated Cardiac Myocytes of Rabbit. *Circ. Res.* 1983; 53:823-829.
- Green WN, Weiss LB, Andersen OS: Batrachotoxin-Modified Sodium Channels in Planar Lipid Bilayers - Ion Permeation and Block. *J. Gen. Physiol.* 1987a; 89:841-872.
- Green WN, Weiss LB, Andersen OS: Batrachotoxin-Modified Sodium Channels in Planar Lipid Bilayers - Characterization of Saxitoxin- and Tetrodotoxin-Induced Channel Closures. *J. Gen. Physiol.* 1987b; 89:873-903.
- Gülden KM, Vogel W: Three Functions of Sodium Channels in the Toad Node of Ranvier are Altered by Trimethyloxonium Ions. *Pflügers Arch.* 1985; 403:13-20.
- Guy HR, Conti F: Pursuing the Structure and Function of Voltage-gated Channels. *Trends Neurosci.* 1990; 13:201-206.
- Halvorsen SW, Nathanson NM: Ontogenesis of Physiological Responsiveness and Guanine Nucleotide Sensitivity of Cardiac Muscarinic Receptors during Chick Embryonic Development. *Biochemistry* 1984; 23:5813-5821.
- Hamill OP, Marty A, Neher E, Sakmann B, Sigworth FJ: Improved Patch-Clamp Techniques for High-Resolution Current Recording from Cells and Cell-Free Membrane Patches. *Pflügers Arch.* 1981; 391:85-100.

- Hess P, Lansman JB, Tsien, RW: Different Modes of Ca Channel Gating Behaviour Favoured by Dihydropyridine Ca Agonist and Antagonists. *Nature* 1984; 311:538-544.
- Hille B: *Ionic Channels of Excitable Membranes*. Sinauer Associates, Inc. Sunderland, MA. 1984.
- Hisatome I, Kiyosme T, Imanishi S, Arita M: Isoproterenol Inhibits Residual Fast Channel via Stimulation of β -Adrenoceptors in Guinea-pig Ventricular Muscle. *J. Mol. Cell. Cardiol.* 1985; 17:657-665.
- Hodgkin AL, Huxley AF: Current Carried by Sodium and Potassium Ions Through the Membrane of the Giant Squid Axon of *Loligo*. *J. Physiol. (London)* 1952a; 116:449-472.
- Hodgkin AL, Huxley AF: A Quantitative Description of Membrane Current and Its Application to Conduction and Excitation in Nerve. *J. Physiol. (London)* 1952b; 117:500-544.
- Hodgkin AL, Huxley AF, Katz B: Ionic Currents Underlying Activity in the Giant Axon of the Squid. *Arch. Sci. Physiol.* 1949; 3:129-150.
- Hodgkin AL, Katz B: The Effect of Sodium Ions on the Electrical Activity of the Giant Axon of the Squid. *J. Physiol.* 1949; 108:37-77.
- Horn R, Vandenberg CA: Inactivation of Single Sodium Channels. *In* Ion Channels in Neural Membranes. G. M. Ritchie, editor. Alan R. Liss, Inc., New York, 1986, 71-83.
- Horn R, Vandenberg CA, Lange K: Statistical Analysis of Single Sodium Channels. Effects of N-bromoacetamide. *Biophys. J.* 1984; 45:323-335.
- Huxley AL, Stämpfli R: Effect of Potassium and Sodium on Resting and Action Potentials of Single Myelinated Nerve Fibres. *J. Physiol.* 1951; 112:496-508.
- Ikeda SR, Schofield GG: Tetrodotoxin-Resistant Sodium Current of Rat Nodose Neurones: Monovalent Cation Selectivity and Divalent Cation Block. *J. Physiol. (London)* 1987; 389:255-270.
- Johnson PN, Freedberg AS, Marshall JM: Action of Thyroid Hormone on the Transmembrane Potentials from Sinoatrial Node Cells and Atrial Muscle Cells in Isolated Atria of Rabbits. *Cardiology* 1973; 58:273-289.

- Jones SW: Sodium Currents in Dissociated Bull-Frog Sympathetic Neurons. *J. Physiol. (London)* 1987; 389:605-627.
- Josephson IR, Sperelakis N: Tetrodotoxin Differentially Blocks Peak and Steady-State Sodium Channel Currents in Early Embryonic Chick Ventricular Myocytes. *Pflügers Arch.* 1989; 414:354-359.
- Kao CY, Walker SE: Active Groups of Saxitoxin and Tetrodotoxin as Deduced from Saxitoxin Analogues on Frog Muscle and Squid Axon. *J. Physiol. (London)* 1982; 323:619-637.
- Kayano T, Noda M, Flockerzi V, Takahashi H, Numa S: Primary Structure of Rat Brain Sodium Channel III Deduced from the cDNA Sequence. *FEBS Lett.* 1988; 228:187-194.
- Kirsch GE, Brown AM: Kinetic Properties of Single Sodium Channels in Rat Heart and Rat Brain. *J. Gen. Physiol.* 1989; 93:85-99.
- Kiyosue T, Arita M: Late Sodium Current and its Contribution to Action Potential Configuration in Guinea Pig Ventricular Myocytes. *Circ. Res.* 1989; 64:389-397.
- Kohlhardt M, Fichtner H, Fröbe U: Metabolites of the Glycolytic Pathway Modulate the Activity of Single Cardiac Na⁺ Channels. *FASEB J.* 1989; 3:1963-1967.
- Kohlhardt M, Fröbe U, Herzig JW: Properties of Normal and Noninactivating Single Cardiac Na⁺ Channels. *Proc. Roy. Soc. Lond. B* 1987; 232:71-93.
- Krafte D, Volberg W, Dillon K, Ezrin A: Characterization of Tetrodotoxin Sensitivity of Cardiac and Neural Na Channels Expressed in *Xenopus* Oocytes. *Biophys. J.* 1990; 57:300a.
- Krueger BK, Ratzlaff RW, Strichartz GR, Blaustein MP: Saxitoxin Binding to Synaptosomes, Membranes, and Solubilized Binding Sites from Rat Brain. *J. Memb. Biol.* 1979; 50:287-310.
- Krueger BK, Worley JF, French RJ: Block of Sodium Channels in Planar Lipid Bilayers by Guanidinium Toxins and Calcium: Are the Mechanisms of Voltage Dependence the Same? *Ann. NY Acad. Sci.* 1986; 479:257-268.
- Kunze DL, Lacerda AE, Wilson DL, Brown AM: Cardiac Na⁺ Currents and the Inactivating, Reopening, and Waiting Properties of Single Sodium Channels. *J. Gen. Physiol.* 1985; 86:691-719.

- Lai C-S, Cheng S-Y: Molecular Dynamics of 3,3',5-Triiodo-L-thyronine in Model Membranes: A Spin Label Study. *Arch. Biochem. Biophys.* 1984; 232:477-481.
- Lee H-C, Matsuda JJ, Lemmer JH, Shibata EF: Regulation of Sodium Currents by β -Adrenergic Stimulation in Isolated Cardiac Myocytes from Rabbit and Human. *J. Mol. Cell. Cardiol.* 1990; 22:S14.
- Lein A, Dowben RM: Uptake and Binding of Thyroxine and Triiodothyronine by Rat Diaphragm in Vitro. *Am. J. Physiol. (London)* 1961; 200:1029-1031.
- Levey GS, Epstein SE: Myocardial Adenyl Cyclase: Activation by Thyroid Hormones and Evidence for Two Adenyl Cyclase Systems. *J. Clin. Invest.* 1969; 48:1663-1669.
- Margolius HS, Gaffney TE: The Effects of Injected Norepinephrine and Sympathetic Nerve Stimulation in Hypothyroid and Hyperthyroid Dogs. *J. Pharmacol. Exp. Ther.* 1965; 149:329-335.
- Matsuda JJ, Lee H, Shibata EF: Modulation of Cardiac Currents by G-Proteins and cAMP-Dependent Phosphorylation. *Biophys. J.* 1991; 59:program addendum.
- McLaughlin S: The Electrostatic Properties of Membranes. *Ann. Rev. Biophys. Biophys. Chem.* 1989; 18:113-136.
- McManus OB, Magleby KL: Kinetic States and Modes of Single Large-Conductance Calcium-Activated Potassium Channels in Cultured Rat Skeletal Muscle. *J. Physiol. (London)* 1988; 402:79-120.
- Meves H, Nagy K: Multiple Conductance States of the Sodium Channel and of Other Ion Channels. *Biochim. Biophys. Acta* 1989; 988:99-105.
- Mikami A, Imoto K, Tanabe T, Niidome T, Mori Y, Takeshima H, Narumiya S, Numa S: Primary Structure and Functional Expression of the Cardiac Dihydropyridine-Sensitive Calcium Channel. *Nature* 1989; 340:230-233.
- Moczydlowski E, Hall S, Garber SS, Strichartz GR, Miller C: Voltage-Dependent Block of Muscle Channels by Guanidinium Toxins. Effect of Toxin Charge. *J. Gen. Physiol.* 1984; 84:687-704.
- Moczydlowski E, Olivera BM, Gray WR, Strichartz GR: Discrimination of Muscle and Neuronal Na-Channel Subtypes by Binding Competition Between [3 H]Saxitoxin and

- μ -Conotoxins. *Proc. Natl. Acad. Sci. USA* 1986a; 83:5321-5325.
- Moczydlowski E, Uehara A, Guo X, Heiney J: Isochannels and Blocking Modes of Voltage-Dependent Sodium Channels. *Ann. NY Acad. Sci.* 1986b; 479:269-292.
- Moczydlowski E, Uehara A, Hall S: Blocking Pharmacology of Batrachotoxin-Activated Sodium Channels. In *Ion Channel Reconstitution*. C. Miller, editor. Plenum Publishing Corp., New York. 1986c; 405-428.
- Moorman JR, Kirsch GE, Lacerda AE, and Brown AM: Angiotensin II Modulates Cardiac Na⁺ Channels in Neonatal Rat. *Circ. Res.* 1989; 65:1804-1809.
- Moorman JR, Kirsch GE, VanDongen AMJ, Joho RH, Brown AM: Fast and Slow Gating of Sodium Channels Encoded by a Single mRNA. *Neuron* 1990; 4:243-252.
- Murray KT, Snyder DS, Bennett PB: Isoproterenol Increases the Cardiac Sodium Current in the Presence of Buffered Ca²⁺_i. *Circulation* 1990; 82:III-522.
- Nagy K: Subconductance States of Single Sodium Channels Modified by Chloramine-T and Sea Anemone Toxin in Neuroblastoma Cells. *Eur. Biophys. J.* 1987; 15:129-132.
- Nagy K, Kiss T, Hof D: Single Na⁺ Channels in Mouse Neuroblastoma Cell Membrane: Indications for Two Open States. *Pflügers Arch.* 1983; 399:302-308.
- Nastuk WL, Hodgkin AL: The Electrical Activity of Single Fibres. *J. Cell. Comp. Physiol.* 1950; 35:39-73.
- Neher E, Steinbach JH: Local Anaesthetics Transiently Block Currents Through Single Acetylcholine-Receptor Channels. *J. Physiol. (London)* 1978; 277:153-176.
- Nilius B: Calcium Block of Guinea-Pig Heart Sodium Channels With and Without Modification by the Piperazinylole DPI 201-106. *J. Physiol. (London)* 1988a; 399:537-558.
- Nilius B: Modal Gating Behavior of Cardiac Sodium Channels in Cell-Free Membrane Patches. *Biophys. J.* 1988b; 53:857-862.
- Nilius B, Vereecke J, Carmeliet E: Subconductance States in Cardiac Sodium Channels. *Biomed. Biochim. Acta* 1989; 48:S354-357.

- Noda M, Ikeda T, Kayano T, Suzuki H, Takeshima H, Kurasaki M, Takahashi H, Numa S: Existence of Distinct Sodium Channel Messenger RNAs in Rat Brain. *Nature* 1986; 320:188-192.
- Noda M, Shimizu S, Tanabe T, Takai T, Kayano T, Ikeda T, Takahashi H, Nakayama H, Kanaoka Y, Minamino N, Kangawa K, Matsuo H, Raftery MA, Hirose T, Inayama S, Hayashida H, Miyata T, Numa S: Primary Structure of *Electrophorus electricus* Sodium Channel Deduced from cDNA Sequence. *Nature* 1984; 312:121-127.
- Noda M, Suzuki H, Numa S, Stühmer W: A Single Point Mutation Confers Tetrodotoxin and Saxitoxin Insensitivity on the Sodium Channel II. *FEBS Lett.* 1989; 259:213-216.
- Numann R, Scheuer T, Catterall WA: Modulation of Rat Brain Type IIA Sodium Channels By Activators of Protein Kinase C. *Biophys. J.* 1991; 59:262a.
- Nyquist H: Thermal Agitation of Electrical Charge in Conductance. *Phys. Rev.* 1928; 32:110-113.
- Olivera BM, Gray WR, Zeikus R, McIntosh JM, Varga J: Peptide Neurotoxins from Fish-Hunting Cone Snails. *Science* 1985; 230:1338-1343.
- Olshausen KV, Bischoff S, Kahaly G, Mohr-Kahaly S, Erbel R, Beyer J, Meyer J: Cardiac Arrhythmias and Heart Rate in Hyperthyroidism. *Am. J. Cardiol.* 1989; 63:930-933.
- Ono K, Fozzard HA: Late Current Through Na⁺ Channels Modified by Forskolin. *Biophys. J.* 1991; 59:72a.
- Ono K, Kiyosue T, Arita M: Isoproterenol, DBcAMP, and Forskolin Inhibit Cardiac Sodium Current. *Am. J. Physiol.* 1989; 256:C1131-C1137.
- Oppenheimer JH: Thyroid Hormone Action at the Nuclear Level. *Ann. Intern. Med.* 1985; 102:374-384.
- Oxford GS, Yeh JZ: Interactions of Monovalent Cations with Sodium Channels in Squid Axon. I. Modification of Physiological Inactivation Gating. *J. Gen. Physiol.* 1985; 85:583-602.
- Patlak JB: The Information Content of Single Channel Data. *In* Membranes, Channels, and Noise. R. S. Eisenberg, M. Frank, and C. F. Stevens, editors. Plenum Publishing Corp., New York. 1984; 197-234.

- Patlak JB: Sodium Channel Subconductance Levels Measured with a New Variance-Mean Analysis. *J. Gen. Physiol.* 1988; 92:413-430.
- Patlak JB: The Effect of pH on Subconductance State Frequency and Duration in Bursting Na⁺ Channels of Skeletal Muscle. *Biophys. J.* 1990; 57:395a.
- Patlak JB, Ortiz M: Slow Currents Through Single Sodium Channels of the Adult Rat Heart. *J. Gen. Physiol.* 1985; 86:89-104.
- Patlak JB, Ortiz M: Two Modes of Gating During Late Na Channel Currents in Frog Sartorius Muscle. *J. Gen. Physiol.* 1986; 87:305-326.
- Patlak JB, Ortiz M: Kinetic Diversity of Na⁺ Channel Bursts in Frog Skeletal Muscle. *J. Gen. Physiol.* 1989; 94:279-301.
- Patlak JB, Ortiz M, Horn R: Open-Time Heterogeneity During Bursting of Sodium Channels in Frog Skeletal Muscle. *Biophys. J.* 1986; 49:773-777.
- Poole RC, Halestrap AP, Price SJ, Levi AJ: The Kinetics of Transport of Lactate and Pyruvate into Isolated Cardiac Myocytes from Guinea Pig. *Biochem. J.* 1989; 264:409-418.
- Rack M, Woll K-H: Effects of Chemical Modification of Carboxyl Groups on the Voltage-Clamped Nerve Fiber of the Frog. *J. Memb. Biol.* 1984; 82:41-48.
- Rando TA, Strichartz GR: Saxitoxin Blocks Batrachotoxin-Modified Sodium Currents in the Node of Ranvier in a Voltage-Dependent Manner. *Biophys. J.* 1986; 49:785-794.
- Rao G: Mode of Entry of Steroid and Thyroid Hormones into Cells. *Mol. Cell. Endocrinol.* 1981; 21:97-108.
- Reed JK, Raftery MA: Properties of the Tetrodotoxin Binding Component in Plasma Membranes Isolated from *Electrophorus electricus*. *Biochemistry* 1976; 15:944-953.
- Renaud JF, Fosset M, Schweitz H, Lazdunski M: The Interaction of Polypeptide Neurotoxins with Tetrodotoxin-Resistant Na⁺ Channels in Mammalian Cardiac Cells. Correlation with Inotropic and Arrhythmic Effects. *Eur. J. Pharmacol.* 1986; 120:161-170.
- Reuter H: Slow Inactivation of Currents in Cardiac Purkinje Fibers. *J. Physiol. (London)* 1968; 197:233-253.

- Rogart RB, Cribbs LL, Muglia LK, Kephart DD, Kaiser MW: Molecular Cloning of a Putative Tetrodotoxin-Resistant Rat Heart Na⁺ Channel Isoform. *Proc. Nat. Acad. Sci. USA* 1989; 86:8170-8174.
- Rudinger A, Mylotte KM, Davis PJ, Davis FB, Blas SD: Rabbit Myocardial Membrane Ca²⁺ Adenosine Triphosphatase Activity: Stimulation In Vitro by Thyroid Hormone. *Arch. Biochem. Biophys.* 1984; 229:379-385.
- Sakmann B, Neher E, eds.: *Single Channel Recording*. Plenum Press. New York. 1983.
- Sakmann B, Neher E: Patch Clamp Techniques for Studying Ionic Channels in Excitable Membranes. *Ann. Rev. Physiol.* 1984; 46:455-472.
- Salgado VL, Yeh JZ, Narahashi T: Use- and Voltage-Dependent Block of the Sodium Channel by Saxitoxin. *Ann. NY Acad. Sci.* 1986; 479:84-95.
- Scanley BE, Fozzard HA: Low Conductance Sodium Channels in Canine Cardiac Purkinje Cells. *Biophys. J.* 1987; 52:489-495.
- Scanley BE, Hanck DA, Chay T, Fozzard HA: Kinetic Analysis of Single Sodium Channels from Canine Cardiac Purkinje Cells. *J. Gen. Physiol.* 1990; 95:411-437.
- Schauf CL: Tetramethylammonium Ions Alter Sodium Channel Gating in *Myxicola*. *Biophys. J.* 1983; 41:269-274.
- Scherer NM, Toro M-J, Entman ML, Birnbaumer L: G Protein Distribution in Canine Cardiac Sarcoplasmic Reticulum and Sarcolemma. Comparison to Rabbit Skeletal Membrane and Brain and Erythrocyte G Proteins. *Arch. Biochem. Biophys.* 1987; 259:431-440.
- Schreibmayer W, Tritthart HA, Schindler H: The Cardiac Sodium Channel Shows Regular Substate Pattern Indicating Synchronized Activity of Several Ion Pathways Instead of One. *Biochim. Biophys. Acta* 1989; 986:172-186.
- Schroeder F: Hormonal Effects of Fatty Acid Binding and Physical Properties of Rat Liver Plasma Membranes. *J. Memb. Biol.* 1982; 68:1-10.
- Schubert B, VanDongen AMJ, Kirsch GE, Brown AM: β -Adrenergic Inhibition of Cardiac Sodium Channels by Dual G-Protein Pathways. *Science* 1989; 245:516-519.

- Schubert B, VanDongen AMJ, Kirsch GE, Brown AM: Inhibition of Cardiac Na⁺ Currents by Isoproterenol. *Am. J. Physiol.* 1990; 258:H977-H982.
- Sculptoreanu A, Scheuer T, Catterall WA: Electrophysiological Characterization of a Cardiac Cell Line. *Biophys. J.* 1991; 59:100a.
- Segal J: Action of the Thyroid Hormone at the Level of the Plasma Membrane. *Endocrine Res.* 1989a; 15:619-649.
- Segal J: Acute Effect of Thyroid Hormone on the Heart: An Extranuclear Increase in Sugar Uptake. *J. Mol. Cell. Cardiol.* 1989b; 21:323-34.
- Segal J: A Rapid, Extranuclear Effect of 3,5,3'-Triiodothyronine on Sugar Uptake by Several Tissues in the Rat In Vivo. Evidence for a Physiological Role for Thyroid Hormone Action at the Level of the Plasma Membrane. *Endocrinology* 1989c; 124:2755-2764.
- Segal J: Calcium is the First Messenger for the Action of Thyroid Hormone at the Level of the Plasma Membrane: First Evidence for an Acute Effect of Thyroid Hormone on Calcium Uptake in the Heart. *Endocrinology* 1990a; 126:2693-2702.
- Segal J: In Vivo Effect of 3,5,3'-Triiodothyronine on Calcium Uptake in Several Tissues in the Rat: Evidence for Calcium as the First Messenger for the Prompt Action of Thyroid Hormone at the Level of the Plasma Membrane. *Endocrinology* 1990b; 127:17-24.
- Segal J, Ingbar SH: Evidence that an Increase in Cytoplasmic Calcium is the Initiating Event in Certain Plasma Membrane-Mediated Responses to 3,5,3'-Triiodothyronine in Rat Thymocytes. *Endocrinology* 1989; 124:1949-1955.
- Sharp NA, Neel DS, Parsons RL: Influence of Thyroid Hormone Levels on the Electrical and Mechanical Properties of Rabbit Papillary Muscle. *J. Mol. Cell. Cardiol.* 1985; 17:119-132.
- Sheets MF, Hanck DA, Fozzard HA: Divalent Cation Block of Sodium Current in Single Canine Cardiac Purkinje Cells. *Biophys. J.* 1988; 53:535a.
- Sheets MF, Scanley BE, Hanck DA, Makielski JC, Fozzard HA: Open Sodium Channel Properties of Single Canine Cardiac Purkinje Cells. *Biophys. J.* 1987; 52:13-22.
- Shrager P, Profera C: Inhibition of the Receptor for Tetrodotoxin in Nerve Membranes by Reagents that Modify Carboxyl Groups. *Biochim. Biophys. Acta* 1973; 318:141-146.

- Sigworth FJ, Spalding BC: Chemical Modification Reduces the Conductance of Sodium Channels in Nerve. *Nature* 1980; 283:293-295.
- Spalding BC: Properties of Toxin-Resistant Sodium Channels Produced by Chemical Modification in Frog Skeletal Muscle. *J. Physiol. (London)* 1980; 305:485-500.
- Stevens CF: Making a Submicroscopic Hole in One. *Nature* 1991; 349:657-658.
- Strichartz G, Rando T, Wang GK: An Integrated View of the Molecular Toxinology of Sodium Channel Gating in Excitable Cells. *Ann. Rev. Neurosci.* 1987; 10:237-267.
- Stühmer W, Conti F, Suzuki H, Wang X, Noda M, Yahagi N, Kubo H, Numa S: Structural Parts Involved in Activation and Inactivation of the Sodium Channel. *Nature* 1989; 339:597-603.
- Tanabe T, Takeshima H, Mikami A, Flockerzi V, Takahashi H, Kangawa K, Kojima M, Matsuo H, Hirose T, Numa S: Primary Structure of the Receptor for Calcium Channel Blockers from Skeletal Muscle. *Nature* 1987; 328:313-318.
- Tanguy J, Yeh JZ: Divalent Cation Block of Normal and BTX-Modified Sodium Channels in Squid Axons. *Biophys. J.* 1988; 53:229a.
- Trimmer JS, Agnew WS: Molecular Diversity of Voltage-Gated Na Channels. *Ann. Rev. Physiol.* 1989; 51:401-418.
- Trimmer JS, Cooperman SS, Tomiko SA, Zhou JY, Crean SM, Boyle MB, Kallen RG, Sheng ZH, Barchi RL, Sigworth FJ, Goodman FS, Agnew WS, Mandel G: Primary Structure and Functional Expression of a Mammalian Skeletal Muscle Sodium Channel. *Neuron* 1989; 3:33-49.
- Tsien RW, Hess P, McCleskey EW, Rosenberg RL: Calcium Channels: Mechanisms of Selectivity, Permeation, and Block. *Ann. Rev. Biophys. Biophys. Chem.* 1987; 16:265-290.
- Tytgat J, Vereecke J, Carmeliet E: A Combined Study of Sodium Current and T-Type Calcium Current in Isolated Cardiac Cells. *Pflügers Arch.* 1990; 417:142-148.
- Ulbricht W, Wagner H-H: The Influence of pH on the Rate of Tetrodotoxin Action on Myelinated Nerve Fibers. *J. Physiol. (London)* 1975; 252:185-202.

- Urban BW, Recio-Pinto E, Duch DS, Parnicas M: Several Conductance Levels in Steady State Sodium Channels. *Pflügers Arch.* 1987; 408:R311.
- Visentin S, Zaza A, Ferroni A, Tromba C, DiFrancesco C: Sodium Current Block Caused by Group IIb Cations in Calf Purkinje Fibres and in Guinea-Pig Ventricular Myocytes. *Pflügers Arch.* 1990; 417:213-222.
- Wagner H-H, Ulbricht W: The Rates of Saxitoxin Action and of Saxitoxin-Tetrodotoxin Interaction at the Node of Ranvier. *Pflügers Arch.* 1975; 359:297-315.
- Weiss RE, Horn R: Functional Differences Between Two Classes of Sodium Channels in Developing Rat Skeletal Muscle. *Science* 1986a; 233:361-364.
- Weiss RE, Horn R: Single-Channel Studies of TTX-Sensitive and TTX-Resistant Sodium Channels in Developing Rat Muscle Reveal Different Open Channel Properties. *Ann. NY Acad Sci.* 1986b; 479:152-161.
- Will-Shahab L, Wollenberger A, Kuttner I: Stimulation of Rat and Cat Heart Adenylate Cyclase by Triiodothyronine in the Presence of 5'-Guanylylimidodiphosphate. *Acta Biol. Med. Germ.* 1976; 35:829-835.
- Woodhull AM: Ionic Blockade of the Sodium Channels in Nerve. *J. Gen. Physiol.* 1973; 61:687-708.
- Worley JF, French RJ, Krueger BK: Trimethyloxonium Modification of Single Batrachotoxin-Activated Sodium Channels in Planar Bilayers. *J. Gen. Physiol.* 1986; 87:327-349.
- Wortsman J, Premachandra BN, Williams K, Burman KD, Hay ID, Davis PJ: Familial Resistance to Thyroid Hormone Associated with Decreased Transport Across the Plasma Membrane. *Ann. Int. Med.* 1983; 98:904-909.
- Yamamoto D, Yeh JZ, Narahashi T: Interactions of Permeant Cations with Sodium Channels of Squid Axon Membranes. *Biophys. J.* 1985; 48:361-368.
- Yellen G: Permeation in Potassium Channels: Implications for Channel Structure. *Ann. Rev. Biophys. Chem.* 1987; 16:227-246.
- Zhou J, Agnew W, Sigworth FJ: The μ I Na Channels Expressed in Oocytes Have At Least Three Gating Modes. *Biophys. J.* 1991; 59:71a.

Vita

